Arabian Journal of Chemistry (2023) **16**, 105137

King Saud University

Arabian Journal of Chemistry

www.ksu.edu.sa
www.sciencedirect.com

REVIEW ARTICLE

Plant polyacetylenoids: Phytochemical, analytical and pharmacological updates

Jia-Xin Lai [1], Su-Fang Dai [1], Bian-Xia Xue, Li-Hua Zhang, Yanxu Chang, Wenzhi Yang, Hong-Hua Wu [*]

State Key Laboratory of Component-based Chinese Medicine, Institute of Traditional Chinese Medicine, Tianjin University of Traditional Chinese Medicine, 10 Poyanghu Road, West Area, Tuanbo New Town, Jinghai District, Tianjin 301617, People's Republic of China

Received 10 February 2023; accepted 3 July 2023
Available online 7 July 2023

KEYWORDS

Plant polyacetylenoids;
Phytochemicals;
Analytical methods;
Pharmacology

Abstract In terrestrial medicinal plants, polyacetylenoids have been isolated from almost 110 species belonging to 11 families including Compositae, Apiaceae, Araliaceae, Campanulaceae, Annonaceae, and Meliaceae. They are a class of natural products derived from fatty acids with carbon chain lengths of $C_{8–19}$, C_{21}, $C_{23–25}$, C_{27}, C_{29}, and C_{33}, possessing a pleiotropic profile of bioactivities such as anti-tumor, anti-inflammatory activities. Herein, this review aims at summarizing the inventory of polyacetylenoids occurring in terrestrial medicinal plants during the last two decades from 2000 to 2023, the NMR characteristics, and the progress on analytical methods and pharmacological investigation of the well-known plant polyacetylenoids.

1. Introduction

According to the fossil records, the human history of using terrestrial medicinal plants as remedies dates back at least 60,000 years. Terrestrial medicinal plants produce constitutive metabolites (primary or secondary) for the purpose of reproduction and survival. It's precisely these metabolites, well-known as phytochemicals, with qualities of a definite chemical diversity, a wide range of biological activities and drug-likeness, give us the possibility to protect against a variety of diseases such as malaria, gastrointestinal disorders, traumatic infection, fever, liver disorders, hypertension, tumor, and cancer. (Sanchez-Ramos et al., 2021). In today's world, the potential of this chemical arsenal has been well-recognized by chemists and pharmacologists to discover molecules functional as lead structures in the search and development of new drugs or as biological probes for physiological investigation (Yeboah et al., 2022).

* Corresponding author at: Institute of Traditional Chinese Medicine, Tianjin University of Traditional Chinese Medicine, 10 Poyanghu Road, West Area, Tuanbo New Town, Jinghai District, Tianjin, 301617, People's Republic of China.
E-mail address: wuhonghua2011@tjutcm.edu.cn (H.-H. Wu).
[1] **Co-first authors:** J.-X. Lai and S-F. Dai contributed equally to this work and should be considered co-first authors.
Peer review under responsibility of King Saud University.

Production and hosting by Elsevier

https://doi.org/10.1016/j.arabjc.2023.105137

Polyacetylenoids are a class of compounds derived from polyacetylenes (or acetylenes) that may be biosynthesized from fatty acids, featuring two or more acetylenic bonds in their nucleus scaffolds (Konovalov 2014; Xie and Wang 2022). So far, naturally occurring polyacetylenoids have been isolated from a wide range of biomasses such as plants, animals, fungi, and marine sponges (Kuklev and Dembitsky, 2014; Negri 2015; Christensen 2020). Until now, more than 1400 plant polyacetylenoids and their relevant derivatives have been isolated, mainly from the higher plants of Compositae, Apiaceae and Araliaceae families and sporadically from the plants of other families (Christensen and Brandt 2006; Patil et al., 2012). And numerous researches have been devoted into the pharmacological and biological properties of polyacetylenoids, such as antitumoral (Kobaek-Larsen et al., 2017), anti-inflammatory (Christensen 2020; Redl et al., 1994), antimicrobial, (Marčetić et al., 2014), hepatoprotective (Utrilla et al., 1995), phototoxic (Chobot et al., 2006), antimalarial (Tobinaga et al., 2009), anti-obesity(Jiao et al., 2014), antioxidative (Lee et al., 2013), allergic (Hansen et al., 1986), anti-Alzheimer's disease (Hao et al., 2005), antidiabetic (Chien et al., 2009), immunoregulatory (Song et al., 2019), neuroprotective (Wang et al., 2016) and insecticidal (Herrmann et al., 2011) activities. Notably, the successful drug development of the polyacetylenoids is exemplified by the case of allyl enediyne antibiotics, which have been the most active antitumoral agents to date. Benefiting from the special molecular structure, the novel mechanism of action, and the broad development prospects (Thorson et al., 2000), enediyne antibiotics have been reported to be highly effective in killing tumor cells, and are very likely to be exploited as novel and highly effective antitumoral drugs.

As far as the literature we can reach, before 2000, people mainly reported the antitumoral (Matsunaga et al., 1990), phototoxic (Towers et al., 1979, Wat et al., 1979), and allergic properties (Hansen et al., 1986, Towers 1986, Gafner et al., 1988) of plant polyacetylenoids, followed by their anti-inflammatory, antioxidative (Redl et al., 1994) and hepatoprotective (Utrilla et al., 1995) activities. For examples, there were clinical trial and *in vitro* study convincing us the contact allergic action of falcarinol (Gafner et al., 1988). Several *in vivo* studies revealed the antioxidative (Cavin. et al., 1998) and hepatoprotective (Utrilla et al., 1995) effects of santolindiacetylene, and the antitumoral efficacy of falcarinol oxylipin in a LOX melanoma mouse xenograft model (Bernart et al., 1996). Since 2000, most studies have focused on their antitumoral, anti-inflammatory, and antimicrobial effects, followed by the bioactivities of antimalarial, anti-obesity, hepatoprotection, and anti-Alzheimer's disease. And numerous *in vivo* studies have illustrated the above-mentioned biological functions of plant polyactylenoids.

Since 1972, several reviews summarized the studies on polyacetylenoids that occurred in families of Araliaceae and Apiaceae, and furtherly the genus of *Bupleurum* and *Echinacea*, focusing on their distribution, phytochemistry, biosynthesis and the bioactive chemicals and their pharmacological properties, as well as the analytical methods of the polyacetylenoids in *Bupleurum* species (Hansen and Boll 1986; Pellati et al., 2012; Chen et al., 2015; Lin et al., 2016). At the same time, biosynthesis progress on the natural polyacetylenoid products and their glycosidal derivatives has also been reviewed by Minto *et al.* (Minto and Blacklock 2008; Gung 2009; Pan et al., 2009; Dawid et al., 2015; Santos et al., 2022). Furthermore, the cytotoxic, anticancer, and anti-inflammatory bioactivities of several specific polyacetylenoids, including natural and synthetic acetylenic lipids, C_{17} and C_{18} acetylenic oxylipins, lobetyolin and its structural analogs, were collected by Dembitsky *et al.* (Bailly 2020; Christensen 2020; Dembitsky 2006). And recently, two reviews covering the advances on bioactivity properties of those polyacetylenoids originated from the terrestrial eukaryotic organisms, especially the herbal medicines, during 2000–2015 and 2014–2021, respectively (Negri 2015; Xie and Wang 2022).

However, there were few reviews focusing on a global classification and the structural spectroscopic characteristics of those terrestrial polyacetylenoids, which intuitively unveiling their molecular shapes and structural characteristics in aid of their structural elucidation. Further, there were few concerns on summarizing the analytical methods that have been developed for those representative terrestrial plant polyacetylenoids, as quality control of polyacetylenoid products plays a more and more important role in their future development and utilization. Under this background, the terrestrial plant polyacetylenoids were re-classified based on their intrinsic molecular characteristics in this Review. And herein, recent research progresses on their phytochemistry, plant origins, NMR characteristics and determination methods of their configurations, analytical methods, and the pharmacological benefits as exemplified by some typical polyacetylenoids (such as falcarinol, falcarindiol and lobetylolin) were updated.

In this Review, 'polyacetylenoids' is introduced to represent the polyacetylenes and their derivatives including polyacetylenic ethers, esters, glycosides, and the thio-products. For better clearness and ease for readers, the polyacetylenoid molecules described in this Review have been divided into two sections (linear polyacetylenoids and cyclic polyacetylenoids) based on their structural features (cyclic or not). And within each section, they have been presented in an order based on the general types of carbon skeletons in the clue of the substitution patterns of the 'acetylenic terminal' concentrated with triple and double bonds. Considering the main differences between polyacetylenoids' structures are the chain length and the cyclic pattern and that C_{17}, C_{14}, C_{18}, C_{10}, C_{13} and C_{15}-polyacetylenoids are the most common polyacetylenoids in terrestrial medicinal plants, the linear polyacetylenoid structures are then divided into seven main classes, *i.e.*, those with 17 carbons, 14 carbons, 18 carbons, 10 carbons, 13 carbons, and 15 carbons, and others. The clyclic polyacetylenoids have been furtherly separated into monocyclic, bicyclic, and polycyclic based on the complexity of ring systems in their structures. Summary tables reporting, for each group of molecules, the names, and sources of the presented structures, as well as their literature references, are embedded in the text (Table 1).

2. Plant polyacetylenoids and their distribution

In the last twenty years, more than 485 polyacetylenoids, with chain lengths of $C_{8–19}$, C_{21}, $C_{23–25}$, C_{27}, C_{29} and C_{33}, have been isolated from the terrestrial medicinal plants. Almost all of them were isolated from the species in families of Compositae, Apiaceae, Araliaceae, Campanulaceae, Annonaceae and Meliaceae. The top 7 chain lengths of polyacetylenoids, occurring mostly in the terrestrial plants, were 17, 14, 13, 18, 10, 15 and 12. Among them, 363 linear polyacetylenoids ($C_{9–19}$ and C_{33}) and 122 cyclic ones (including 78 monocyclic, 35 bicyclic, 4 tricyclic and 1 tetracyclic; C_8, $C_{11–19}$, C_{21}, $C_{23–25}$, C_{27}, and C_{29}) have been isolated from almost 110 species of terrestrial medicinal plants as listed in Supplementary Table S1.

2.1. Linear polyacetylenoids

Linear polyacetylenoids accounted for about 80% of all the polyacetylenoids isolated from terrestrial medicinal plants in the last two decades. As summarized in Table 1, the linear polyacetylenoids mainly consist of C_{17}, C_{14}, C_{13}, C_{18}, C_{10}, and C_{15} polyacetylenoids. And based on the numbers and substitution sites of triple and double bonds, the polyacetylenic terminals of linear polyacetylenoids can be mainly sorted into 14 types, as shown in Fig. 1. In most linear polyacetylenoids, carbon–carbon triple bonds prefer to be situated at C-4,5 or C-6,7, and carbon–carbon double bonds tend to be at C-1,2 or C-2,3. In the last two decades, liner polyacetylenoids were mainly isolated from the plants of Compositae, Apiaceae, Araliaceae, Campanulaceae, Annonaceae and Meliaceae fam-

Table 1 Polyacetylenoids isolated from terrestrial medicinal plants from 2000 to 2022.

No.	Name	Formula	Origin	Part	Reference
1	(3*R*,8*S*)-Heptadec-1-ene-4,6-diyne-3,8-diol	$C_{17}H_{26}O_2$	*L. tenuissimum*	Roots	(Choi et al., 2016)
2	8-Hydroxyheptadec-1-ene-4,6-diyn-3-yl acetate	$C_{19}H_{28}O_3$	*C. zimmermannii*	Roots	(Baur et al., 2005; Senn et al., 2007)
3	10-Chloro-1-heptadecene-4,6-diyne-3,8,9-triol	$C_{17}H_{25}ClO_3$	*N. ternata*	Aerial parts	(Nakagawa et al., 2004)
4	Panaxydol chlorohydrin	$C_{17}H_{25}ClO_2$	*P. ginseng*	Roots	(Suzuki et al., 2017)
5	Baisanqisaponin B	$C_{63}H_{96}O_{20}$	*P. japonicus*	Roots	(Liu et al., 2016)
6	Baisanqisaponin A	$C_{59}H_{90}O_{16}$	*P. japonicus*	Roots	(Liu et al., 2016)
7	Baisanqisaponin C	$C_{59}H_{90}O_{16}$	*P. japonicus*	Roots	(Liu et al., 2016)
8	(3*R*,9*R*,10*R*)-Panaxytriol	$C_{17}H_{26}O_3$	*P. ginseng*	Roots	(Yang et al., 2008; Herrmann et al., 2013; Suzuki et al., 2017)
9	10-Methoxyheptadec-1-ene-4, 6-diyne-3,9-diol	$C_{18}H_{28}O_3$	*P. ginseng*	Roots	(Yang et al., 2008)
10	Ac-panaxytriol	$C_{23}H_{32}O_6$	*P. ginseng*	Roots	(Suzuki et al., 2017)
11	*cis*-Panaxydiol	$C_{17}H_{24}O_2$	*E. triquetrum*	Aerial parts	(Bouzergoune et al., 2016)
12	Panaxydiol	$C_{17}H_{24}O_2$	*A. graveolens*	Roots	(Zidorn et al., 2005)
			G. littoralis	Whole plant	(Um et al., 2010)
			O. horridus	Root barks	(Resetar et al., 2020)
			P. sativa	Roots	(Roman et al., 2011)
			S. divaricata	Roots and rhizomes	(Yokosuka et al., 2017)
13	(8*E*)-10-Hydroperoxy-1,8-heptadecadiene-4,6-diyn-3-ol	$C_{17}H_{24}O_3$	*S. divaricata*	Roots and rhizomes	(Yokosuka et al., 2017)
14	1,8-Heptadeca-diene-4,6-diyne-3,10-diol	$C_{17}H_{24}O_2$	*P. ginseng*	Roots	(Washida and Kitanaka 2003; Suzuki et al., 2017)
15	(8*E*)-Heptadeca-1,8-diene-4,6-diyne-(3*S*),10-diol	$C_{17}H_{24}O_2$	*D. morbiferus*	Leaves	(Chung et al., 2011)
			E. triquetrum	Aerial parts	(Bouzergoune et al., 2016)
16	(8*E*)-1,8-Heptadecadiene-4,6-diyne-3,10-diol	$C_{17}H_{24}O_2$	*G. littoralis*	Roots	(Zhang et al., 2020)
17	Heptadeca-1,8-diene-4,6-diyne-3-ol-10-one	$C_{17}H_{22}O_2$	*E. triquetrum*	Aerial parts	(Bouzergoune et al., 2016)
18	Cadiyenol	$C_{24}H_{36}O_6$	*C. asiatica*	Aerial parts	(Govindan et al., 2007)
19	Falcarinol	$C_{17}H_{24}O$	*P. pseudoginseng*	Roots and rhizomes	(Tanaka et al., 2000)
			N. ternata	Aerial parts	(Nakagawa et al., 2004)
			C. aureum	Aerial parts	(Rollinger et al., 2003)
			A. graveolens	Roots	(Zidorn et al., 2005)
			E. yuccifolium	Aerial parts	(Ayoub et al., 2006)
			L. officinale	Roots	(Zloh et al., 2007; Schinkovitz et al., 2008)
			P. ginseng	Roots	(Washida and Kitanaka 2003; Liu et al., 2007; Yang et al., 2008; Qian et al., 2009; Herrmann et al., 2013; Suzuki et al., 2017)
			G. littoralis	Whole plant	(Um et al., 2010; Zhang et al., 2020)
			N. incisum	Roots	(Blunder et al., 2014)
			S. divaricata	Roots and rhizomes	(Yokosuka et al., 2017)
			E. triquetrum	Aerial parts	(Bouzergoune et al., 2016)
			E. platyloba	Aerial parts	(Chianese et al., 2018)
			A. furcijuga	Roots	(Yoshikawa et al., 2006)
			C. pilosula	Roots	(Bailly 2020)
			P. quinquefolius	Roots	(Baranska et al., 2006; Christensen et al., 2006)
			D. carota	Roots	(Purup et al., 2009; Kramer et al., 2011; Killeen et al., 2013)
			P. sativa	\	(Rawson et al., 2010; Roman et al., 2011; Corell et al., 2013)
			P. quinquefolius	Roots	(Wang et al., 2010)
19a[a]	(*R*)-Falcarinol	$C_{17}H_{24}O$	*D. guatemalense*	Flowers, leaves, and twigs	(Grant et al., 2020)
			O. horridus	Root barks	(Resetar et al., 2020)

(*continued on next page*)

Table 1 (*continued*)

No.	Name	Formula	Origin	Part	Reference
20	Falcarindiol	$C_{17}H_{24}O_2$	*N. ternata*	Aerial parts	(Nakagawa et al., 2004)
			S. taiwaniana	Leaves	(Kuo et al., 2002)
			L. mutellina	Roots	(Renate et al., 2002)
			S. yunnanensis	Roots	(Wang et al., 2003)
			C. barteri	Leaves	(Kraus 2003)
			A. cordata	Roots	(Dang et al., 2005)
			H. rhombea	Leaves	(Yamazoe et al., 2006; Yamazoe et al., 2007)
			C. zimmermannii	Roots	(Senn et al., 2007)
			A. sylvestris	Roots	(Jeong et al., 2007)
			C. maritimum	Leaves	(Meot-Duros et al., 2010)
			G. littoralis	Whole plant	(Um et al., 2010; Zhang et al., 2020)
			O. horridus	Root barks	(Sun et al., 2010; Resetar et al., 2020)
			O. elatus	Stems	(Yang et al., 2010)
			N. incisum	Roots	(Blunder et al., 2014; Zheng et al., 2019)
			P. praeruptorum	Roots	(Lee et al., 2015)
			S. divaricata	Roots and rhizomes	(Yokosuka et al., 2017)
			B. chinense	Roots	(Liu et al., 2017)
			H. dissectum	Roots	(Gao et al., 2019)
			A. furcijuga	Roots	(Yoshikawa et al., 2006)
			P. ginseng	Roots	(Herrmann et al., 2013)
			C. officinale	Rhizomes	(Venkatesan et al., 2018)
			C. pilosula	Roots	(Bailly 2020)
			D. carota	Roots	(Purup et al., 2009; Kramer et al., 2011; Koidis et al., 2012; Killeen et al., 2013)
			P. sativa	\	(Rawson et al., 2010; Roman et al., 2011)
			D. guatemalense	Flowers, leaves, and twigs	(Grant et al., 2020)
			L. tenuissimum	Roots	(Choi et al., 2016)
20a	(+)-Falcarindiol	$C_{17}H_{24}O_2$	*A. scott-thomsonii*	Subaerial parts	(Perry et al., 2001)
20b	(3*R*,8*S*)-Falcarindiol	$C_{17}H_{24}O_2$	*A. graveolens*	Roots	(Zidorn et al., 2005)
			L. officinale	Roots	(Zloh et al., 2007; Schinkovitz et al., 2008)
			H. maximum	Roots	(Johnson et al., 2013)
			O. fistulosa	Underground parts	(Appendino et al., 2009)
20c	(3*S*,8*S*)-Falcarindiol	$C_{17}H_{24}O_2$	*E. tricuspidatum*	Aerial parts	(Djebara et al., 2019)
			D. morbiferus	Leaves	(Chung et al., 2011)
21	8-Acetoxyfalcarinol	$C_{20}H_{28}O_2$	*N. ternata*	Aerial parts	(Nakagawa et al., 2004)
			H. rhombea	Leaves	(Yamazoe et al., 2006)
			N. incisum	Roots	(Blunder et al., 2014)
22	8-*O*-Methylfalcarindiol	$C_{18}H_{26}O_2$	*P. sativa*	Roots	(Roman et al., 2011)
			A. graveolens	Roots	(Zidorn et al., 2005)
23	Falcarindiol 8-acetate	$C_{19}H_{26}O_3$	*A. cordata*	Roots	(Dang et al., 2005)
24	Notoether D	$C_{32}H_{50}O_4$	*N. incisum*	Roots and rhizomes	(Liu et al., 2014)
25	Notoether F	$C_{32}H_{50}O_4$	*N. incisum*	Roots and rhizomes	(Liu et al., 2014)
26	Notoether B	$C_{32}H_{50}O_3$	*N. incisum*	Roots and rhizomes	(Liu et al., 2014)
27	Notoether H	$C_{32}H_{50}O_4$	*N. incisum*	Roots and rhizomes	(Liu et al., 2014)
28	(*Z*)-3-Hydroxyheptadeca-1,9-diene-4,6-diyn-8-yl-11-(1*H*-indol-3-yl) acetate	$C_{27}H_{31}NO_3$	*H. rhombea*	Flower buds	(Yamazoe et al., 2007)
29	Notoincisol A	$C_{27}H_{32}O_5$	*N. incisum*	Roots and rhizomes	(Liu et al., 2014)
30	Japoangelol A	$C_{34}H_{40}O_8$	*L. officinale*	Roots	(Zloh et al., 2007)
31	Japoangelol C	$C_{33}H_{38}O_7$	*L. officinale*	Roots	(Zloh et al., 2007)
32	Falcarindiol 3-*O*-acetate	$C_{19}H_{26}O_3$	*L. mutellina*	Roots	(Renate et al., 2002)
33	Notoether C	$C_{32}H_{50}O_4$	*N. incisum*	Roots and	(Liu et al., 2014)

Table 1 (*continued*)

No.	Name	Formula	Origin	Part	Reference
				rhizomes	
34	Notoether E	$C_{32}H_{50}O_4$	*N. incisum*	Roots and rhizomes	(Liu et al., 2014)
35	Notoether A	$C_{32}H_{50}O_3$	*N. incisum*	Roots and rhizomes	(Liu et al., 2014)
36	Notoether G	$C_{32}H_{50}O_4$	*N. incisum*	Roots and rhizomes	(Liu et al., 2014)
37	Japoangelol B	$C_{34}H_{40}O_8$	*L. officinale*	Roots	(Zloh et al., 2007)
38	Japoangelol D	$C_{33}H_{38}O_7$	*L. officinale*	Roots	(Zloh et al., 2007)
39	Falcarinaiol 3-acetate	$C_{19}H_{26}O_3$	*D. carota*	Roots	(Kramer et al., 2011; Koidis et al., 2012; Killeen et al., 2013)
			P. sativa	Roots	(Roman et al., 2011)
40	(3*S*,8*S*)-Falcarindiol-3,8-diacetate	$C_{21}H_{28}O_4$	*E. tricuspidatum*	Aerial parts	(Djebara et al., 2019)
41	11-Hydroxyfalcarindiol	$C_{17}H_{24}O_3$	*O. horridus*	Root barks	(Resetar et al., 2020)
42	(3*S*,8*S*)-11-Acetoxyfalcarindiol	$C_{19}H_{26}O_4$	*E. tricuspidatum*	Aerial parts	(Djebara et al., 2019)
43	Falcarinone	$C_{17}H_{22}O$	*E. yuccifolium*	The parts	(Ayoub et al., 2006)
			P. ginseng	Roots	(Murata et al., 2017)
			D. carota	Roots	(Purup et al., 2009)
			P. sativa	Roots	(Roman et al., 2011)
44	Falcarinolone	$C_{17}H_{22}O_2$	*P. sativa*	\	(Rawson et al., 2010; Roman et al., 2011)
45	(*Z*)-8-Acetoxy-3-oxoheptadeca-1,9-diene-4,6-diyne	$C_{19}H_{24}O_3$	*H. rhombea*	Leaves	(Yamazoe et al., 2006)
46	Falcarindione	$C_{17}H_{20}O_2$	*P. sativa*	\	(Rawson et al., 2010)
47	8-Acetoxy-heptadeca-1,9-diene-4,6-diyn-8-ol	$C_{19}H_{26}O_3$	*L. officinale*	Roots	(Zloh et al., 2007)
48	Triquetridiol	$C_{17}H_{24}O_2$	*E. triquetrum*	Aerial parts	(Bouzergoune et al., 2016)
49	Arteordoyn A	$C_{17}H_{24}O_2$	*A. ordosica*	Aerial parts	(Wang et al., 2020)
50	(3*R*,8*S*)-Heptadeca-1,16-diene-4,6-diyne-3,8-diol	$C_{17}H_{24}O_2$	*A. halodendron*	\	(Jin et al., 2021)
51	Ginsenoyne C	$C_{17}H_{24}O_3$	*P. ginseng*	Roots	(Yang et al., 2008)
52	11,12-Dehydrofalcarinol	$C_{17}H_{22}O$	*H. rhombea*	Leaves	(Yamazoe et al., 2007)
53	(9*Z*,11*Z*)-Heptadeca-1,9,11-triene-4,6-diyne-3,8-diol	$C_{17}H_{22}O_2$	*H. rhombea*	Flower buds	(Yamazoe et al., 2007)
54	Dendroarboreol B	$C_{17}H_{22}O_2$	*A. capillaris*	Aerial parts	(Zhao et al., 2014)
			D. guatemalense	Flowers, leaves, and twigs	(Grant et al., 2020)
			T. procumbens	Aerial parts	(Chen et al., 2008)
55	2,9,16-heptadecatriene-4,6-diyn-8-ol	$C_{17}H_{22}O$	*G. koraiensis*	Roots	(Jung et al., 2002)
56	Dehydrofalcarindiol	$C_{17}H_{22}O_2$	*A. cordata*	Roots	(Dang et al., 2005)
56a	(3*R*,8*R*)-Dehydrofalcarindiol	$C_{17}H_{22}O_2$	*A. ordosica*	Aerial parts	(Wang et al., 2020)
			A. monosperma	Aerial parts	(Stavri et al., 2005)
			L. officinale	Roots	(Zloh et al., 2007; Schinkovitz et al., 2008)
57	Dehydrofalcarinol	$C_{17}H_{22}O$	*A. capillaris*	Aerial parts	(Zhao et al., 2014)
			A. ordosica	Aerial parts	(Wang et al., 2020)
			P. sativa	\	(Rawson et al., 2010)
			D. guatemalense	Flowers, leaves, and twigs	(Grant et al., 2020)
			T. procumbens	Roots	(Larque-Garcia et al., 2020)
58	Dehydrofalcarindiol 8-acetate	$C_{19}H_{24}O_3$	*A. cordata*	Roots	(Dang et al., 2005)
59	1,9,16-Heptadecatriene-4,6-diyne-3,8-diol	$C_{17}H_{22}O_2$	*G. koraiensis*	Roots	(Jung et al., 2002)
60	Gymnasterkoreayne C	$C_{19}H_{24}O_3$	*G. koraiensis*	Roots	(Jung et al., 2002)
61	Dehydrofalcarinone	$C_{17}H_{20}O$	*P. sativa*	\	(Rawson et al., 2010)
62	10-Methoxyheptadeca-4,6-diyne-3,9-diol	$C_{18}H_{30}O_3$	*S. macrophylla*	Roots	(Mi et al., 2019)
63	Dihydropanaxacol	$C_{17}H_{28}O_3$	*P. ginseng*	Roots	(Fukuyama et al., 2012; Suzuki et al., 2017)
64	Oploxyne B	$C_{18}H_{30}O_4$	*O. elatus*	Stems	(Yang et al., 2010)
65	8-Hydroxyheptadeca-4,6-diyn-3-yl acetate	$C_{19}H_{30}O_3$	*C. zimmermannii*	Roots	(Baur et al., 2005; Senn et al., 2007)
66	1-Hydroxydihydropanaxacol	$C_{17}H_{28}O_4$	*P. ginseng*	Roots	(Fukuyama et al., 2012)
67	Toonasindiyne A	$C_{17}H_{26}O_2$	*T. sinensis*	Root barks	(Xu et al., 2020)

(*continued on next page*)

Table 1 (*continued*)

No.	Name	Formula	Origin	Part	Reference
			C. pilosula	Roots	(Bailly 2020)
68	Herpecaudene A	$C_{17}H_{26}O_3$	*H. caudigerum*	Fruits	(Feng et al., 2017)
69	Herpecaudene B	$C_{17}H_{26}O_3$	*H. caudigerum*	Fruits	(Feng et al., 2017)
70	Heptadec-8-ene-4,6-diyne-3,10-diol	$C_{17}H_{26}O_2$	*P. stipuleanatus*	Roots	(Tuyen et al., 2018)
70a	(3*R*,8*E*,10*S*)-Heptadec-8-ene-4,6-diyne-3,10-diol	$C_{17}H_{26}O_2$	*S. macrophylla*	Roots	(Mi et al., 2019)
			T. sinensis	Root barks	(Xu et al., 2020)
70b	Panaxjapyne B	$C_{17}H_{26}O_2$	*E. triquetrum*	Aerial parts	(Bouzergoune et al., 2016)
70c	1,2-Dihydropanaxydiol	$C_{17}H_{26}O_2$	*O. horridus*	Root barks	(Resetar et al., 2020)
71	(*E*)-Heptadec-8-ene-4,6-diyne-3,10,11-triol	$C_{17}H_{26}O_3$	*S. macrophylla*	Roots	(Mi et al., 2019)
72	Toonasindiyne F	$C_{17}H_{26}O_3$	*T. sinensis*	Root barks	(Xu et al., 2020)
73	Toonasindiyne C	$C_{17}H_{24}O_2$	*T. sinensis*	Root barks	(Xu et al., 2020)
		$C_{17}H_{24}O_2$	*C. pilosula*	Roots	(Bailly 2020)
74	Sadivaethyne D	$C_{17}H_{26}O_4$	*S. divaricata*	Roots	(Sun et al., 2022)
75	Sadivaethyne C	$C_{17}H_{26}O_4$	*S. divaricata*	Roots	(Sun et al., 2022)
76	1,2-Dihydrofalcarinol	$C_{17}H_{26}O$	*O. horridus*	Inner stem barks	(Cheung et al., 2019)
77	(9*Z*)-1,9-Heptadecadiene-4,6-diyne-3,8,11-triol	$C_{17}H_{26}O_3$	*L. officinale*	Roots	(Zloh et al., 2007)
78	Panaxjapyne A	$C_{17}H_{26}O$	*T. sinensis*	Root barks	(Xu et al., 2020)
79	Oplopandiol	$C_{17}H_{26}O_2$	*O. horridus*	Root barks	(Sun et al., 2010; Resetar et al., 2020)
			O. elatus	Stems	(Yang et al., 2010)
			L. tenuissimum	Roots	(Choi et al., 2016)
80	(3*S*,8*S*)-1,2-Dihydro-11-acetoxy-falcarindiol	$C_{19}H_{28}O_4$	*E. tricuspidatum*	Aerial parts	(Djebara et al., 2019)
81	Sadivaethyne B	$C_{17}H_{26}O_4$	*S. divaricata*	Roots	(Sun et al., 2022)
82	(9*Z*)-Heptadecene-4,6-diyn-1-ol	$C_{17}H_{26}O$	*N. incisum*	Roots	(Blunder et al., 2014)
83	Hederyne A	$C_{17}H_{26}O_3$	*H. rhombea*	Leaves	(Yamazoe et al., 2007)
			O. horridus	Root barks	(Resetar et al., 2020)
84	(9*Z*)-1-Methoxy-9-heptadecene-4,6-diyn-3-ol	$C_{18}H_{26}O_2$	*S. divaricata*	Roots and rhizomes	(Yokosuka et al., 2017)
85	(*Z*)-8-Acetoxy-1-methoxy-3-oxoheptadec-9-ene-4,6-diyne	$C_{20}H_{28}O_4$	*H. rhombea*	Leaves	(Yamazoe et al., 2006)
86	Heptadec-9-ene-4,6-diyne-3,11-diol	$C_{17}H_{26}O_2$	*S. macrophylla*	Roots	(Mi et al., 2019)
87	Cirussuryne C	$C_{17}H_{28}O_3$	*C. japonicum*	Roots	(Lee et al., 2022)
88	Ciryneol C	$C_{17}H_{25}ClO_2$	*C. rhinoceros*	Whole plant	(Yim et al., 2003)
89	Cirussuryne G	$C_{18}H_{26}O_3$	*C. japonicum*	Roots	(Lee et al., 2022)
90	Cirussuryne D	$C_{18}H_{26}O_2$	*C. japonicum*	Roots	(Lee et al., 2022)
91	1,2-Dihydrodendroarboreol B	$C_{17}H_{24}O_2$	*D. guatemalense*	Flowers, leaves, and twigs	(Grant et al., 2020)
			T. procumbens	Aerial parts	(Chen et al., 2008)
92	1,2-Dihydro-16,17-dehydrofalcarinol	$C_{17}H_{24}O$	*D. guatemalense*	Flowers, leaves, and twigs	(Grant et al., 2020)
93	Dendroarboreol A	$C_{17}H_{24}O_2$	*T. procumbens*	Aerial parts	(Chen et al., 2008)
94	Gymnasterkoreayne G	$C_{17}H_{24}O_3$	*G. koraiensis*	Leaves	(Dat et al., 2005)
95	Gymnasterkoreayne E	$C_{17}H_{24}O_3$	*G. koraiensis*	Roots	(Jung et al., 2002)
96	Cirussuryne H	$C_{18}H_{28}O_3$	*C. japonicum*	Roots	(Lee et al., 2022)
97	Dihydrooenanthotoxin	$C_{17}H_{24}O_2$	*O. fistulosa*	Underground parts	(Appendino et al., 2009)
98	Cicutol	$C_{17}H_{22}O$	*Cicuta maculata*	The tuber or seed	(Panter et al., 2011)
99	Cicutoxin	$C_{17}H_{22}O_2$	*O. fistulosa*	Underground parts	(Appendino et al., 2009)
			C. maculata	The tubers or seeds	(Panter et al., 2011)
100	(2*Z*,9*Z*)-Heptadecadiene-4,6-diyn-1-ol	$C_{17}H_{24}O$	*B. longiradiatum*	Whole plant	(Huang et al., 2009)
			N. incisum	Roots	(Blunder et al., 2014)
101	Cirussuryne A	$C_{17}H_{24}O_3$	*C. japonicum*	Roots	(Lee et al., 2022)
102	Cirussuryne F	$C_{18}H_{26}O_3$	*C. japonicum*	Roots	(Lee et al., 2022)

Table 1 (*continued*)

No.	Name	Formula	Origin	Part	Reference
103	Cirussuryne E	$C_{19}H_{26}O_2$	*C. japonicum*	Roots	(Lee et al., 2022)
104	(2*Z*,8*Z*,10*E*)-Heptadecatriene-4,6-diyn-1-ol	$C_{17}H_{22}O$	*B. scorzonerifolium*	Roots	(Liu et al., 2015)
105	(2*Z*,8*Z*,10*E*)-Heptadecatriene-4,6-diyne-1,14-diol	$C_{17}H_{22}O_2$	*B. longiradiatum*	Roots	(Huang et al., 2011)
106	(2*Z*,8*Z*,10*E*)-1-Hydroxyheptadecatriene-4,6-diyn-14-yl acetate	$C_{19}H_{24}O_3$	*B. longiradiatum*	Roots	(Huang et al., 2011)
107	Bupleurynol	$C_{17}H_{22}O$	*B. longiradiatum*	Whole plant	(Huang et al., 2009; Huang et al., 2011)
			B. scorzonerifolium	Roots	(Liu et al., 2015)
108	Acetylbupleurotoxin	$C_{19}H_{24}O_3$	*B. longiradiatum*	Roots	(Huang et al., 2009; Huang et al., 2011)
109	Bupleurotoxin	$C_{17}H_{22}O_2$	*B. longiradiatum*	Whole plant	(Huang et al., 2009; Huang et al., 2011; Zhang et al., 2014)
110	Bupleuronol	$C_{17}H_{20}O_2$	*B. longiradiatum*	Whole plant	(Huang et al., 2009)
111	(2*Z*,8*E*,10*E*)-14*S*-Hydroxyheptadecatriene-4,6-diyn-1-yl acetate	$C_{19}H_{24}O_3$	*B. longiradiatum*	Whole plant	(Huang et al., 2009)
112	(2*Z*,8*E*)-Heptadecadiene-10-oxo-4,6-diyn-1-ol	$C_{17}H_{22}O_2$	*B. chinense*	Roots	(Cao et al., 2020)
113	Oenanthotoxin	$C_{17}H_{22}O_2$	*O. fistulosa*	Underground parts	(Appendino et al., 2009)
			E. platyloba	Aerial parts	(Chianese et al., 2018)
114	Gymnasterkoreayne F	$C_{17}H_{22}O_2$	*G. koraiensis*	Roots	(Jung et al., 2002)
115	Gymnasterkoreayne D	$C_{19}H_{24}O_3$	*G. koraiensis*	Roots	(Jung et al., 2002)
116	(8*E*,15*E*)-Heptadeca-8,15-diene-11,13-diynoic acid	$C_{17}H_{22}O_2$	*A. japonica*	Rhizomes	(Rui and Chou 2022)
117	4,5-Dihydropanaxynol	$C_{17}H_{26}O$	*N. incisum*	Roots	(Blunder et al., 2014)
118	Crithmumdiol	$C_{17}H_{26}O_2$	*N. incisum*	Roots	(Blunder et al., 2014)
119	(2*E*,4*E*,9*Z*)-Heptadecatrien-6-yn-1-yl acetate	$C_{19}H_{28}O_2$	*B. longiradiatum*	Whole plant	(Huang et al., 2009; Huang et al., 2011)
120	(2*E*,4*E*,8*E*,10*E*)-Heptadecatetraen-6-yn-1-yl acetate	$C_{19}H_{26}O_2$	*B. longiradiatum*	Whole plant	(Huang et al., 2009)
121	Panaxacol	$C_{17}H_{26}O_3$	*P. ginseng*	Roots	(Fukuyama et al., 2012)
122	17-Hydroxypanaxacol	$C_{17}H_{26}O_4$	*P. ginseng*	Roots	(Fukuyama et al., 2012)
123	Cirussuryne B	$C_{17}H_{24}O_3$	*C. japonicum*	Roots	(Lee et al., 2022)
124	(2*E*)-10*R*-Tetradecaene-4,6-diyne-1,10,14-triol-1-*O*-*β*-D-glucopyranoside	$C_{20}H_{30}O_8$	*C. tinctorius*	Florets	(He et al., 2011; Baek et al., 2021)
125	(2*E*,8*Z*)-12*R*-Tetradecadiene-4,6-diyne-1,12,14-triol-1-*O*-*β*-D-glucopyranoside	$C_{20}H_{28}O_8$	*C. tinctorius*	Florets	(He et al., 2011)
126	Ritroyne A	$C_{21}H_{30}O_6S$	*E. ritro*	Whole plant	(Li et al., 2019)
127	Coreoside E	$C_{21}H_{30}O_7$	*C. tinctoria*	Fresh buds	(Guo et al., 2017)
128	Coreoside F	$C_{26}H_{38}O_{11}$	*C. tinctoria*	Fresh buds	(Guo et al., 2017)
129	(6*E*,12*E*)-6,12-Tetradecadiene-8,10-diyne-1,3-diol	$C_{14}H_{18}O_2$	*A. japonica*	Rhizomes	(Rui and Chou 2022)
130	(6*E*,12*E*)-1-Acetoxytetradeca-6,12-diene-8,10-diyn-3-ol	$C_{16}H_{20}O_3$	*A. japonica*	Rhizomes	(Rui and Chou 2022)
			A. macrocephala	Rhizomes	(Jeong et al., 2019)
131	Bidensyneoside E	$C_{20}H_{28}O_7$	*L. capitata*	Aerial parts	(Emad et al., 2020)
132	1,3-Diacetoxy-tetradeca-(6*E*,12*E*)-diene-8,10-diyne	$C_{18}H_{22}O_4$	*A. japonica*	Rhizomes	(Rui and Chou 2022)
			A. macrocephala	Rhizomes	(Kim et al., 2018; Jeong et al., 2019)
133	Bidensyneoside F	$C_{23}H_{30}O_{10}$	*L. capitata*	Aerial parts	(Emad et al., 2020)
134	Coreoside A	$C_{25}H_{36}O_{11}$	*C. tinctoria*	Capitula	(Zhang et al., 2013)
135	(6*E*,12*E*)-3-Oxo-tetradeca-6,12-diene-8,10-diyn-1-ol	$C_{14}H_{16}O_2$	*B. pilosa*	Aerial parts	(Wang et al., 2010)
136	Codonopilodiynoside E	$C_{26}H_{38}O_{12}$	*C. pilosula*	Roots	(Jiang et al., 2015)
137	(6*E*,12*E*)-Tetradecadiene-8,10-diyne-	$C_{14}H_{18}O_3$	*B. bipinnata*	Whole plant	(Wang et al., 2013)

(*continued on next page*)

Table 1 (*continued*)

No.	Name	Formula	Origin	Part	Reference
	1,3,14-triol				
137a	(2*E*,8*E*)-Tetradecadiene-4,6-diyne-1,11,14-triol	$C_{14}H_{18}O_3$	*C. tinctorius*	Florets	(He et al., 2011)
138	3-*O*-*β*-D-Glucosyl-tetradeca-(6*E*,12*E*)-diene-8,10-diyne-1,14-diol	$C_{20}H_{28}O_8$	*B. bipinnata*	Whole plant	(Wang et al., 2013)
			B. gardneri	Leaves and stems	(Silva et al., 2015)
			C. tinctoria	Capitula	(Zhang et al., 2013)
139	Coreoside B	$C_{25}H_{36}O_{12}$	*C. tinctoria*	Capitula	(Zhang et al., 2013)
140	(6*E*,12*E*)-3-Oxo-tetradecadiene-8,10-diyne-14-hydroxy-1-*O*-*β*-D-glucopyranoside	$C_{20}H_{26}O_8$	*B. bipinnata*	Whole plant	(Wang et al., 2013)
			B. gardneri	Leaves and stems	(Silva et al., 2015)
141	Cordifolioidyne B	$C_{20}H_{28}O_8$	*C. cordifolioidea*	Roots	(Mei et al., 2008)
			C. tangshen	Roots	(Sun et al., 2016)
			B. chinense	Roots	(Phan et al., 2022)
			C. pilosula	Roots	(He et al., 2014; He et al., 2014; Bailly 2020)
141a	Codonopilodiynoside A	$C_{20}H_{28}O_8$	*C. pilosula*	Roots	(Jiang et al., 2015)
142	Codonopilodiynoside B	$C_{26}H_{38}O_{13}$	*C. pilosula*	Roots	(Jiang et al., 2015)
			C. lanceolata	Roots	(Hu et al., 2018)
143	Coreoside C	$C_{27}H_{38}O_{13}$	*C. tinctoria*	Capitula	(Zhang et al., 2013)
144	(2*E*,8*E*)-12*R*-Tetradecadiene-4,6-diyne-1,12,14-triol-1-*O*-*β*-D-glucopyranoside	$C_{20}H_{28}O_8$	*C. tinctorius*	Florets	(He et al., 2011; Baek et al., 2021)
145	Codonopilodiynoside C	$C_{26}H_{38}O_{13}$	*C. pilosula*	Roots	(Jiang et al., 2015)
146	Cordifolioidyne C	$C_{20}H_{28}O_7$	*C. cordifolioidea*	Roots	(Mei et al., 2008)
147	Codonopilodiynoside F	$C_{26}H_{38}O_{12}$	*C. pilosula*	Roots	(Jiang et al., 2015)
148	Lobetyol	$C_{14}H_{18}O_3$	*P. nummularia*	Callus and hairy root	(Ishimaru et al., 2003)
			C. cordifolioidea	Roots	(Mei et al., 2008)
			L. chinensis	Aerial part	(Yang et al., 2014)
			C. tangshen	Roots	(Sun et al., 2016)
			P. grandiflorus	Roots	(Li 2022)
			B. chinense	Roots	(Phan et al., 2022)
			C. pilosula	Roots	(He et al., 2014; He et al., 2014; Bailly 2020)
149	Lobetyolin	$C_{20}H_{28}O_8$	*P. nummularia*	Callus and hairy roots	(Ishimaru et al., 2003)
			C. cordifolioidea	Roots	(Mei et al., 2008)
			C. tangshen	Roots	(Sun et al., 2016)
			P. grandiflorus	Roots	(Chen et al., 2018; Li 2022)
			C. lanceolata	Roots	(Hu et al., 2018)
			B. chinense	Roots	(Phan et al., 2022)
			C. pilosula	Roots	(He et al., 2014; He et al., 2014; Bailly 2020)
			L. inflata	Roots	(Bálványos et al., 2004)
150	Tangshenyne B	$C_{26}H_{38}O_{13}$	*C. tangshen*	Roots	(Sun et al., 2016)
			C. pilosula	Roots	(Bailly 2020)
151	Lobetyolinin	$C_{26}H_{38}O_{13}$	*P. nummularia*	Callus and hairy roots	(Ishimaru et al., 2003)
			C. tangshen	Roots	(Sun et al., 2016)
			B. chinense	Roots	(Phan et al., 2022)
			C. pilosula	Roots	(He et al., 2014; He et al., 2014; Bailly 2020)
			L. inflata	Roots	(Bálványos et al., 2004)
152	Pratialin B	$C_{32}H_{48}O_{18}$	*P. nummularia*	Callus and hairy roots	(Ishimaru et al., 2003)
			C. pilosula	Roots	(Bailly 2020)
153	Pratialin A	$C_{26}H_{38}O_{12}$	*P. nummularia*	Callus and hairy roots	(Ishimaru et al., 2003)
			C. pilosula	Roots	(Bailly 2020)
154	Tangshenyne A	$C_{20}H_{28}O_9$	*C. tangshen*	Roots	(Sun et al., 2016)

Table 1 (*continued*)

No.	Name	Formula	Origin	Part	Reference
			C. pilosula	Roots	(Bailly 2020)
155	Choushenpilosulyne A	$C_{36}H_{58}O_9$	*C. pilosula*	Roots	(Bailly 2020)
156	*threo*-Tetradeca-2,10-diene-4,6-diyne-1,8,9,14-tetraol	$C_{14}H_{18}O_4$	*C. cordifolioidea*	Roots	(Mei et al., 2008)
156a	(4*E*,12*Z*)-*threo*-Tetradeca-4,12-diene-8,10-diyne-1,6,7,14-tetraol	$C_{14}H_{18}O_4$	*C. lanceolata*	Roots	(Hu et al., 2018)
157	Cordifolioidyne A	$C_{20}H_{28}O_9$	*C. cordifolioidea*	Roots	(Mei et al., 2008)
158	Atractylodemayne A	$C_{19}H_{22}O_3$	*A. macrocephala*	Rhizomes	(Yao and Yang 2014)
159	14-Acetoxy-12-α-methylbutyryltetradeca-(2*E*,8*Z*,10*E*)-triene-4,6-diyn-1-ol	$C_{21}H_{26}O_5$	*A. macrocephala*	Rhizomes	(Yao and Yang 2014)
160	14-Acetoxy-12-senecioyloxytetradeca-(2*E*,8*Z*,10*E*)-triene-4,6-diyn-1-ol	$C_{21}H_{24}O_5$	*A. macrocephala*	Rhizomes	(Yao and Yang 2014)
161	Atractylodemayne F	$C_{20}H_{24}O_5$	*A. macrocephala*	Rhizomes	(Yao and Yang 2014)
162	Atractylodemayne D	$C_{23}H_{28}O_6$	*A. macrocephala*	Rhizomes	(Yao and Yang 2014)
163	Atractylodemayne C	$C_{23}H_{26}O_6$	*A. macrocephala*	Rhizomes	(Yao and Yang 2014)
164	(4*E*,6*E*,12*E*)-Tetradecatriene-8,10-diyn-1-ol	$C_{14}H_{16}O$	*A. japonica*	Rhizomes	(Rui and Chou 2022)
165	(4*E*,6*E*,12*E*)-1-Acetoxytetradecatriene-8,10-diyne	$C_{16}H_{18}O_2$	*A. japonica*	Rhizomes	(Rui and Chou 2022)
166	1-*O*-Feruloyl-(4*E*,6*E*,12*E*)-tetradecatriene-8,10-diyne	$C_{24}H_{24}O_4$	*A. japonica*	Rhizomes	(Rui and Chou 2022)
167	1-*O*-Feruloyl-(4*E*,6*E*,12*E*)-tetradecatriene-8,10-diyne-1,3-diol	$C_{24}H_{24}O_5$	*A. japonica*	Rhizomes	(Rui and Chou 2022)
168	(4*E*,6*E*,12*E*)-Tetradecatriene-8,10-diyne-1,3-diyl diacetate	$C_{18}H_{20}O_4$	*A. lancea*	Rhizomes	(Resch et al., 2001; Jiao et al., 2014)
169	1-*O*-Feruloyl-(4*E*,6*E*,12*E*)-tetradecatriene-8,10-diyne-1,3,14-triol	$C_{24}H_{24}O_5$	*A. japonica*	Rhizomes	(Rui and Chou 2022)
170	Atractylodemayne B	$C_{19}H_{24}O_3$	*A. macrocephala*	Rhizomes	(Yao and Yang 2014)
171	14-α-Methylbutyryltetradeca-(2*E*,8*E*,10*E*)-triene-4,6-diyn-1-ol	$C_{19}H_{24}O_4$	*A. macrocephala*	Rhizomes	(Yao and Yang 2014)
172	14-β-Methylbutyryltetradeca-(2*E*,8*E*,10*E*)-triene-4,6-diyn-1-ol	$C_{19}H_{24}O_4$	*A. macrocephala*	Rhizomes	(Yao and Yang 2014)
173	12-Senecioyloxytetradeca-(2*E*,8*E*,10*E*)-triene-4,6-diyn-1-ol	$C_{19}H_{22}O_4$	*A. macrocephala*	Rhizomes	(Yao and Yang 2014)
174	14-Acetoxy-12-α-methylbutyl-(2*E*,8*E*,10*E*)-triene-4,6-diyn-1-ol	$C_{21}H_{26}O_5$	*A. lancea*	Rhizomes	(Nur et al., 2020)
			A. macrocephala	Rhizomes	(Yao and Yang 2014)
175	14-Acetoxy-12-senecioyloxytetradeca-(2*E*,8*E*,10*E*)-triene-4,6-diyn-1-ol	$C_{21}H_{24}O_5$	*A. lancea*	Rhizomes	(Yao and Yang 2014)
			A. macrocephala	Rhizomes	(Yao and Yang 2014)
176	Atractylodemayne G	$C_{20}H_{24}O_5$	*A. macrocephala*	Rhizomes	(Yao and Yang 2014)
177	14-Acetoxy-12-β-methylbutyl-(2*E*,8*E*,10*E*)-triene-4,6-diyn-1-ol	$C_{21}H_{26}O_5$	*A. lancea*	Rhizomes	(Yao and Yang 2014)
			A. macrocephala	Rhizomes	(Yao and Yang 2014)
178	(2*E*,8*E*,10*E*,12*R*)-Tetradeca-2,8,10-triene-4,6-diyne-1,12,14-triol-1-*O*-β-D-glucopyranoside	$C_{20}H_{26}O_8$	*A. lancea*	Rhizomes	(Xu et al., 2017)
179	(2*E*,8*E*,10*E*,12*R*)-Tetradeca-2,8,10-triene-4,6-diyne-1,12,14-triol-1-*O*-β-D-apiofuranosyl-(1–6)-β-D-glucopyranoside	$C_{25}H_{34}O_{12}$	*A. lancea*	Rhizomes	(Xu et al., 2017)
180	Atractylodemayne E	$C_{23}H_{26}O_6$	*A.*	Rhizomes	(Yao and Yang 2014)

(*continued on next page*)

Table 1 (*continued*)

No.	Name	Formula	Origin	Part	Reference
			macrocephala		
181	(5*R*)-5-Acetoxy-8,10,12-tetradecatriyne-1-*O*-*β*-D-glucopyranoside	$C_{22}H_{30}O_8$	*C. tinctorius*	Florets	(Li et al., 2021)
182	1,3-Dihydroxy-6(*E*)-tetradecene-8,10,12-triyne	$C_{14}H_{16}O_2$	*B. pilosa*	Whole plant; leaves	(Wu et al., 2004; Chen et al., 2020; Chung et al., 2021)
183	3-*β*-D-Glucopyranosyloxy-1-hydroxy-6(*E*)-tetradecene-8,10,12-triyne	$C_{20}H_{26}O_7$	*B. pilosa*	Leaves	(Chien et al., 2009; Wang et al., 2010; Wen-Chin et al., 2013; Wei et al., 2016; Chen et al., 2021; Chung et al., 2021)
184	Artemisiaketone	$C_{14}H_{14}O$	*T. vulgare*	Flowers	(Moricz et al., 2018)
185	(5*R*,6*E*)-tetradecene-8,10,12-triyne-1-ol-5-*O*-β-glucoside	$C_{20}H_{26}O_7$	*C. lanceolata*	Flowers	(Kim et al., 2020)
186	Platetyolin A	$C_{20}H_{26}O_8$	*P. grandiflorus*	Roots	(Chen et al., 2018)
187	1-Acetoxy-3-angeloyloxy-(4*E*,6*Z*)-tetradeca-4,6-diene-8,10,12-triyne	$C_{21}H_{22}O_4$	*L. alpinum*	Sub aerial parts	(Schwaiger et al., 2004)
188	3-*O*-*β*-D-Glucopyranosyloxy-1-hydroxy-(4*E*,6*E*)-tetradecene-8,10,12-triyne	$C_{20}H_{24}O_7$	*E. prostrata*	Aerial parts	(Xi et al., 2014)
189	1-Acetoxy-3-angeloyloxy-(4*E*,6*E*)-tetradeca-4,6-diene-8,10,12-triyne	$C_{21}H_{22}O_4$	*L. alpinum*	Sub aerial parts	(Schwaiger et al., 2004)
190	Tetradeca-1,3-diyne-6,7,8-triol	$C_{14}H_{22}O_3$	*S. macrophylla*	Roots	(Mi et al., 2019)
191	6,7,8,9-Tetraacetoxytetradeca-1,3-diyne	$C_{23}H_{32}O_7$	*S. macrophylla*	Roots	(Mi et al., 2019)
192	Panaxyne	$C_{14}H_{20}O_2$	*P. ginseng*	Roots	(Yang et al., 2008)
193	8-Hydroxy-tetradec-(9*E*)-ene-11,13-diyn-2-one	$C_{14}H_{18}O_2$	*E. pallida*	Roots	(Pellati et al., 2007; Tacchini et al., 2017)
194	Tetradec-(8*Z*)-ene-11,13-diyn-2-one	$C_{14}H_{18}O$	*E. pallida*	Roots	(Pellati et al., 2007; Pellati et al., 2012; Tacchini et al., 2017)
195	(2*Z*,8*Z*)-12*R*-Tetradecadiene-4,6-diyne-1,12,14-triol-1-*O*-*β*-D-glucopyranoside	$C_{20}H_{28}O_8$	*C. tinctorius*	Florets	(He et al., 2011)
196	(2*Z*,8*E*)-12*R*-Tetradecadiene-4,6-diyne-1,12,14-triol-1-*O*-*β*-D-glucopyranoside	$C_{20}H_{28}O_8$	*C. tinctorius*	Florets	(He et al., 2011)
197	Platetyolin B	$C_{20}H_{28}O_8$	*P. grandiflorus*	Roots	(Chen et al., 2018)
198	(2*E*,4*E*,12*Z*)-*N*-Isobutyltetradeca-2,4,12-triene-8,10-diynamide	$C_{18}H_{23}NO$	*C. zawadskii*	Roots	(Rahman et al., 2007)
199	Pilosulyne G	$C_{14}H_{20}O_4$	*C. lanceolata*	Roots	(Hu et al., 2018)
200	Codonopilodiynoside D	$C_{20}H_{30}O_8$	*C. pilosula*	Roots	(Jiang et al., 2015)
201	16-Acetoxy-11-hydroxyoctadec-17-ene-12,14-diynyl acetate	$C_{22}H_{32}O_5$	*C. zimmermannii*	Roots	(Senn et al., 2007)
201	16-Acetoxy-11-hydroxyoctadec-17-ene-12,14-diynyl acetate	$C_{22}H_{32}O_5$	*C. zimmermannii*	Whole plant	(Baur et al., 2005)
202	11,16-Diacetoxyoctadec-17-ene-12,14-diynyl acetate	$C_{24}H_{34}O_6$	*C. zimmermannii*	Roots	(Senn et al., 2007)
203	(8*E*)-Octadeca-1,8-diene-4,6-diyne-3,10-diol	$C_{18}H_{26}O_2$	*P. ginseng*	Roots	(Murata et al., 2017)
203a	Stipudiol	$C_{18}H_{26}O_2$	*C. pilosula*	Roots	(Bailly 2020)
204	Fruticotriol	$C_{18}H_{26}O_3$	*B. fruticosum*	Aerial parts	(Fois et al., 2017)
204a	Oplopantriol C	$C_{18}H_{26}O_3$	*O. horridus*	Root barks	(Resetar et al., 2020)
205	Oplopantriol C 18-acetate	$C_{20}H_{28}O_4$	*O. horridus*	Root barks	(Resetar et al., 2020)
206	Octadeca-1,9-diene-4,6-diyne-3,8,18-triol	$C_{18}H_{26}O_3$	*A. gigas*	Roots	(Choi et al., 2000)
206a	Oplopantriol A	$C_{18}H_{26}O_3$	*C. barteri*	Leaves	(Kraus 2003)
			C. zimmermannii	Roots	(Senn et al., 2007)
			O. horridus	Root barks	(Resetar et al., 2020)
206b	(+)-9(*Z*),17-Octadecadiene-12,14-diyne-1,11,16-triol	$C_{18}H_{26}O_3$	*A. scott-thomsonii*	Sub aerial parts	(Perry et al., 2001)
207	(*Z*)-11,16-Dihydroxyoctadeca-9,17-dien-12,14-diyn-1-yl acetate	$C_{20}H_{28}O_4$	*A. gigas*	Roots	(Choi et al., 2000)
			S. taiwaniana	Leaves	(Kuo et al., 2002)
207a	(9*Z*,11*S*,16*S*)-Octadeca-9,17-diene-12,14-diyne-1,11,16-triol 1-Acetate	$C_{20}H_{28}O_4$	*C. zimmermannii*	Roots	(Senn et al., 2007)

Table 1 (*continued*)

No.	Name	Formula	Origin	Part	Reference
		$C_{20}H_{28}O_4$	*O. horridus*	Root barks	(Sun et al., 2010; Resetar et al., 2020)
207b	(11*R*,16*R*,*Z*)-11,16-Dihydroxyoctadeca-9,17-dien-12,14-diyn-1-yl acetate	$C_{20}H_{28}O_4$	*O. horridus*	inner stem bark	(Tai et al., 2014; Cheung et al., 2019)
207c	(+)-9(*Z*),17-Octadecadiene-12,14-diyne-1,11,16-triol 1-acetate	$C_{20}H_{28}O_4$	*A. scott-thomsonii*	Leaves	(Perry et al., 2001)
208	Homopanaxynol	$C_{18}H_{26}O$	*P. ginseng*	Roots	(Murata et al., 2017)
209	Dendrotrifidiol	$C_{18}H_{26}O_2$	*O. horridus*	Root barks	(Resetar et al., 2020)
210	Dendrotrifidiol 18-acetate	$C_{20}H_{28}O_3$	*O. horridus*	Root barks	(Resetar et al., 2020)
211	*cis*-9,17-Octadecadiene-12,14-diyne-1,16-diol	$C_{18}H_{26}O_2$	*B. fruticosum*	Aerial parts	(Fois et al., 2017)
212	(9*Z*,16*S*)-16-Hydroxyl-9,17-octadecadiene-12,14-diynoic acid	$C_{18}H_{24}O_3$	*D. morbiferus*	Leaves	(Park et al., 2004; Kang et al., 2018)
213	*cis*-16-Oxo-octadeca-9,17-diene-12,14-diyn-1-al	$C_{18}H_{22}O_2$	*P. sativa*	Roots	(Roman et al., 2011)
214	3,8,18-Triacetoxyloctadeca-1,9-diene-4,6-diyne	$C_{24}H_{32}O_6$	*A. gigas*	Roots	(Choi et al., 2000)
215	1-Acetoxymethylfalcarindiol	$C_{24}H_{32}O_6$	*C. barteri*	Leaves	(Kraus 2003)
216	Toonasindiyne B	$C_{18}H_{28}O_3$	*T. sinensis*	Root barks	(Xu et al., 2020)
			C. pilosula	Roots	(Bailly 2020)
217	(3*R*,10*S*,8*E*)-8-Octadecene-4,6-diyne-3,10,18-triol	$C_{18}H_{28}O_3$	*O. horridus*	Root barks	(Resetar et al., 2020)
218	(3*R*,10*S*,8*E*)-8-Octadecene-4,6-diyne-3,10,18-triol 18-acetate	$C_{20}H_{30}O_4$	*O. horridus*	Root barks	(Resetar et al., 2020)
219	Octadec-10-ene-12,14-diyne-1,9,16-triol	$C_{18}H_{28}O_3$	*T. sinensis*	Root barks	(Xu et al., 2020)
220	9,16-Dihydroxyoctadec-10-ene-12,14-diyn-1-yl acetate	$C_{20}H_{30}O_4$	*T. sinensis*	Root barks	(Xu et al., 2020)
221	Toonapolyyne A	$C_{18}H_{28}O_4$	*T. sinensis*	Root barks	(Xu et al., 2020)
222	Toonasindiyne D	$C_{18}H_{26}O_3$	*T. sinensis*	Root barks	(Xu et al., 2020)
			C. pilosula	Roots	(Bailly 2020)
223	Toonasindiyne E	$C_{20}H_{28}O_4$	*T. sinensis*	Root barks	(Xu et al., 2020)
			C. pilosula	Roots	(Bailly 2020)
224	Toonapolyyne C	$C_{18}H_{28}O_2$	*T. sinensis*	Root barks	(Xu et al., 2020)
225	Oplopandiol acetate	$C_{20}H_{30}O_4$	*O. horridus*	Root barks	(Sun et al., 2010; Resetar et al., 2020)
226	Oplopantriol B	$C_{18}H_{28}O_3$	*O. horridus*	Root barks	(Resetar et al., 2020)
227	1-Hydroxyoplopantriol B	$C_{18}H_{28}O_4$	*O. horridus*	Root barks	(Resetar et al., 2020)
228	1-Hydroxyoplopantriol B 18-acetate	$C_{20}H_{30}O_5$	*O. horridus*	Root barks	(Resetar et al., 2020)
229	13,14-Dihydrooropheic acid	$C_{18}H_{24}O_2$	*M. tomentosa*	Leaves and twigs	(Wongsomboon et al., 2021)
230	(-)-(7*R*,8*S*)-Mitrephentosin B	$C_{41}H_{50}O_8$	*M. tomentosa*	Leaves and twigs	(Wongsomboon et al., 2021)
231	(-)-(7*R*,8*S*)-Mitrephentosin A	$C_{39}H_{48}O_7$	*M. tomentosa*	Leaves and twigs	(Wongsomboon et al., 2021)
232	(-)-(7*R*,8*S*)-Mitrephentosin C	$C_{39}H_{48}O_7$	*M. tomentosa*	Leaves and twigs	(Wongsomboon et al., 2021)
233	Oropheic acid	$C_{18}H_{22}O_2$	*M. glabra*	The stem bark	(Li et al., 2009)
			M. tomentosa	Leaves and twigs	(Wongsomboon et al., 2021)
234	Methylooropheate	$C_{19}H_{24}O_2$	*M. glabra*	The stem bark	(Li et al., 2009)
235	(-)-(7*R*,8*S*)-Mitrephentosin E	$C_{41}H_{48}O_8$	*M. tomentosa*	Leaves and twigs	(Wongsomboon et al., 2021)
236	(-)-(7*R*,8*S*)-Mitrephentosin D	$C_{39}H_{46}O_7$	*M. tomentosa*	Leaves and twigs	(Wongsomboon et al., 2021)
237	(2*E*,4*E*,9*Z*)-Octadecatrien-6-yne-1,18-diol	$C_{18}H_{28}O_2$	*B. longiradiatum*	Whole plant	(Huang et al., 2009)
238	(2*E*,4*E*,9*Z*)-1-Hydroxyoctadecatrien-6-yn-18-yl acetate	$C_{20}H_{30}O_3$	*B. longiradiatum*	Whole plant	(Huang et al., 2009)
239	(2*E*,4*E*,9*Z*)-Octadecatrien-6-yne-1,18-diyl diacetate	$C_{22}H_{32}O_4$	*B. longiradiatum*	Whole plant	(Huang et al., 2009; Huang et al., 2011)
240	(2*Z*,9*Z*)-Octadecadiene-4,6-diyne-1,18-diol	$C_{18}H_{26}O_2$	*B. longiradiatum*	Whole plant	(Huang et al., 2009)
241	Octadec-17-ene-9,11-diynoate ethyl	$C_{20}H_{30}O_2$	*O. gore*	The seeds	(Ntumba et al., 2018)

(*continued on next page*)

Table 1 (*continued*)

No.	Name	Formula	Origin	Part	Reference
242	(-)-17-Hydroxy-9,11,13,15-octadecatetraynoic acid/ Minquartynoic acid	$C_{18}H_{20}O_3$	*O. amentacea*	The branches	(Rashid et al., 2001)
243	Minquartynoic acid methyl ester	$C_{19}H_{22}O_3$	*O. amentacea*	The branches	(Rashid et al., 2001)
244	(*S*)-17,18-Dihydroxy-9,11,13,15-octadecatetraynoic acid	$C_{18}H_{20}O_4$	*O. amentacea*	The twigs	(Ito et al., 2001)
245	8-Hydroxy-octadec-13-ene-9,11-diynoate ethyl	$C_{20}H_{30}O_3$	*O. gore*	The seeds	(Ntumba et al., 2018)
246	(-)-(7*R*,8*S*)-Mitrephentosin F	$C_{39}H_{50}O_7$	*M. tomentosa*	Leaves and twigs	(Wongsomboon et al., 2021)
247	8-Hydroxy-octadeca-13,17-diene-9,11-diynoate ethyl	$C_{20}H_{28}O_3$	*O. gore*	The seeds	(Ntumba et al., 2018)
248	Octadeca-9,11,13-triynoic acid	$C_{18}H_{24}O_2$	*M. glabra*	The stem barks	(Li et al., 2009)
249	(*E*)-15,16-Dihydrominquartynoic acid \(*S*)-17-Hydroxy-15*E*-octadecene-9,11,13-triynoic acid	$C_{18}H_{22}O_3$	*O. amentacea*	The dried twigs	(Ito et al., 2001)
250	(8*E*)-Decene-4,6-diyne-1-ol-1-*O*-*β*-D-glucopyranoside	$C_{16}H_{22}O_6$	*C. tinctorius*	Florets	(He et al., 2011; Baek et al., 2021)
251	(8*E*)-Decaene-4,6-diyne-1-*O*-*β*-D-glucopyranosyl-(1–2)-*β*-D-glucopyranoside	$C_{22}H_{32}O_{11}$	*C. morifolium*	Flowers	(Li et al., 2021)
252	(8*E*)-Decaene-4,6-diyne-1-*O*-*β*-D-glucopyranosyl-(1–6)-*β*-D-glucopyranosyl-(1–2)-*β*-D-glucopyranoside	$C_{28}H_{42}O_{16}$	*H. dissectum*	Roots	(Gao et al., 2019)
253	Gymnasterkoreayne A	$C_{10}H_{12}O_2$	*G. koraiensis*	Roots	(Jung et al., 2002; Park et al., 2002)
254	Bidensyneoside A1	$C_{16}H_{22}O_7$	*B. parviflora*	Whole plant	(Wang et al., 2001)
			C. pilosula	Roots	(Bailly 2020)
			L. capitata	Aerial parts	(Emad et al., 2020)
255	6-*O*-Acetylbidensyneoside A1	$C_{18}H_{24}O_8$	*L. capitata*	Aerial parts	(Emad et al., 2020)
256	(*E*,*E*)-Matricarianol	$C_{10}H_{10}O$	*T. angulata*	Roots	(Pan et al., 2006)
257	(2*E*,8*E*)-Decadiene-4,6-diyne-1-*O*-*β*-D-glucopyranoside	$C_{16}H_{20}O_6$	*C. tinctorius*	Florets	(Li et al., 2021)
258	(3*R*,8*E*)-Decene-4,6-diyne-1,3,10-triol	$C_{10}H_{12}O_3$	*B. parviflora*	Whole plant material	(Li et al., 2008)
259	3-Deoxybidensyneoside B	$C_{16}H_{22}O_7$	*B. parviflora*	Whole plant	(Wang et al., 2001)
260	(*E*)-Dec-2-ene-4,6-diyne-1,10-diol-1-O-*β*-D-apiofuranosyl-(1–6)-*β*-D-glucopyranoside	$C_{21}H_{30}O_{11}$	*A. lancea*	Rhizomes	(Xu et al., 2016)
261	(*E*)-Dec-2-ene-4,6-diyne-1,10-diol-1-*O*-*β*-D-glucopyranoside	$C_{16}H_{22}O_7$	*A. lancea*	Rhizomes	(Xu et al., 2016)
262	(2*E*,8*E*)-Deca-2,8-diene-4,6-diyne-1,10-diol-1-*O*-*β*-D-apiofuranosyl-(1–6)-*β*-D-glucopyranoside	$C_{21}H_{28}O_{11}$	*A. lancea*	Rhizomes	(Xu et al., 2016)
263	(2*Z*,8*E*)-Deca-2,8-diene-4,6-diyne-1,10-diol-1-*O*-*β*-D-glucopyranoside	$C_{16}H_{20}O_7$	*A. lancea*	Rhizomes	(Xu et al., 2016)
264	Bidensyneoside C	$C_{16}H_{22}O_8$	*B. parviflora*	Whole plant	(Wang et al., 2001)
			C. pilosula	Roots	(Bailly 2020)
265	(2*E*)-Decaene-4,6-diyne-1-*O*-*β*-D-glucopyranoside	$C_{16}H_{22}O_6$	*C. tinctorius*	Florets	(Li et al., 2021)
266	(8*R*)-Deca-2-*trans*-2-ene-4,6-diyne-1,8-diol	$C_{10}H_{12}O_2$	*T. angulata*	Roots	(Pan et al., 2006)
267	(2*E*,8*R*)-Decene-4,6-diyne-1,8-diol-8-*O*-*β*-D-glucopyranoside	$C_{16}H_{22}O_7$	*A. lancea*	Rhizomes	(Xu et al., 2017)
268	(2*E*,8*R*)-Decene-4,6-diyne-1,8-diol-*O*-di-*β*-D-glucopyranoside	$C_{22}H_{32}O_{12}$	*A. lancea*	Rhizomes	(Xu et al., 2017)
269	(2*E*,8*S*)-Decene-4,6-diyne-1,8-diol-8-*O*-*β*-D-glucopyranoside	$C_{16}H_{22}O_7$	*A. lancea*	Rhizomes	(Xu et al., 2017)
270	Bidenoside C	$C_{16}H_{22}O_6$	*C. tinctorius*	Florets	(He et al., 2011)
			C. tinctorius	Florets	(Baek et al., 2021; Li et al., 2021; Ngo et al., 2021)
			C. lanceolata	Flowers	(Kim et al., 2020)

Table 1 (*continued*)

No.	Name	Formula	Origin	Part	Reference
271	Kamiohnoyneoside B	$C_{22}H_{32}O_{11}$	*C. morifolium*	Flowers	(Kurimoto et al., 2021; Li et al., 2021)
272	(8*Z*)-Decene-4,6-diyne-1-*O*-*β*-D-glucopyranosyl-(1–6)-*β*-D-glucopyranosyl-(1–2)-*β*-D-glucopyranoside	$C_{28}H_{42}O_{16}$	*H. dissectum*	Roots	(Gao et al., 2019)
273	(8*Z*)-8-Decene-4,6-diyn-1-yl 2-*O*-*β*-D-glucopyranuronosyl-*β*-D-glucopyranoside	$C_{22}H_{32}O_{11}$	*C. tinctorius*	Flowers	(Ngo et al., 2021)
274	(8*Z*)-Decene-4,6-diyn-1-ol-1-*O*-*β*-D-glucuronyl-(1′′-2′)-*β*-D-glucopyranoside	$C_{22}H_{30}O_{12}$	*C. tinctorius*	Florets	(He et al., 2011)
275	(8*Z*)-1-[(3-*O*-*β*-D-Glucosyl)-isovaleroyloxy]-8-decene-4,6-diyne	$C_{21}H_{30}O_8$	*C. tinctorius*	Florets	(Li et al., 2021)
276	Bidensyneoside A2	$C_{16}H_{22}O_7$	*B. parviflora*	Whole plant	(Wang et al., 2001)
277	(8*Z*)-Decene-4,6-diyne-1,10-diol-1-*O*-*β*-D-glucopyranoside	$C_{16}H_{22}O_7$	*C. tinctorius*	Florets	(Baek et al., 2021)
278	(8*Z*)-Decene-4,6-diyne-1,3,10-triol	$C_{10}H_{12}O_3$	*A. capillaris*	Aerial parts	(Zhao et al., 2014)
279	(8*Z*)-Decen-1-isovaleroyloxy-4,6-diyne-10-*O*-*β*-D-glucopyranoside	$C_{21}H_{30}O_8$	*C. tinctorius*	Florets	(Li et al., 2021)
280	(2*E*,8*Z*)-Deca-2,8-diene-4,6-diyne-1,10-diol-1-*O*-*β*-D-glucopyranoside	$C_{16}H_{20}O_7$	*A. lancea*	Rhizomes	(Xu et al., 2016)
281	(2*E*,8*Z*)-Deca-2,8-diene-4,6-diyne-1,10-diol-1-*O*-*β*-D-apiofuranosyl-(1–6)-*β*-D-glucopyranoside	$C_{21}H_{28}O_{11}$	*A. lancea*	Rhizomes	(Xu et al., 2017)
282	(2*E*,8*Z*)-Decadiene-4,6-diyne-1-ol-1-*O*-*β*-D-glucopyranoside	$C_{16}H_{20}O_6$	*C. tinctorius*	Florets	(He et al., 2011)
283	Echinacetylene	$C_{11}H_{12}O_3$	*E. purpurea*	Roots	(Chang et al., 2020)
284	(8*S*)-Deca-2-*trans*-2,9-diene-4,6-diyne-1,8-diol	$C_{10}H_{10}O_2$	*T. angulata*	Roots	(Pan et al., 2006)
285	3, 8-Dihydroxydec-9-en-4, 6-yne-1-*O*-*β*-D-glucopyranoside	$C_{16}H_{22}O_8$	*A. monosperma*	Aerial parts	(Stavri et al., 2005)
286	(1,3*R*,8*R*)-Trihydroxydec-9-en-4,6-yne	$C_{10}H_{12}O_3$	*A. monosperma* *L. officinale*	Aerial parts Roots	(Stavri et al., 2005) (Zloh et al., 2007)
287	(1,3*S*,8*S*)-Trihydroxydec-9-en-4,6-yne	$C_{10}H_{12}O_3$	*A. capillaris*	Aerial parts	(Zhao et al., 2014)
288	(3*S*,8*S*)-Dihydroxydec-9-en-4,6-yne	$C_{25}H_{28}O_{11}$	*A. scoparia*	Aerial parts	(Geng et al., 2015)
289	(3*S*,8*S*)-Dihydroxydec-9-en-4,6-yne-1-*O*-(6′-*O*-caffeoyl)-*β*-D-glucopyranoside	$C_{25}H_{28}O_{11}$	*A. scoparia*	Aerial parts	(Geng et al., 2015)
290	4,6-Decadiyne-1-*O*-*β*-D-glucopyranoside	$C_{16}H_{24}O_6$	*C. tinctorius*	Florets	(Li et al., 2021)
291	4,6-Decadiyne-1-*O*-*β*-D–glucopyranosyl-(1–6)-*β*-D-glucopyranosyl-(1–2)-*β*-D-glucopyranoside	$C_{28}H_{44}O_{16}$	*H. dissectum*	Roots	(Gao et al., 2019)
292	(8*S*)-Deca-4,6-diyne-1,8-diol-1-*O*-*β*-D-glucopyranoside	$C_{16}H_{24}O_7$	*C. tinctorius*	Florets	(Baek et al., 2021)
293	(8*S*)-Deca-4,6-diyne-1,8-diol-8-*O*-*β*-D-glucopyranoside	$C_{16}H_{24}O_7$	*C. tinctorius*	Florets	(Baek et al., 2021)
294	(8*S*)-Deca-4,6-diyne-1,8-di-*O*-*β*-D-glucopyranoside	$C_{22}H_{34}O_{12}$	*C. tinctorius*	Flowers	(Ngo et al., 2021)
295	(2*Z*)-Decene-4,6,8-triyne-1-*O*-*β*-D-glucopyranoside	$C_{16}H_{18}O_6$	*C. tinctorius*	Florets	(Li et al., 2021)
296	Dehydromatricaria ester	$C_{11}H_8O_2$	*A. ordosica*	Aerial parts	(Wang et al., 2020)
297	Kamiohnoyneoside A	$C_{22}H_{30}O_{11}$	*C. morifolium*	Flowers	(Kurimoto et al., 2021)
298	Bidensyneoside B	$C_{16}H_{20}O_7$	*B. parviflora* *C. pilosula*	Whole plant Roots	(Wang et al., 2001) (Bailly 2020)
299	(2*S*) (5*E*,11*E*)-Tridecadiene-7,9-diyne-1,2,13-triol	$C_{13}H_{16}O_3$	*B. bipinnata*	Whole plant	(Wang et al., 2013)
300	(12*R*)-Trideca-(2*E*,8*E*)-diene-4,6-diyne-1,14-diol 12-*O*-*β*-D-glucopyranoside	$C_{19}H_{26}O_8$	*B. parviflora*	Whole plant	(Zhu et al., 2021)
301	(3*Z*,5*E*,11*E*)-Tridecatriene-7,9-diynyl 1-*O*-(*E*)-ferulate	$C_{23}H_{22}O_4$	*A. lancea*	Rhizomes	(Resch et al., 2001)
302	(3*Z*,5*E*,11*E*)-3,5,11-Tridecatriene-7,9-diyne 1-*O*-acetate	$C_{15}H_{16}O_2$	*A. lancea*	Rhizomes	(Jiao et al., 2014)

(*continued on next page*)

Table 1 (*continued*)

No.	Name	Formula	Origin	Part	Reference
303	(3*Z*,5*E*,11*E*)-3,5,11-Tridecatriene-7,9-diyne 1,2-diacetate	$C_{17}H_{18}O_4$	*A. lancea*	Rhizomes	(Jiao et al., 2014)
304	(3*E*,5*E*,11*E*)-Tridecatriene-7,9-diyne-1,2,13-triol-2-*O*-*β*-D-glucopyranoside	$C_{19}H_{24}O_8$	*B. frondosa*	Aerial parts	(Le et al., 2015)
305	(2*E*,8*E*,10*E*)-12R-Tridecatriene-4,6-diyne-1,12,13-triol-1-*O*-*β*-D-glucopyranoside	$C_{19}H_{24}O_8$	*C. tinctorius*	Flowers	(He et al., 2011; Ngo et al., 2021)
306	*syn*-(5*E*,11*E*)-3-Acetoxy-4-*O*-(3-methylbutanoyl)-1,5,11-tridecatriene-7,9-diyne-3,4-diol	$C_{20}H_{24}O_4$	*A. lancea*	Rhizomes	(Jiao et al., 2014)
307	(5*E*,11*E*)-1,5,11-Tridecatriene-7,9-diyne 3,4-diacetate	$C_{17}H_{18}O_4$	*A. lancea*	Rhizomes	(Jiao et al., 2014)
308	(1,3*Z*,11*E*)-Tridecatriene-7,9-diyne-5-hydroxyl 6-*O*-*β*-D-glucopyranoside	$C_{19}H_{24}O_7$	*A. lancea*	Rhizomes	(Ji et al., 2010)
309	*erythro*-(1,3*Z*,11*E*)-Tridecatriene-7,9-diyne-5,6-diyl diacetate	$C_{17}H_{18}O_4$	*A. lancea*	Rhizomes	(Resch et al., 2001)
310	1,2-Dihydroxy-(5*E*)-tridecene-7,9,11-triyne	$C_{13}H_{14}O_2$	*B. pilosa*	Leaves	(Chen et al., 2020; Chen et al., 2021; Chung et al., 2021)
311	2-*β*-D-Glucopyranosyloxy-1-hydroxy-5(*E*)-tridecene-7,9,11-triyne	$C_{19}H_{24}O_7$	*B. pilosa*	Leaves	(Chien et al., 2009; Wen-Chin et al., 2013; Wei et al., 2016; Chen et al., 2020; Chen et al., 2021; Chung et al., 2021)
312	(+)-*threo*-(5*E*)-Trideca-1,5-diene-7,9,11-triyne-3,4-diol	$C_{13}H_{12}O_2$	*A. annua*	Aerial parts	(Ivarsen et al., 2014)
313	(5*E*)-Trideca-1,5-diene-7,9,11-triyne-3,4-diol-4-*O*-*β*-D-glucopyranoside	$C_{19}H_{22}O_7$	*B. bipinnata*	Whole plant	(Hu et al., 2018)
			E. prostrata	Aerial parts	(Xi et al., 2014)
313a	(3*S*,4*S*,5*E*)-Trideca-1,5-diene-7,9,11-triyne-3,4-diol-4-*O*-*β*-glucopyranoside	$C_{19}H_{22}O_7$	*C. lanceolata*	Flowers	(Kim et al., 2020)
314	*erythro*-(5*E*)-1,5-Didecadiene-7,9,11-triyne 3,4-diacetate	$C_{17}H_{16}O_4$	*P. tatsienense*	Stems and leaves	(Lu et al., 2020)
315	(2*S*,3*Z*,11*E*)-Decadiene-5,7,9-triyne-1,2-diol	$C_{13}H_{12}O_2$	*C. tinctoria*	Capitula	(Liu et al., 2015)
316	(2*S*,3*E*,11*E*)-Decadiene-5,7,9-triyne-1,2-diol	$C_{13}H_{12}O_2$	*C. tinctoria*	Capitula	(Liu et al., 2015)
317	(3*E*,11*E*)-Tridecadiene-6,8,10-triyne-1,2,13-triol	$C_{13}H_{12}O_3$	*B. bipinnata*	Whole plant	(Wang et al., 2013)
318	(3*E*,11*E*)-Tridecadiene-6,8,10-triyne-1,13-diol-2-*O*-*β*-D-glucopyranoside	$C_{19}H_{22}O_8$	*B. bipinnata*	Whole plant	(Wang et al., 2013)
			B. gardneri	Leaves and stems	(Silva et al., 2015)
319	2-*O*-*β*-D-Glucosyl-13-acetyltrideca-(3*E*,11*E*)-diene-5,7,9-triyn-1-ol	$C_{21}H_{24}O_9$	*B. gardneri*	Leaves and stems	(Silva et al., 2015)
320	(10*S*)-Tridecane-2*E*,12-diene-4,6,8-triyne-1-ol 10-*O*-*β*-D-glucopyranoside	$C_{19}H_{22}O_7$	*B. parviflora*	Whole plant	(Zhu et al., 2021)
321	1,2-Dihydroxytrideca-5,7,9,11-tetrayne	$C_{13}H_{12}O_2$	*B. pilosa*	Whole plant	(Wu et al., 2004; Chung et al., 2021)
322	2-*β*-D-Glucopyranosyloxy-1-hydroxytrideca-5,7,9,11-tetrayne	$C_{19}H_{22}O_7$	*B. pilosa*	Leaves	(Chien et al., 2009; Wen-Chin et al., 2013; Wei et al., 2016; Chen et al., 2020; Chung et al., 2021)
323	2-*O*-*β*-D-Glucosyltridec-(11*E*)-ene-3,5,7,9-tetrayne-1,13-diol	$C_{19}H_{20}O_8$	*B. gardneri*	Leaves and stems	(Silva et al., 2015)
324	2-*O*-*β*-D-Glucosyl-13-acetyltridec-(11*E*)-ene-3,5,7,9-tetrayn-1-ol	$C_{21}H_{22}O_9$	*B. gardneri*	Leaves and stems	(Silva et al., 2015)
325	(*R*)-1,2-Dihydroxytrideca-3,5,7,9,11-pentayne	$C_{13}H_8O_2$	*B. pilosa*	Aerial parts	(Tobinaga et al., 2009)
326	2-*β*-D-Glycopyrasyloxy-1-hydroxytrideca-3,5,7,9,11-pentayne	$C_{19}H_{18}O_7$	*B. pilosa*	Aerial parts	(Tobinaga et al., 2009; Chen et al., 2021)
327	(5*E*)-1,5-Tridecadiene-7,9-diyne-3,4,12-triol	$C_{13}H_{16}O_3$	*B. pilosa*	Aerial parts	(Wang et al., 2010)
328	(2*R*,3*E*,11*Z*)-Decadiene-5,7,9-triyne-1,2-diol	$C_{13}H_{12}O_2$	*C. tinctoria*	Capitula	(Liu et al., 2015)
329	Pentaynene	$C_{13}H_6$	*A. maritima*	Roots	(AbouZid et al., 2007)
330	8-Acetoxycentellynol	$C_{17}H_{22}O_3$	*C. asiatica*	Leaves	(Randriamampionona et al., 2007)
331	(*E*)-Pentadeca-1,9-diene-4,6-diyne-3,8-	$C_{15}H_{20}O_2$	*D. carota*	Roots	(Ahmed et al., 2005)

Table 1 (*continued*)

No.	Name	Formula	Origin	Part	Reference
	diol				
332	Cofalcarinol D	$C_{15}H_{18}O$	*D. guatemalense*	Flowers, leaves, and twigs	(Grant et al., 2020)
333	(3*R*,*Z*)-3-Hydroxypentadeca-1,9,14-triene-4,6-diyn-8-yl acetate	$C_{17}H_{20}O_3$	*D. guatemalense*	Flowers, leaves, and twigs	(Grant et al., 2020)
333a	(*Z*)-8-Acetoxy-3-hydroxy-1,9,14-pentadecatriene-4,6-diyne	$C_{17}H_{20}O_3$	*H. annuus*	Seeds of sunflower	(Shigemori et al., 2011)
334	(*Z*)-3,8-Dihydroxy-1,9,14-pentadecatriene-4,6-diyne	$C_{15}H_{18}O_2$	*H. annuus*	Seeds of sunflower	(Shigemori et al., 2011)
335	(3*R*,8*S*,*Z*)-Pentadeca-1,9,14-triene-4,6-diyne-3,8-diol	$C_{15}H_{20}O_2$	*D. guatemalense*	Flowers, leaves, and twigs	(Grant et al., 2020)
336	(*Z*)-3,8-Diacetoxy-1,9,14-pentadecatriene-4,6-diyne	$C_{19}H_{22}O_4$	*H. annuus*	Seeds of sunflower	(Shigemori et al., 2011)
337	Saikodiyne A	$C_{15}H_{20}O_2$	*B. chinense*	Roots	(Liu et al., 2017)
338	(2*Z*,9*Z*)-Pentadecadiene-4,6-diyn-1-ol	$C_{15}H_{20}O$	*B. longiradiatum*	Roots	(Huang et al., 2011)
339	Saikodiyne F	$C_{15}H_{20}O_2$	*B. chinense*	Roots	(Liu et al., 2017)
340	(2*Z*,8*Z*,10*E*)-Pentadecatriene-4,6-diyn-1-ol	$C_{15}H_{18}O$	*B. scorzonerifolium*	Roots	(Liu et al., 2015)
341	(2*Z*,8*E*,10*E*)-Pentadecatriene-4,6-diyn-1-ol	$C_{15}H_{18}O$	*B. longiradiatum*	Roots	(Huang et al., 2009; Huang et al., 2011)
			B. scorzonerifolium	Roots	(Liu et al., 2015)
342	8-Hydroxy-pentadeca-(9*E*,13*Z*)-dien-11-yn-2-one	$C_{15}H_{22}O_2$	*E. pallida*	Roots	(Pellati et al., 2006; Pellati et al., 2007; Pellati et al., 2012; Tacchini et al., 2017)
343	Pentadeca-(9*E*,13*Z*)-dien-11-yne-2,8-dione	$C_{15}H_{20}O_2$	*E. pallida*	Roots	(Pellati et al., 2006; Pellati et al., 2007; Pellati et al., 2012; Tacchini et al., 2017)
344	Pentadeca-(8*Z*,13*Z*)-dien-11-yn-2-one	$C_{15}H_{22}O$	*E. pallida*	Roots	(Pellati et al., 2006; Pellati et al., 2007; Pellati et al., 2012; Tacchini et al., 2017)
345	8-Hydroxy-pentadec-(9*E*)-ene-11,13-diyn-2-one	$C_{15}H_{20}O_2$	*E. pallida*	Roots	(Pellati et al., 2006; Pellati et al., 2007; Pellati et al., 2012; Tacchini et al., 2017)
346	Pentadec-(9*E*)-ene-11,13-diyne-2,8-dione	$C_{15}H_{18}O_2$	*E. pallida*	Roots	(Pellati et al., 2006; Pellati et al., 2007; Pellati et al., 2012)
347	Pentadec-(8*Z*)-ene-11,13-diyn-2-one	$C_{15}H_{20}O$	*E. pallida*	Roots	(Pellati et al., 2006; Pellati et al., 2007; Pellati et al., 2012)
348	Saikodiyne E	$C_{15}H_{22}O_2$	*B. chinense*	Roots	(Liu et al., 2017)
349	(*Z*)-3-Hydroxy-9,14-pentadecatriene-4,6-diyne	$C_{15}H_{20}O$	*H. annuus*	Seeds of sunflower	(Shigemori et al., 2011)
350	Saikodiyne D	$C_{15}H_{20}O_2$	*B. chinense*	Roots	(Liu et al., 2017)
351	Nona-3,5-diyne	C_9H_{12}	*S. tenuifolium*	Roots	(Chauhan et al., 2012)
352	Nona-3,5-diyn-2-ol	$C_9H_{12}O$	*S. tenuifolium*	Roots	(Chauhan et al., 2012)
353	Nona-3,5-diyn-2-one	$C_9H_{10}O$	*S. tenuifolium*	Roots	(Chauhan et al., 2012)
354	Nona-4,6-diyn-3-ol	$C_9H_{12}O$	*S. tenuifolium*	Roots	(Chauhan et al., 2012)
355	Nona-4,6-diyn-3-one	$C_9H_{10}O$	*S. tenuifolium*	Roots	(Chauhan et al., 2012)
356	Sadivaethyne A	$C_{12}H_{16}O_5$	*S. divaricata*	Roots	(Sun et al., 2022)
357	Cofalcarinol C	$C_{16}H_{22}O_2$	*D. guatemalense*	Flowers, leaves, and twigs	(Grant et al., 2020)
358	Cofalcarinol B	$C_{16}H_{20}O_2$	*D. guatemalense*	Flowers, leaves, and twigs	(Grant et al., 2020)
359	Cofalcarinol A	$C_{16}H_{20}O$	*D. guatemalense*	Flowers, leaves, and twigs	(Grant et al., 2020)
360	Eprostrata I	$C_{17}H_{22}O_7$	*E. prostrata*	Stems	(Meng et al., 2019)
361	Echinalkamide	$C_{22}H_{31}NO_7$	*E. purpurea*	Roots	(Chang et al., 2020)
362	Yuccifolol (nonadeca-1,11-diene-4,6,8-triyne-3,10-diol)	$C_{19}H_{24}O_2$	*E. yuccifolium*	Aerial parts	(Ayoub et al., 2006)
363	Aciphyllal	$C_{34}H_{42}O_5$	*A. scott-thomsonii*	Sub aerial parts	(Perry et al., 2001)

(*continued on next page*)

Table 1 (*continued*)

No.	Name	Formula	Origin	Part	Reference
364	Pontica epoxide	$C_{13}H_{10}O$	*T. vulgare*	Flowers	(Moricz et al., 2018)
364a	Pontica epoxide	$C_{13}H_{10}O$	*A. annua*	Aerial parts	(Zhai and Zhong 2010; Ivarsen et al., 2014)
365	Panaxydol	$C_{17}H_{24}O_2$	*N. ternata*	Aerial parts	(Nakagawa et al., 2004)
			P. ginseng	Roots	(Washida and Kitanaka 2003; Liu et al., 2007; Yang et al., 2008; Qian et al., 2009; Herrmann et al., 2013; Suzuki et al., 2017)
			O. horridus	Root barks	(Resetar et al., 2020)
			P. quinquefolius	Roots	(Baranska et al., 2006; Christensen et al., 2006)
			D. carota	Roots	(Purup et al., 2009)
			P. quinquefolius	Roots	(Wang et al., 2010)
			P. sativa	Roots	(Roman et al., 2011)
366	Homopanaxydol	$C_{18}H_{26}O_2$	*P. ginseng*	Roots	(Murata et al., 2017)
367	Ginsenoyne A	$C_{17}H_{22}O_2$	*P. ginseng*	Roots	(Yang et al., 2008)
368	9-Epoxyfalcarindiol	$C_{17}H_{24}O_3$	*F. campestris*	Roots	(Dall'Acqua et al., 2010)
			N. incisum	Roots	(Blunder et al., 2014)
			O. fistulosa	Underground parts	(Appendino et al., 2009)
369	*trans*-Epoxytriquetrol	$C_{17}H_{24}O_3$	*E. triquetrum*	Aerial parts	(Bouzergoune et al., 2016)
370	α-Hexy-3-(6-hydroxy-2,4-ocadiynyl) oxiranemethanol	$C_{17}H_{26}O_3$	*S. macrophylla*	Roots	(Mi et al., 2019)
371	Oploxyne A	$C_{17}H_{26}O_3$	*O. elatus*	Stems	(Yang et al., 2010)
372	Ginsenoyne D	$C_{17}H_{26}O_2$	*P. ginseng*	Roots	(Fukuyama et al., 2012)
373	(9*R*,10*S*)-Epoxyheptadeca-4,6-diyn-3-one	$C_{17}H_{24}O_2$	*P. ginseng*	Roots	(Lee et al., 2004)
			O. horridus	Root barks	(Resetar et al., 2020)
374	(9*R*,10*S*)-Epoxy-16-heptadecene-4,6-diyn-3-one	$C_{17}H_{22}O_2$	*O. horridus*	Root barks	(Resetar et al., 2020)
375	1-Methoxy-(9*R*,10*S*)-epoxyheptadeca-4,6-diyn-3-one	$C_{18}H_{26}O_3$	*P. ginseng*	Roots	(Lee et al., 2004)
376	(*Z*)-8-Acetoxyl-1,2-epoxy-9,14-pentadecatriene-4,6-diyne	$C_{17}H_{18}O_4$	*H. annuus*	Seeds of sunflower	(Shigemori et al., 2011)
377	(*Z*)-8-Acetoxy-1,2-epoxy-3-oxoheptadec-9-ene-4,6-diyne	$C_{19}H_{24}O_4$	*H. rhombea*	Leaves	(Yamazoe et al., 2006)
378	Gymnasterkoreayne B	$C_{17}H_{22}O_2$	*G. koraiensis*	The plant material	(Butler et al., 2013)
378a	(5*S*,*Z*)-1-(3-methyloxiran-2-yl) tetradeca-6,13-diene-1,3-diyn-5-ol	$C_{17}H_{22}O_2$	*G. koraiensis*	Roots	(Jung et al., 2002; Park et al., 2002)
379	19-(2-furyl)nonadec-5-ynoic acid	$C_{21}H_{32}O_3$	*P. evecta*	Roots	(Kanokmedhakul et al., 2006)
380	Notopolyenol A	$C_{17}H_{20}O_2$	*N. incisum*	Roots and rhizomes	(Zheng et al., 2019)
381	(1*Z*)-Atractylodin	$C_{13}H_{10}O$	*A. lancea*	Rhizomes	(Jiao et al., 2014)
382	1-(2-Furanyl)-7-nonene-3,5-diyne 1,2-diacetate	$C_{17}H_{16}O_5$	*A. lancea*	Rhizomes	(Jiao et al., 2014)
383	(1*Z*)-Atractylodinol	$C_{13}H_{10}O_2$	*A. lancea*	Rhizomes	(Resch et al., 2001; Jiang et al., 2015)
384	(1*Z*)-Acetylatractylodinol	$C_{15}H_{12}O_3$	*A. lancea*	Rhizomes	(Resch et al., 2001)
385	19-(2-Furyl)nonadeca-5,7-diynoic acid	$C_{23}H_{32}O_3$	*P. evecta*	Roots	(Resch et al., 2001)
386	1-(2- furyl)pentacosa-7,9-diyne	$C_{29}H_{46}O$	*P. evecta*	Roots	(Kanokmedhakul et al., 2006)
387	Panaxfurayne A	$C_{23}H_{32}O_{12}$	*P. ginseng*	Roots	(Lee et al., 2009)
388	Panaxfurayne B	$C_{23}H_{32}O_{12}$	*P. ginseng*	Roots	(Lee et al., 2009)
389	2-[(1*E*,8*E*)-Deca-1,8-diene-4,6-diyn-1-yl]tetrahydrofuran	$C_{14}H_{16}O$	*C. cordifolioidea*	Roots	(Mei et al., 2008)
390	3,4-Dihydrovernoniyne-4-*O*-β-glucoside	$C_{18}H_{20}O_8$	*V. scorpioides*	Aerial parts	(Pollo et al., 2018)
391	4-β-Hydroxy-3,4-dihydrovernoniyne	$C_{12}H_{10}O_3$	*V. scorpioides*	Leaves	(Pollo et al., 2013)
392	5-Octa-2,4,6-triynyl-furan-2(5H)-one	$C_{12}H_8O_2$	*V. scorpioides*	Flowers and leave	(Buskuhl et al., 2009)
392a	Vernoniyne	$C_{12}H_8O_2$	*V. scorpioides*	Leaves	(Klein et al., 2013; Pollo et al., 2013)
393	8′-Hydroxy-3,4-dihydrovernoniyne	$C_{12}H_{10}O_3$	*V. scorpioides*	Leaves	(Klein et al., 2013; Pollo et al., 2013)
394	3,4-Dihydrovernoniyne-8′-*O*-β-glucoside	$C_{18}H_{20}O_8$	*V. scorpioides*	Leaves	(Pollo et al., 2013)
395	1′,8′-Dihydroxy-3,4-dihydrovernoniyne	$C_{12}H_{10}O_4$	*V. scorpioides*	Leaves	(Pollo et al., 2013)
396	4,8′-Dihydroxy-3,4-dihydrovernoniyne	$C_{12}H_{10}O_4$	*V. scorpioides*	Leaves	(Pollo et al., 2013)

Table 1 (*continued*)

No.	Name	Formula	Origin	Part	Reference
397	4-*β*-Hydroxy-3,4-dihydrovernoniyne-8′-*O*-*β*-glucoside	$C_{18}H_{20}O_9$	*V. scorpioides*	Leaves	(Pollo et al., 2013)
398	8′-Hydroxy-3,4-dihydrovernoniyne-4-*O*-*β*-glucoside	$C_{18}H_{20}O_9$	*V. scorpioides*	Leaves	(Pollo et al., 2013)
399	Junipic acid	$C_8H_6O_2S$	*E. ritro*	Whole plant	(Li et al., 2019)
400	Atracthioenyneside B	$C_{17}H_{22}O_8S$	*A. lancea*	Rhizomes	(Feng et al., 2018)
401	4-(5-(Penta-1,3-diyn-1-yl)thiophen-2-yl)but-3-yne-1,2-diol	$C_{13}H_{10}O_2S$	*A. repens*	Roots	(Quintana et al., 2008)
			E. ritro	Whole plant	(Li et al., 2019)
			E. transiliensis	Roots	(Nakano et al., 2011)
			E. prostrata	Aerial parts	(Xi et al., 2014)
402	3′-Chloro-1′-(5-penta-1,3-diyn-1-yl-2-thienyl)-but-2′-yn-4′-ol	$C_{13}H_9ClOS$	*A. repens*	Roots	(Quintana et al., 2008)
403	4′-Chloro-1′-(5-penta-1,3-diyn-1-yl-2-thienyl)-but-2′-yn-3′-ol	$C_{13}H_9ClOS$	*A. repens*	Roots	(Quintana et al., 2008)
404	Echinopsacetylene B	$C_{31}H_{40}O_3S$	*E. transiliensis*	Roots	(Nakano et al., 2011)
405	(*E*)-1-[5-(Hept-5-ene-1,3-diynyl)-2-thienyl]ethan-1,2-diol	$C_{13}H_{12}O_2S$	*L. carthamoides*	Roots	(Chobot et al., 2006)
406	Atracthioenyneside A	$C_{19}H_{26}O_8S$	*A. lancea*	Rhizomes	(Feng et al., 2018)
407	5′-Methyl-1′-(5-prop-1-yn-1-yl-2-thienyl)-hexa-2′,4′-diyn-6′-yl acetate	$C_{16}H_{14}O_3S$	*A. repens*	Roots	(Quintana et al., 2008)
408	Thiarubrine A diol	$C_{13}H_{10}O_2S_2$	*A. maritima*	Roots	(AbouZid et al., 2007)
409	Thiarubrine A	$C_{13}H_8S_2$	*A. maritima*	Roots	(AbouZid et al., 2007)
410	(3*R*,5*S*)-5-(Hydroxymethyl)-3-(tetradec-13-en-5-yn-1-yl) dihydrofuran-2(3H)-one	$C_{19}H_{30}O_3$	*P. debilis*	Roots	(Panthama et al., 2010)
411	9,10-Dihydrooropheolide	$C_{21}H_{28}O_3$	*M. glabra*	The stem bark	(Li et al., 2009)
412	Oropheolide	$C_{21}H_{26}O_3$	*M. glabra*	The stem bark	(Li et al., 2009)
413	Debilisone B	$C_{25}H_{40}O_4$	*P. debilis*	Roots	(Panthama et al., 2010)
414	Saccopetrin A	$C_{25}H_{42}O_3$	*P. debilis*	Roots	(Panthama et al., 2010)
415	Debilisone A	$C_{25}H_{40}O_3$	*P. debilis*	Roots	(Panthama et al., 2010)
416	Debilisone C	$C_{25}H_{38}O_3$	*P. debilis*	Roots	(Panthama et al., 2010)
417	Debilisone D	$C_{25}H_{36}O_3$	*P. debilis*	Roots	(Panthama et al., 2010)
418	Debilisone E	$C_{25}H_{36}O_3$	*P. debilis*	Roots	(Panthama et al., 2010)
419	Longifolione A	$C_{25}H_{38}O_3$	*E. longifolia*	Roots	(Wang et al., 2017)
420	Debilisone F	$C_{27}H_{42}O_3$	*P. debilis*	Roots	(Panthama et al., 2010)
421	Longifolione C	$C_{27}H_{42}O_3$	*E. longifolia*	Roots	(Wang et al., 2017)
422	Longifolione B	$C_{27}H_{40}O_3$	*E. longifolia*	Roots	(Wang et al., 2017)
423	Longifolione E	$C_{29}H_{46}O_3$	*E. longifolia*	Roots	(Wang et al., 2017)
424	Longifolione D	$C_{29}H_{44}O_3$	*E. longifolia*	Roots	(Wang et al., 2017)
425	Echinophorin C	$C_{12}H_{10}O_2$	*E. cinerea*	Aerial parts	(Jelodarian et al., 2017)
426	Echinophorin A	$C_{14}H_{14}O_2$	*E. cinerea*	Aerial parts	(Jelodarian et al., 2017)
			E. platyloba	Aerial parts	(Chianese et al., 2018)
427	Echinophorin B	$C_{14}H_{12}O_2$	*E. cinerea*	Aerial parts	(Jelodarian et al., 2017)
			E. platyloba	Aerial parts	(Chianese et al., 2018)
428	Echinophorin D	$C_{14}H_{10}O_2$	*E. platyloba*	Aerial parts	(Chianese et al., 2018)
429	Ichthyothereol	$C_{14}H_{14}O_2$	*P. tatsienense*	Stems and leaves	(Lu et al., 2020)
430	Icthyothereol acetate	$C_{17}H_{18}O_3$	*B. pilosa*	Whole plant	(Chen et al., 2021)
431	Codojavanyol	$C_{14}H_{18}O_3$	*B. chinense*	Roots	(Phan et al., 2022)
432	Isolobetyol	$C_{14}H_{20}O_4$	*P. grandiflorus*	Roots	(Li 2022)
433	9-(Tetrahydropyran-2-yl)–non-*trans*-8-en-4,6-yn-l-ol	$C_{14}H_{18}O_2$	*C. tangshen*	Roots	(Sun et al., 2016)
434	(2*E*,8*E*)-9-(Tetrahydro-2H-pyran-2-yl) nona-2,8-diene-4,6-diyn-1-ol	$C_{14}H_{16}O_2$	*C. cordifolioidea*	Roots	(Mei et al., 2008)
			C. tangshen	Roots	(Sun et al., 2016)
			B. chinense	Roots	(Phan et al., 2022)
435	Codonopilodiynoside G	$C_{26}H_{38}O_{12}$	*C. pilosula*	Roots	(Jiang et al., 2015)
436	Artemisidiyne A	$C_{14}H_{16}O_4$	*A. lactiflora*	Aerial parts	(Xiao et al., 2014)
437	*o*-Hydroxycapillene	$C_{12}H_{10}O$	*A. ordosica*	Aerial parts	(Wang et al., 2020)
438	1-Phenyl-hepta-1,3,5-triyne	$C_{13}H_8$	*B. pilosa*	Aerial parts	(Wang et al., 2010; Chen et al., 2020; Chung et al., 2021)
439	4-Chloro-2-(hepta-1,3,5-triyn-1-yl)-	$C_{13}H_7ClO$	*H. aureonitens*	Aerial parts	(Ziaratnia et al., 2009)

(*continued on next page*)

Table 1 (*continued*)

No.	Name	Formula	Origin	Part	Reference
	phenol				
440	7-Phenyl-hepta-2,4,6-triyn-2-ol	$C_{13}H_8O$	*B. pilosa*	Aerial parts	(Wang et al., 2010)
441	7-Phenyl-2-heptene-4,6-diyn-1-ol	$C_{13}H_{10}O$	*B. pilosa*	Aerial parts	(Wang et al., 2010)
			C. tinctoria	Capitula	(Liu et al., 2015)
442	7-Phenyl-hepta-4,6-diyn-2-ol	$C_{13}H_{12}O$	*B. pilosa*	Aerial parts	(Wang et al., 2010)
443	7-Phenyl-hepta-4,6-diyne-1,2-diol	$C_{13}H_{12}O_2$	*B. pilosa*	Aerial parts	(Wang et al., 2010)
444	Arteordoyn B	$C_{13}H_{12}O_3$	*A. ordosica*	Aerial parts	(Wang et al., 2020)
445	Arctic acid	$C_{12}H_8O_2S_2$	*E. ritro*	Whole plant	(Li et al., 2019)
446	Arctinol A	$C_{12}H_{10}OS_2$	*E. ritro*	Whole plant	(Li et al., 2019)
447	Arctinal	$C_{12}H_8OS_2$	*E. ritro*	Whole plant	(Li et al., 2019)
448	Arctinol B	$C_{13}H_{12}O_2S_2$	*E. ritro*	Whole plant	(Li et al., 2019)
449	4-(5′-Methyl-[2,2′-bithiophen]-5-yl)but-3-yn-1-ol	$C_{13}H_{12}OS_2$	*E. ritro*	Whole plant	(Li et al., 2019)
450	4-([2,2′-Bithiophen]-5-yl)but-3-yn-1-ol	$C_{12}H_{10}OS_2$	*E. ritro*	Whole plant	(Li et al., 2019)
451	5′-Isovaleryloxymethyl-5-(4-isovaleryloxy-but-1-ynyl)-2,2′-bithiophene	$C_{23}H_{28}O_4S_2$	*E. prostrata*	Aerial parts	(Xi et al., 2014)
452	4-([2,2′-Bithiophen]-5-yl) but-3-yne-1,2-diol	$C_{12}H_{10}O_2S_2$	*E. ritro*	Whole plant	(Li et al., 2019)
453	5′-(3,4-Dihydroxybut-1-yn-1-yl)-[2,2′-bithiophene]-5-carboxylic acid	$C_{13}H_{10}O_4S_2$	*E. ritro*	Whole plant	(Li et al., 2019)
454	5′-(3,4-Dihydroxybut-1-yn-1-yl)-[2,2′-bithiophene]-5-carbaldehyde	$C_{13}H_{10}O_3S_2$	*E. ritro*	Whole plant	(Li et al., 2019)
455	5-(But-3-yne-1,2-diol)-5′-hydroxymethyl-2,2′-bithiophene	$C_{13}H_{12}O_3S_2$	*E. prostrata*	Aerial parts	(Xi et al., 2014)
456	Thiarubrine A epoxide	$C_{13}H_8OS_2$	*A. maritima*	Roots	(Quintana et al., 2008)
457	3′-(5-Penta-1,3-diynylthiophen-2-ylethynyl)-oxirane	$C_{13}H_8OS$	*A. repens*	Roots	(Quintana et al., 2008)
458	5-(2-Phenylethynyl)-2-thiophene methanol	$C_{13}H_{10}OS$	*B. pilosa*	Aerial parts	(Wang et al., 2010)
459	5-(2-Phenylethynyl)-2-β-glucosylmethyl-thiophene	$C_{19}H_{20}O_6S$	*B. pilosa*	Aerial parts	(Wang et al., 2010)
460	(*Z*)-1,6-Dioxaspiro[4.4]non-3-ene	$C_{13}H_{12}O_2$	*C. indicum*	Flowers	(Liu et al., 2011)
461	(*E*)-1,6-Dioxas-piro[4.4]non-3-ene	$C_{13}H_{12}O_2$	*C. indicum*	Flowers	(Liu et al., 2011)
462	Dendrazawayne A	$C_{14}H_{14}O_3$	*C. zawadskii*	Roots	(Rahman et al., 2007)
463	Tonghaosu	$C_{13}H_{12}O_2$	*M. chamomilla*	Flower heads	(Avula et al., 2014; Avonto et al., 2017)
464	Dendrazawayne B	$C_{14}H_{14}O_3$	*C. zawadskii*	Roots	(Rahman et al., 2007)
465	*trans*-2-(2,4-Hexadiynylidene)-1,6-dioxaspiro[4.5]dec-3-ene	$C_{14}H_{14}O_2$	*T. vulgare*	Flowers	(Moricz et al., 2018)
466	*cis*-2-(2,4-Hexadiynylidene)-1,6-dioxaspiro[4.5]dec-3-ene	$C_{14}H_{14}O_2$	*T. vulgare*	Flowers	(Moricz et al., 2018)
467	*cis*-Spiroketalenolether polyyne	$C_{14}H_{14}O_2$	*C. indicum*	Flowers	(Liu et al., 2011)
468	Chrysindin A	$C_{13}H_{12}O_2$	*C. indicum*	Flowers	(Liu et al., 2011)
469	2-(Hexa-2,4-diyn-1-ylidene)-1,6-dioxaspiro[4.5]decane	$C_{14}H_{16}O_2$	*C. zawadskii*	Roots	(Rahman et al., 2007)
470	2-(Hexa-2,4-diyn-1-ylidene)-1,6-dioxaspiro[4.5]decan-8-ol	$C_{14}H_{16}O_3$	*C. zawadskii*	Roots	(Rahman et al., 2007)
471	(+)-(3*S*,4*S*,5*R*)-(*E*)-4-Hydroxyl-3-isovaleroyloxy-2-(*hexa*-2,4-diynyliden)-1,6-dioxaspiro[4, 5]decane	$C_{19}H_{24}O_5$	*C. indicum*	Flowers	(Liu et al., 2011)
472	(−)-(3*S*,4*S*,5*R*)-(*E*)-3,4-Diacetoxy-2-(*hexa*-2,4-diynyliden)-1,6-dioxa-spiro [4, 5]decane	$C_{18}H_{20}O_6$	*C. indicum*	Flowers	(Liu et al., 2011)
473	Chrysindin C	$C_{16}H_{18}O_5$	*C. indicum*	Flowers	(Liu et al., 2011)
474	Chrysindin D	$C_{14}H_{16}O_4$	*C. indicum*	Flowers	(Liu et al., 2011)
475	Artemiselenol C	$C_{14}H_{16}O_5$	*A. selengensis*	Whole plant	(Wang et al., 2016)
476	Artemiselenol B	$C_{19}H_{24}O_6$	*A. selengensis*	Whole plant	(Wang et al., 2016)
477	(+)-(3*S*,4*S*,5*R*,8*S*)-(*E*)-8-Acetoxy-4-hydroxyl-3-isovaleroyloxy-2-(*hexa*-2,4-diynyliden)-1,6-dioxaspiro[4, 5]decane	$C_{21}H_{26}O_7$	*C. indicum*	Flowers	(Liu et al., 2011)
478	Artemiselenol A	$C_{19}H_{23}ClO_5$	*A. selengensis*	Whole plant	(Wang et al., 2016)
479	Carlina oxide	$C_{13}H_{10}O$	*C. acaulis*	Roots	(Herrmann et al., 2011; Strzemski et al., 2019)

Table 1 (*continued*)

No.	Name	Formula	Origin	Part	Reference
480	Ester 21-(2-furyl)heneicosa-14,16-diyne-19-(2-furyl)nonadeca-5,7-diynoate	$C_{48}H_{66}O_4$	*P. evecta*	Roots	(Kanokmedhakul et al., 2006)
481	Chrysindin B	$C_{13}H_{12}O_3$	*C. indicum*	Flowers	(Zhang et al., 2013)
482	2-(2,4-Hexadiynylidene)-3,4-epoxy-1,6-dioxaspiro-[4.5]-decane	$C_{14}H_{14}O_3$	*T. vulgare*	Flowers	(Moricz et al., 2018)
483	Notoincisol C	$C_{27}H_{32}O_4$	*N. incisum*	Roots and rhizomes	(Liu et al., 2014)
484	Notoincisol B	$C_{27}H_{32}O_4$	*N. incisum*	Roots and rhizomes	(Liu et al., 2014)
485	Echinopsacetylene A	$C_{25}H_{16}OS_4$	*E. transiliensis*	Roots	(Nakano et al., 2011)

[a] The compound with a letter (a, b, c, or d) in the compound number represents a different configurational isomer of the compound.

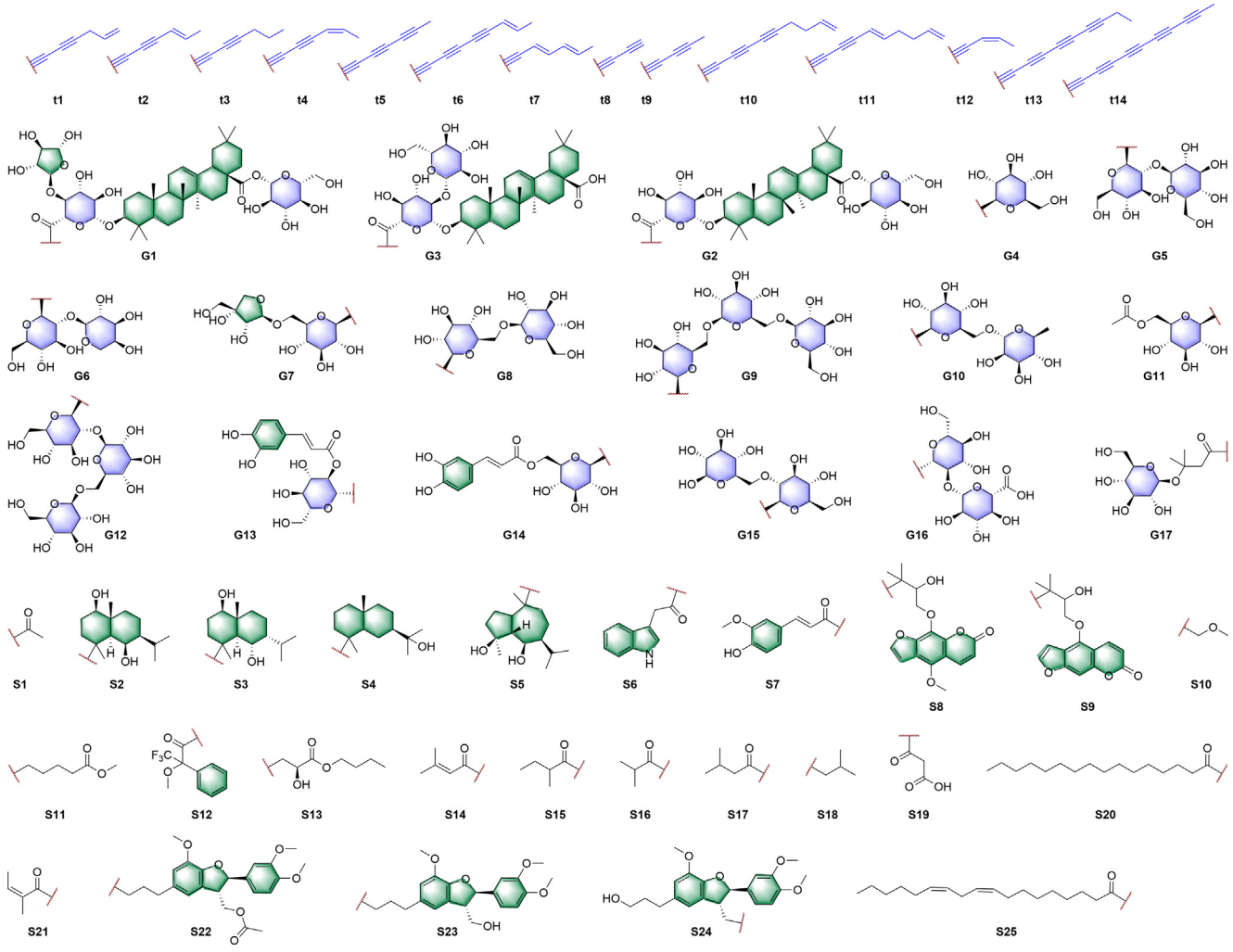

Fig. 1 The acetylenic terminal types of polyacetylenic phytochemicals and the glycosyl, acyl and ether substituents.

ilies, among which, 251 and 113 polyacetylenoids, were obtained from plants of the top 2 families, Compositae (45 species) and Apiaceae (34 species), respectively.

2.1.1. C_{17} polyacetylenoids

C_{17} polyacetylenoids (Fig. 2), such as falcarinol (**19**) and falcarindiol (**20**), are the most common linear polyacetylenoids that have ever been discovered from terrestrial medicinal

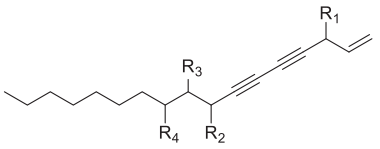

1 R_1 = α-OH, R_2 = β-OH, R_3 = R_4 = H
2 R_1 = OS_1, R_2 = OH, R_3 = R_4 = H
3 R_1 = OH, R_2 = OH, R_3 = OH, R_4 = Cl
4 R_1 = α-OH, R_2 = H, R_3 = OH, R_4 = α-Cl
5 R_1 = α-OH, R_2 = H, R_3 = α-OH, R_4 = α-OG_1
6 R_1 = α-OH, R_2 = H, R_3 = α-OH, R_4 = α-OG_2
7 R_1 = α-OH, R_2 = H, R_3 = α-OH, R_4 = α-OG_3
8 R_1 = β-OH, R_2 = H, R_3 = α-OH, R_4 = α-OH
9 R_1 = β-OH, R_2 = H, R_3 = α-OH, R_4 = α-OCH_3
10 R_1 = α-OS_1, R_2 = H, R_3 = OS_1, R_4 = α-OS_1

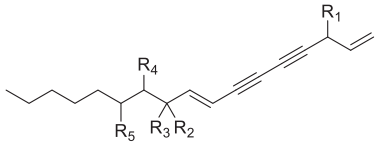

12 R_1 = OH, R_2 = OH, R_3 = R_4 = R_5 = H
13 R_1 = OH, R_2 = OOH, R_3 = R_4 = R_5 = H
14 R_1 = α-OH, R_2 = OH, R_3 = R_4 = R_5 = H
15 R_1 = β-OH, R_2 = OH, R_3 = R_4 = R_5 = H
16 R_1 = β-OH, R_2 = β-OH, R_3 = α-H, R_4 = R_5 = H
17 R_1 = β-OH, R_2 = R_3 = O, R_4 = R_5 = H
18 R_1 = OH, R_2 = OCH_3, R_3 = H, R_4 = OS_{11}, R_5 = OH

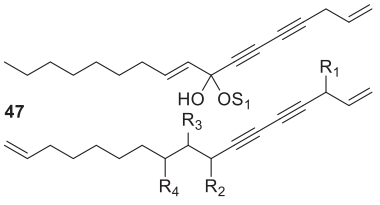

49 R_1 = α-OH, R_2 = α-OH, R_3 = R_4 = H
50 R_1 = α-OH, R_2 = β-OH, R_3 = R_4 = H
51 R_1 = β-OH, R_2 = H, R_3 = α-OH, R_4 = α-OH

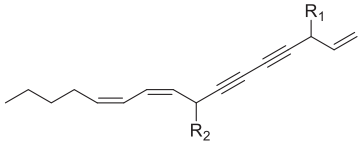

52 R_1 = OH, R_2 = H
53 R_1 = α-OH, R_2 = α-OH

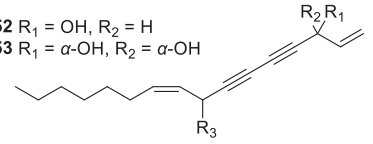

55 R_1 = H, R_2 = β-H, R_3 = β-OH
56 R_1 = R_3 = OH, R_2 = H
56a R_1 = R_3 = α-OH, R_2 = β-H
57 R_1 = α-OH, R_2 = β-H, R_3 = H
58 R_1 = α-OH, R_2 = β-H, R_3 = OS_1
59 R_1 = β-OH, R_2 = α-H, R_3 = β-OH
60 R_1 = β-OS_1, R_2 = α-H, R_3 = β-OH
61 R_1 = R_2 = O, R_3 = H

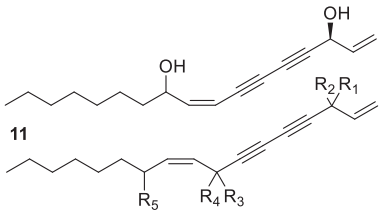

19 R_1 = OH, R_2 = R_3 = R_4 = R_5 = H
19a R_1 = α-OH, R_2 = R_3 = R_4 = R_5 = H
20 R_1 = R_3 = OH, R_2 = R_4 = R_5 = H
20a R_1 = OH, R_3 = β-OH, R_2 = R_4 = R_5 = H
20b R_1 = α-OH, R_3 = β-OH, R_2 = R_4 = R_5 = H
20c R_1 = R_3 = β-OH, R_2 = R_4 = R_5 = H
21 R_1 = α-OH, R_3 = β-OS_1, R_2 = R_4 = R_5 = H
22 R_1 = α-OH, R_3 = β-OCH_3, R_2 = R_4 = R_5 = H
23 R_1 = α-OH, R_3 = OS_1, R_2 = R_4 = R_5 = H
24 R_1 = α-OH, R_3 = β-OS_2, R_2 = R_4 = R_5 = H
25 R_1 = α-OH, R_3 = β-OS_3, R_2 = R_4 = R_5 = H
26 R_1 = α-OH, R_3 = β-OS_4, R_2 = R_4 = R_5 = H
27 R_1 = α-OH, R_3 = β-OS_5, R_2 = R_4 = R_5 = H
28 R_1 = α-OH, R_3 = β-OS_6, R_2 = R_4 = R_5 = H
29 R_1 = α-OH, R_3 = β-OS_7, R_2 = R_4 = R_5 = H
30 R_1 = α-OH, R_3 = α-OS_8, R_2 = R_4 = R_5 = H
31 R_1 = α-OH, R_3 = α-OS_9, R_2 = R_4 = R_5 = H
32 R_1 = OS_1, R_3 = α-OH, R_2 = R_4 = R_5 = H
33 R_1 = α-OS_2, R_3 = α-OH, R_2 = R_4 = R_5 = H
34 R_1 = α-OS_3, R_3 = α-OH, R_2 = R_4 = R_5 = H
35 R_1 = α-OS_4, R_3 = β-OH, R_2 = R_4 = R_5 = H
36 R_1 = α-OS_5, R_3 = β-OH, R_2 = R_4 = R_5 = H
37 R_1 = α-OS_8, R_3 = α-OH, R_2 = R_4 = R_5 = H
38 R_1 = α-OS_9, R_3 = α-OH, R_2 = R_4 = R_5 = H
39 R_1 = α-COOH, R_3 = α-OH, R_2 = R_4 = R_5 = H
40 R_1 = R_3 = β-OS_1, R_2 = R_4 = R_5 = H
41 R_1 = R_3 = β-OH, R_5 = OH, R_2 = R_4 = H
42 R_1 = R_3 = β-OH, R_5 = OS_1, R_2 = R_4 = H
43 R_1 = R_2 = O, R_3 = R_4 = R_5 = H
44 R_1 = R_2 = O, R_3 = R_5 = H, R_4 = OH
45 R_1 = R_2 = O, R_3 = R_5 = H, R_4 = β-OS_1
46 R_1 = R_2 = O, R_3 = R_4 = O, R_5 = H

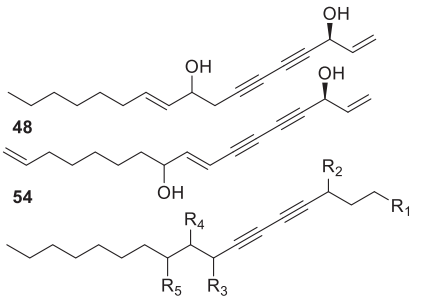

62 R_1 = H, R_2 = OH, R_3 = H, R_4 = OH, R_5 = OCH_3
63 R_1 = H, R_2 = β-OH, R_3 = H, R_4 = R_5 = α-OH
64 R_1 = H, R_2 = R_3 = β-OH, R_4 = α-OH, R_5 = α-OCH_3
65 R_1 = H, R_2 = OS_1, R_3 = OH, R_4 = R_5 = H
66 R_1 = R_2 = OH, R_3 = H, R_4 = R_5 = α-OH

Fig. 2 Chemical structures of the linear C_{17}-polyacetylenoids.

plants (Hansen and Boll 1986). A hepta-4,6-diyne moiety is normally embedded in their polyacetylenic terminals, whose styles include mainly **t1**, **t3**, **t4**, **t5**, **t6** and **t7**. C_{17} Polyacetylenoids are widely distributed in plants of Apiaceae (eg. *Notopterygium incisum*), Araliaceae (eg. *Panax ginseng*) and Compositae families. There were few glycosylated C_{17} polyacetylenoids except baisanqisaponins A–C (**5**–**7**), which have been isolated from *Panax japonicus* (Araliaceae) by Liu *et al* (Liu et al., 2016).

2.1.2. C_{14} polyacetylenoids

Lobetyol (**148**), lobetyolin (**149**), lobetyolinin (**151**) and cordifolioidyne B (**141**) are the representative C_{14} polyacetylenoids originated from terrestrial medicinal plants,

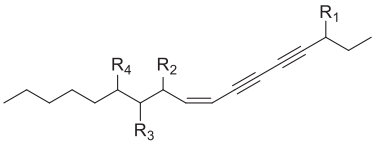

67 R_1 = β-OH, R_2 = α-OH, R_3 = R_4 = H
68 R_1 = R_3 = R_4 = α-OH, R_2 = H
69 R_1 = α-OH, R_2 = H, R_3 = R_4 = β-OH

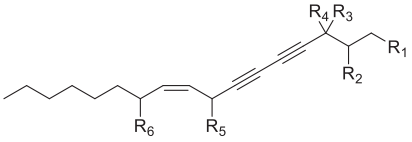

76 R_1 = R_2 = R_4 = R_5 = R_6 = H, R_3 = OH
77 R_1 = R_2 = R_4 = H, R_3 = R_5 = R_6 = OH
78 R_1 = R_2 = R_4 = R_5 = R_6 = H, R_3 = β-OH
79 R_1 = R_2 = R_4 = R_6 = H, R_3 = R_5 = β-OH
80 R_1 = R_2 = R_4 = H, R_3 = R_5 = β-OH, R_6 = OS_1
81 R_1 = OH, R_2 = R_3 = R_5 = β-OH, R_4 = R_6 = H
82 R_1 = OH, R_2 = R_3 = R_4 = R_5 = R_6 = H
83 R_1 = OH, R_3 = β-OH, R_2 = R_4 = R_6 = H, R_5 = β-OH
84 R_1 = OCH_3, R_3 = R_4 = O, R_2 = R_5 = R_6 = H
85 R_1 = OCH_3, R_2 = R_6 = H, R_3 = R_4 = O, R_5 = β-OS_1

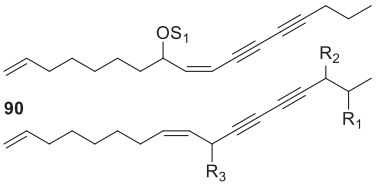

90

92 R_1 = H, R_2 = OH, R_3 = H
93 R_1 = H, R_2 = R_3 = β-OH
94 R_1 = R_2 = *erythro*-OH, R_3 = β-OH
95 R_1 = R_2 = *threo*-OH, R_3 = β-OH

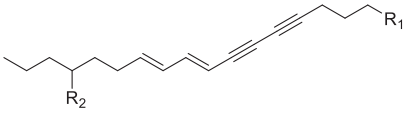

97 R_1 = OH, R_2 = α-OH

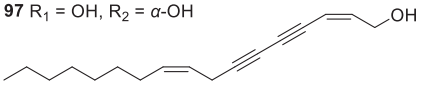

100

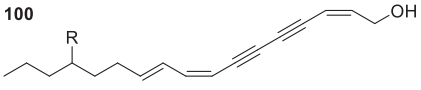

104 R = H
105 R = OH
106 R = OS_1

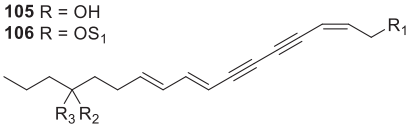

107 R_1 = OH, R_2 = R_3 = H
108 R_1 = OH, R_2 = H, R_3 = α-OS_1
109 R_1 = OH, R_2 = H, R_3 = β-OH
110 R_1 = OH, R_2 = R_3 = O
111 R_1 = OS_1, R_2 = H, R_3 = β-OH

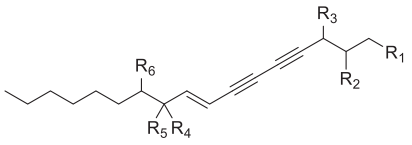

70 R_1 = R_2 = H, R_3 = R_4 = OH, R_5 = R_6 = H
70a R_1 = R_2 = H, R_3 = R_4 = α-OH, R_5 = R_6 = H
70b R_1 = R_2 = H, R_3 = β-OH, R_4 = OH, R_5 = R_6 = H
70c R_1 = R_2 = H, R_3 = α-OH, R_4 = β-OH, R_5 = R_6 = H
71 R_1 = R_2 = H, R_3 = OH, R_4 = β-OH, R_5 = H, R_6 = OH
72 R_1 = R_2 = H, R_3 = β-OH, R_4 = OOH, R_5 = R_6 = H
73 R_1 = R_2 = H, R_3 = β-OH, R_4 = R_5 = O, R_6 = H
74 R_1 = OH, R_2 = R_3 = R_4 = α-OH, R_5 = R_6 = H
75 R_1 = OH, R_2 = R_3 = β-OH, R_4 = α-OH, R_5 = R_6 = H

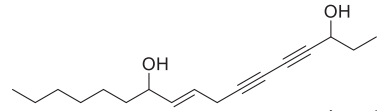

86

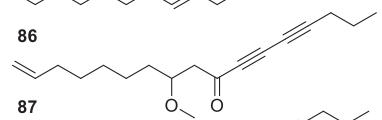

87

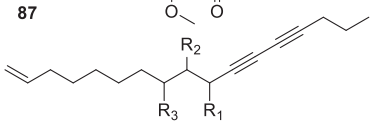

88 R_1 = β-OH, R_2 = α-OH, R_3 = β-Cl
89 R_1 = α-OCH_3, R_2 = β-OH, R_3 = β-OH

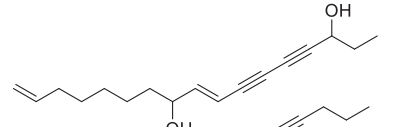

91

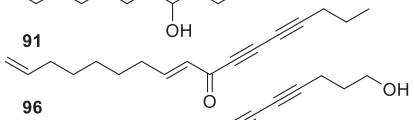

96

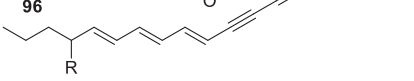

98 R = H
99 R = α-OH

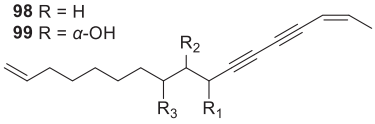

101 R_1 = α-OH, R_2 = β-OH, R_3 = β-OH
102 R_1 = β-OH, R_2 = α-OH, R_3 = α-OCH_3
103 R_1 = α-OCH_3, R_2 = α-OH, R_3 = β-OH

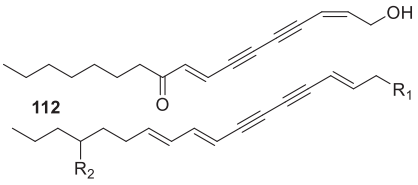

112

113 R_1 = OH, R_2 = β-OH

Fig. 2 (*continued*)

whose polyacetylenic terminals are grouped into the styles of **t2**, **t5**, **t8** and **t4**. The C_{14} polyacetylenoids are extremely abundant in Compositae (eg. *Atractylodes macrocephala*) and Campanulaceae (eg. *Codonopsis pilosula*) species. Unlike C_{17} polyacetylenoids, nearly half of the known C_{14} polyacetylenoids (Fig. 3) are glycosylated.

2.1.3. C_{18} polyacetylenoids

Similar as C_{17} linear polyacetylenoids, the polyacetylenic terminal styles of C_{18} linear polyacetylenoids are mainly **t1**, **t3**, **t11**, **t12**, **t8** and **t14**, featuring with a same hepta-4,6-diyne moiety as C_{17} polyacetylenoids. Till now, C_{18} polyacetylenoids were most frequently isolated from Araliaceae plants, such

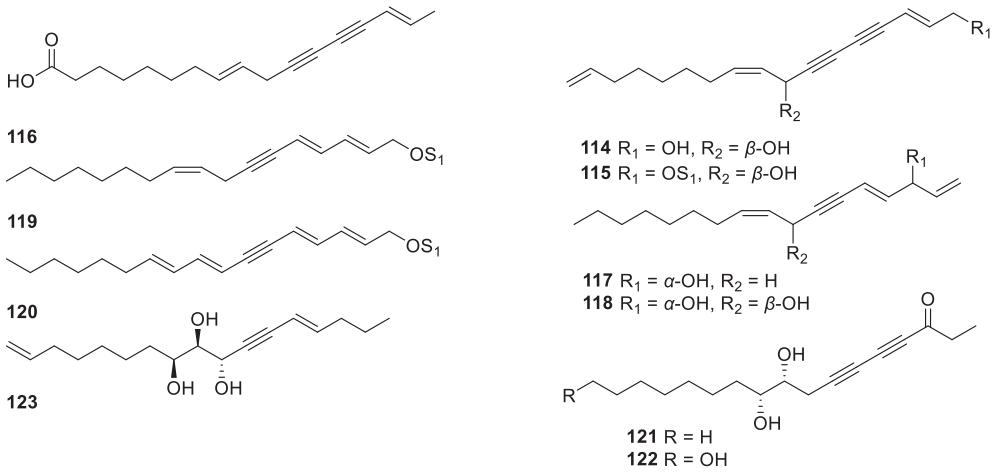

Fig. 2 (*continued*)

as *Oplopanax horridus*. In the last two decades, no glycosylated C_{18} polyacetylenoids (Fig. 4) have been isolated from terrestrial medicinal plants.

2.1.4. C_{10} polyacetylenoids

Deca-4,6-diyne is the basic skeleton of C_{10} linear polyacetylenoids, as exemplified by bidensyneosides A1 (**254**), B (**298**) and C (**264**), that have been isolated from terrestrial medicinal plants in the last two decades. As shown in Fig. 5, the styles of polyacetylenic terminals of C_{10} linear polyacetylenoids are mainly **t2**, **t4**, **t3** and **t1**. Most of the C_{10} linear polyacetylenoids are glycosylated at C-1, C-8 or C-10 of the skeleton, and C-10 glycosylated C_{10} linear polyacetylenoids are the most common ones. In the last two decades, C_{10} polyacetylenoids have been mostly afforded by Compositae plants, such as *Carthamus tinctorius*.

2.1.5. C_{13} polyacetylenoids

The polyacetylenic terminal styles of C_{13} linear polyacetylenoids are mainly **t2**, **t3**, **t5**, and **t6**. As shown in Fig. 6, the structural frameworks of C_{13} linear polyacetylenoids are quite diverse, including the classic 4,6-diyne moiety, the hepta-2,4,6-triayne and the non-2-ene-4,6,8-triyne. Nearly half of the known C_{13} linear polyacetylenoids are glycosylated at the C-1, C-12, or C-13 of the skeleton. Notably, C_{13} linear polyacetylenoids have only been discovered from Compositae plants, mostly from the *Bidens* and *Atractylodes* species.

2.1.6. C_{15} polyacetylenoids

As shown in Fig. 7, more than twenty unglycosylated C_{15} polyacetylenoids, with polyacetylenic terminal styles of **t1**, **t3**, **t4**, **t9**, and **t13**, have been isolated from Compositae and Apiaceae plants in the last twenty years.

2.1.7. Other linear polyacetylenoids

In addition to the above linear polyacetylenoids, there were more than 10 linear polyacetylenoids with other carbon chains of C_9, C_{11}, C_{16}, C_{19}, and C_{34} isolated from terrestrial medicinal plants in the last two decades. Among them (Fig. 8), five C_9 linear polyacetylenoids came from *Selinum tenuifolium* (Chauhan et al., 2012), three C_{16} polyacetylenoids originated from *Desmanthodium* (Grant et al., 2020), while a C_{19} polyacetylenoid (yuccifolol, **362**) was isolated from *Eryngium yuccifolium* (Ayoub et al., 2006). Notably, aciphyllal (**363**) isolated from a New Zealand plant *Aciphylla scott-thomsonii* with a chain length of C_{33}, was a linear polyacetylenoid with the longest carbon chain ever found in terrestrial medicinal plants (Perry et al., 2001).(See Fig. 8).

2.2. Cyclic polyacetylenoids

2.2.1. Monocyclic polyacetylenoids

Monocyclic polyacetylenoids are those cyclic polyacetylenoids with one oxygen or sulfur heterocycle, or a carbon ring system in their structures, possessing a chain length of C_8–C_{29}. Till now, there are oxirane, furan or α-furanone, thiofuran, pyran or α-pyrone, cyclopentanone and benzene rings that have ever been reported to be existied in the monocyclic polyacetylenoids.

In those polyacetylenoids with an orian ring in their structures, the expoxidation always occurs between C-9 and C-10, occasionally between C-10 and C-11 (**364**), between C-2 and C-3 (**378**), or between C-1 and C-2 (**376** and **377**). They all possess a hepta-4,6-diyne moiety at the polyacetylenic terminal. And the majority of monocyclic polyacetylenoids is C_{17} polyacetylenoid, followed by C_{13}, C_{15} and C_{18} polyacetylenoids, mainly obtained from the plants of Apiaceae, Araliaceae (eg. *Panax ginseng*), Compositae and Meliaceae.

Furan or α-furanone-type monocyclic polyacetylenoids, with chain lengths of $C_{11–14}$, C_{17}, C_{19}, C_{21}, C_{25}, C_{27} and C_{29}, were isolated from species of *Panax ginseng*, *Vernonia scorpioides*, *Atractylodes lancea*, *Codonopsis cordifolioidea*, *Notopterygium incisum*, *Polyalthia debilis*, *Mitrephora glabra* and *Eurycoma longifolia*. Most of them contain a hepta-4,6-diyne or a heptyl-2,4,6-triyne moiety at their polyacetylenic terminals. For example, notopolyenol A (**380**) may be derived from falcarindiol by C-8,11 epoxidation in view of the biogenetic pathway (Zheng et al., 2019).

Further, in the last two decades, nine thiofuran-type monocyclic polyacetylenoids (Fig. 9), exemplified by 4-(5-(penta-1,3-diyn-1-yl)thiophen-2-yl)but-3-yne-1,2-diol (**401**), have been isolated from Compositae plants including *Echinops ritro*,

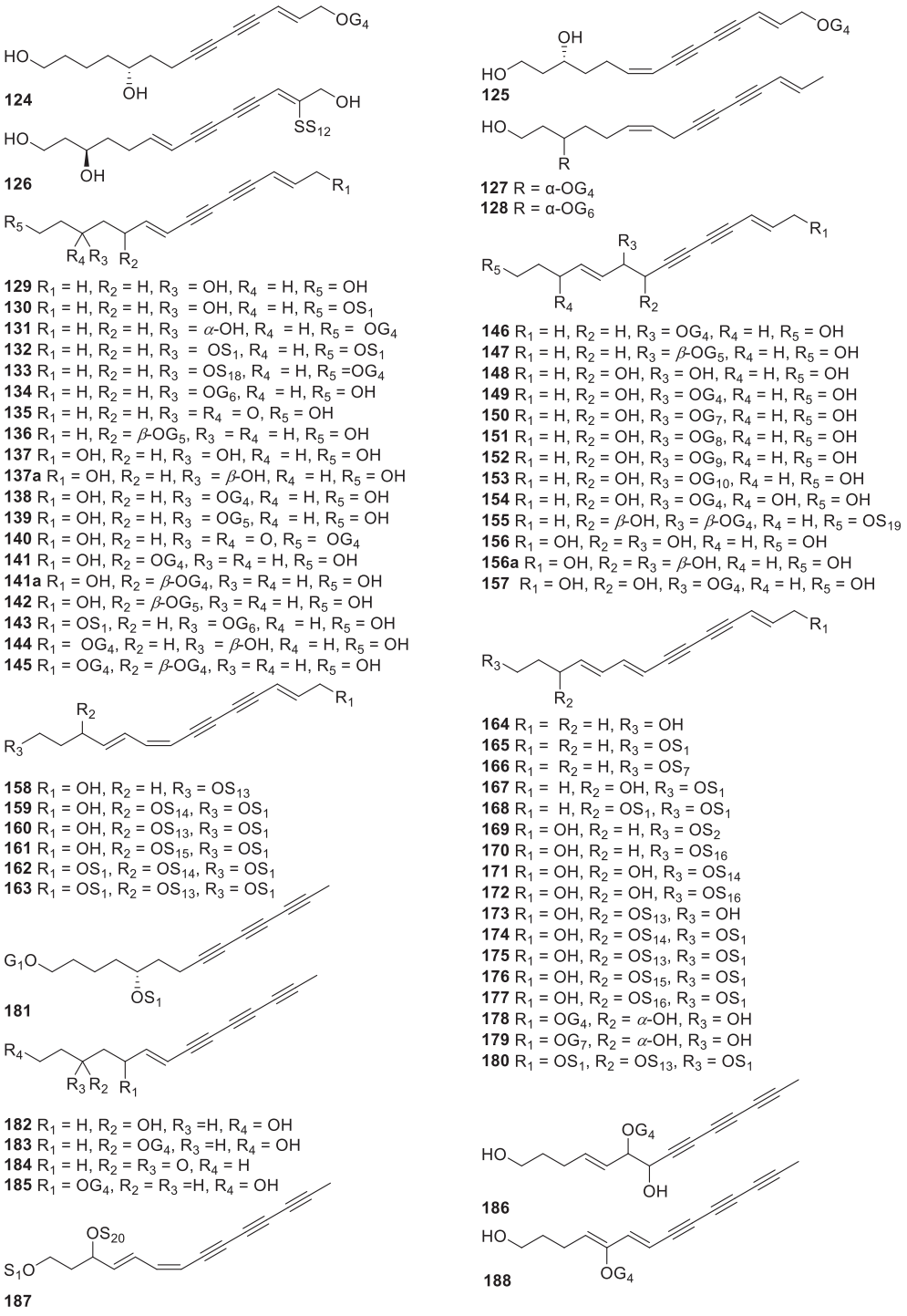

Fig. 3 Chemical structures of the linear C_{14}-polyacetylenoids.

Acroptilon repens, *Atractylodes lancea*, *Eclipata prostrata*, *Echinops transiliensis*, and *Leuzea carthamoides*. And eleven pyran or α-pyrone-type monocyclic polyacetylenoids (Fig. 9), with hepta-4,6-diyne, hepta-2,4,6-triyne or penta-2,4-diyne moiety in their structures, was isolated from *Bidens pilosa*, *Pyrethrum tatsienense*, *Bupleurum chinense*, *Codonopsis cordifolioidea*, *Codonopsis tangshen*, *Echinophora cinerea*, *Echinophora platyloba* and *Codonopsis pilosula*, belonging to Compositae, Apiaceae and Campanulaceae families. Pyran or α-pyrone-type monocyclic polyacetylenoids are mainly C_{14} polyacetylenoids and mostly unglycosylated).

The above-mentioned monocyclic polyacetylenoids are heterocyclic compounds, mostly oxygen heterocyclic compounds. It is worth mentioning that some non-heterocyclic polyacetylenoids, containing benzene rings, have been found to be distributed in Compositae plants, including *Bidens pilosa*, *Coreopsis tinctoria*, *Artemisia ordosica* and *Helichrysum aureonitens*. In the last two decades, non-heterobicyclic or non-

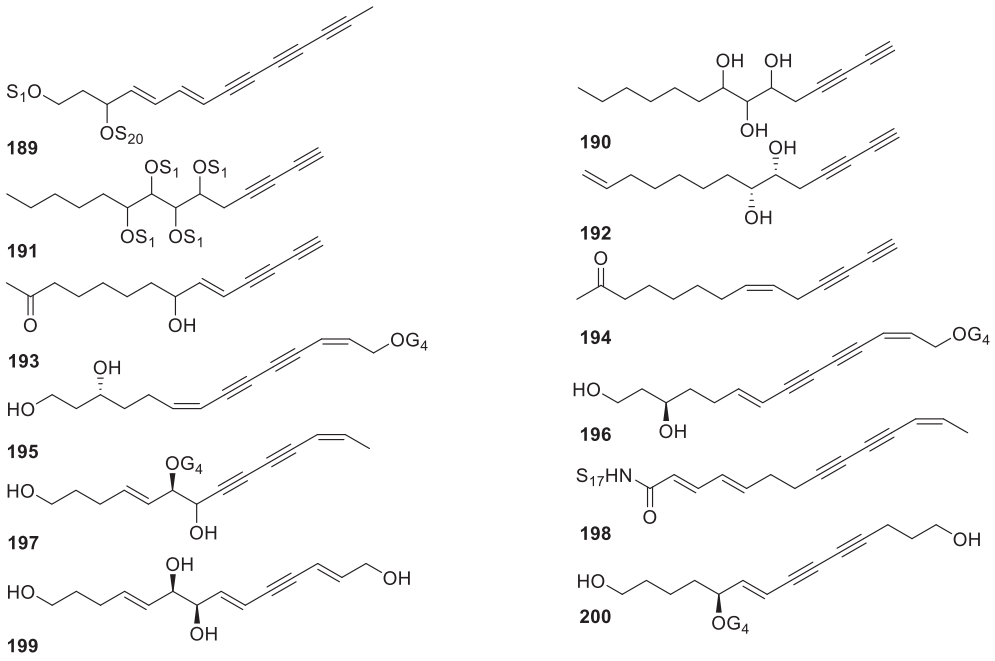

Fig. 3 (*continued*)

heteromonocyclic polyacetylenoids were only found to be distributed in these Compositae plants, with a hepta-2,4,6-triyne, a hepta-4,6-diyne or a penta-2,4-diyne at their polyacetylenic terminals. What's more, there occurs compound **436** (artemisidiyne A) featuring one cyclopentanone ring, possessing a penta-2,4-diyne moiety at its polyacetylenic terminal (Xiao et al., 2014).

2.2.2. Bicyclic polyacetylenoids

In the past twenty years, bicyclic polyacetylenoids with chain lengths of C_{12}, C_{13} and C_{14}, were mostly isolated from *Echinops ritro*, *Bidens pilosa*, *Chrysanthemum indicum*, *Eclipata prostrata*, *Acroptilon repens*, *Ambrosia maritima*, *Matricaria chamomilla*, *Carlina acaulis*, *Tanacetum vulgare*, *Artemisia selengensis* and *Chrysanthemum zawadskii* in Compositae family. As shown in Fig. 10, compounds **445**–**455** are a series of 2,2′-bithiofurphen-type bicyclic polyacetylenoids that distributed mostly in plants of *Echinops ritro* (Li et al., 2019) and *Eclipata prostrate* (Xi et al., 2014). And compounds **460**–**478** come to be a series of dioxaspirocyclic polyacetylenoids isolated with beneficial antibacterial activities (Li et al., 2019), mostly from the *Chrysanthemum* and *Artemisia* plants.

2.2.3. Other cyclic polyacetylenoids

Polycyclic polyacetylenoids (**481**–**485**) have also been found to be existed in terrestrial medicinal plants. For examples, two naphthyl tricyclic polyacetylenoids, notoincisols B (**484**) and C (**483**), have been isolated from *Notopterygium incisum* (family Apiaceae) (Liu et al., 2014), and one tetracyclic polyacetylenoid with four thiofuran rings, echinopsacetylene A (**485**), was isolated from *Echinops transiliensis* (Nakano et al., 2011).(See Fig. 11)

2.3. NMR characteristics and assignment of their configurations

2.3.1. ^{1}H and ^{13}C chemical shift behaviors of the linear polyacetylenoids

In general, polyacetylenic phytochemicals were commonly afforded as colorless oils or white amorphous powder, with planar structures and the concerned relative configurations established by analysis of their extensive spectroscopic and spectrometric data (UV, IR, 1D and 2D NMR, and HRESIMS). As far as we know, NMR analysis plays a vital role in the elucidation of the chemical structures of polyacetylenoids. The common deuterated solvents used are $CDCl_3$, CD_3OD, and DMSO d_6 followed by D_2O, C_6D_6 and so on. As summarized in Tables S1 and S2, in NMR spectra of plant polyacetylenoids, acetylenic carbons often exhibited quaternary carbon resonances at δ_C 58.9–91.0, which easily and frequently overlap with those carbon resonances of sugars and saturated alcohol carbons, making the assignments of these acetylenic carbons more challenging. In $CDCl_3$, the terminal methyl adjacent to an acetylenic bond showed a proton resonance at δ_H 1.93–2.07 (3H, s) and a highly shielded carbon resonance at δ_C 3.7–4.8, while a terminal methyl adjacent to an olefinic bond exhibited a proton resonance at δ_H 1.83–1.95 (3H, d, br d, or m, $^{3}J_{HH} \approx 7.0$ Hz and $^{4}J_{HH} \approx 1.8$ Hz) and a carbon resonance at δ_C 14.0–19.0. Interestingly, in common plant polyacetylenoids, the terminal hydroxymethyl group was only found to be adjacent to an olefinic bond rather than an acetylenic bond, with NMR resonances at δ_H 4.17–4.66 (2H, m), and δ_C 61.1–61.3 (*cis*-olefinic bond) or 62.6–64.4 (*trans*-olefinic bond). Acetylation (acylation) of the saturated tertiary carbinol adjacent to an acetylenic bond, as exemplified by **t1**- and **t3**- types of polyacetylenic terminals, will cause downfield proton and carbon shifts with $\Delta\delta_H$ 0.86–1.01 and $\Delta\delta_C$ 0.7–1.1, respectively. Glycosylation of the saturated tertiary and secondary carbinols in polyacetylenoids perturbs the

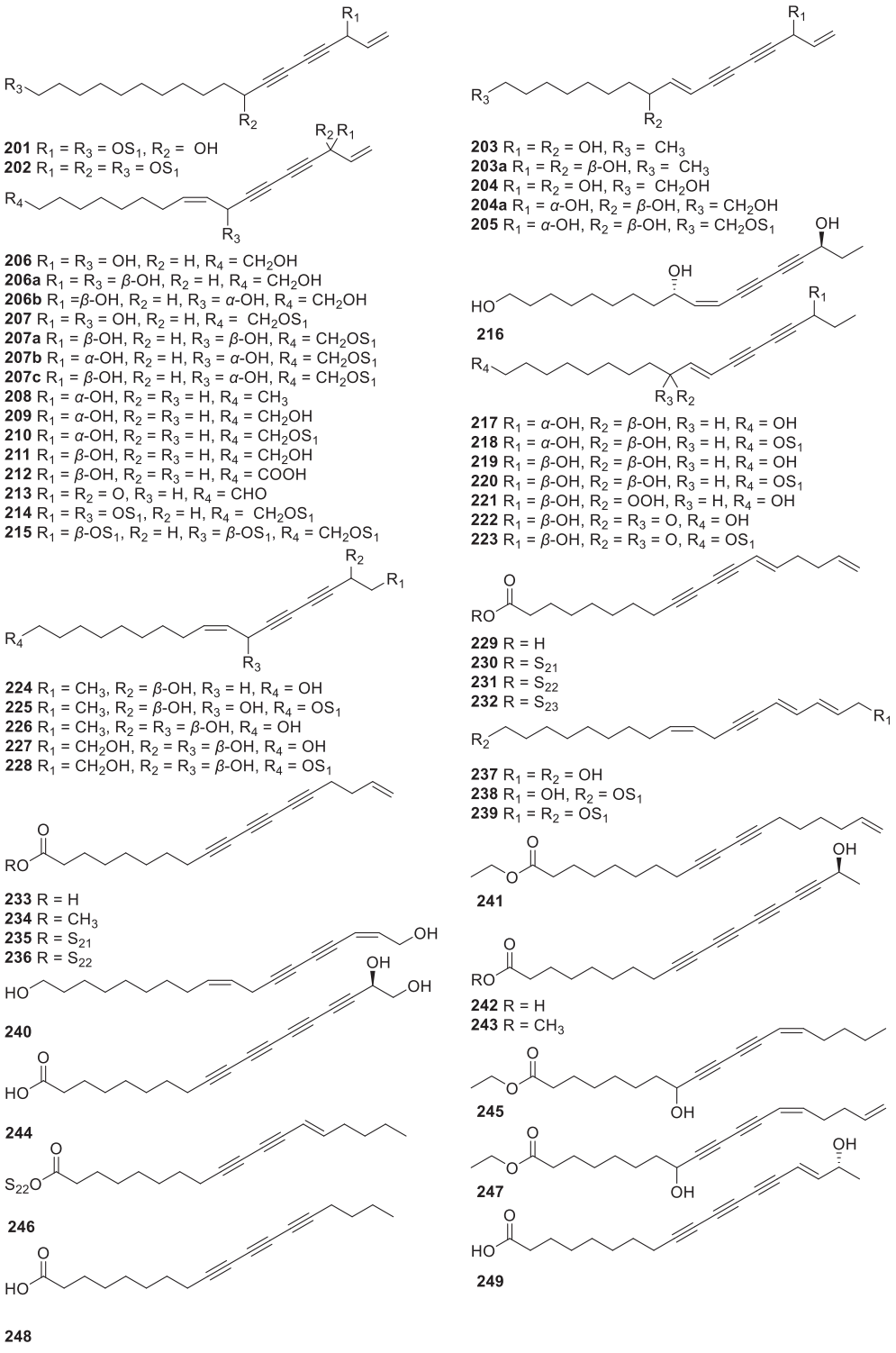

Fig. 4 Chemical structures of the linear C_{18}-polyacetylenoids.

chemical shifts of their protons and carbons following the common glycosidation chemical shift rules.

2.3.2. Determination of the configurations of polyacetylenoids

It can be found from Table 1, the saturated acyclic tertiary carbinols and/or vicinal diol groups (**74**, **75, 81, 94, 95, 356**) occur frequently in natural polyacetylenoids originating from terrestrial medicinal plants, due to biological oxidation of their conjugated olefinic bonds. For typical cyclic polyacetylenoids with three- to six- membered rings displaying predictable conformational behavior, the relative configurations can be deduced using simple NMR parameters such as the $^3J_{HH}$ values and/or the nuclear overhauser effect (NOE) intensities (Guo et al., 2017). However, to determine the relative configurations

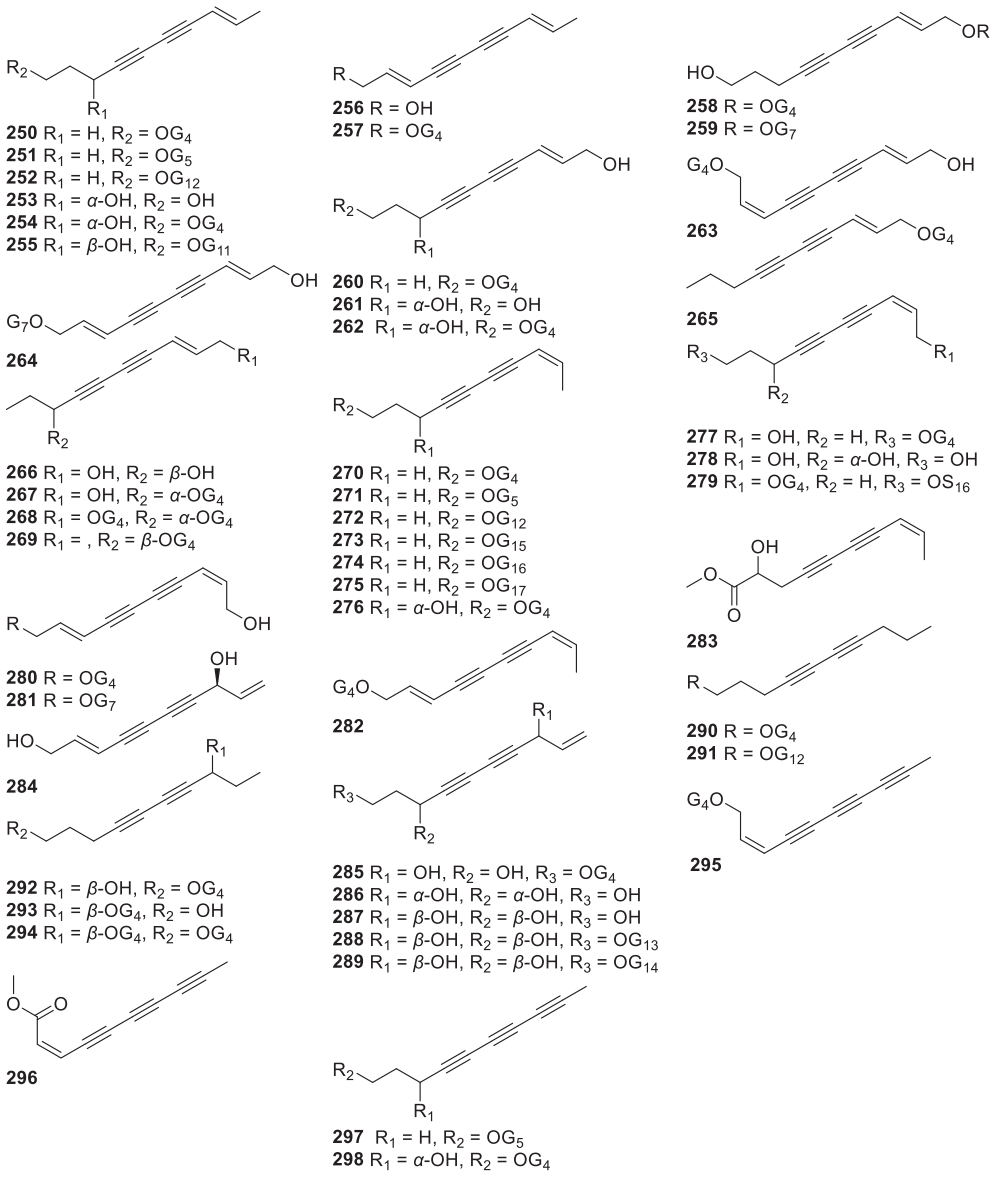

Fig. 5 Chemical structures of the linear C_{10}-polyacetylenoids.

of conformationally flexible linear polyacetylenic chains are significantly more challenging. The NMR profiles (δ_H, δ_C, $\delta_{H(OH)}$, $^3J_{HH}$, and $^{2,3}J_{HC}$) of acyclic *threo* and *erythro* diols in achiral solvents were found to be very similar to each other. So, in the last two decades, optimization of the NMR experiment (such as recording solvent, NMR parameters, pulse sequence, and use of a higher-resolution NMR spectrometer) (Wongsomboon et al., 2021; Zhu et al., 2021), and chemical derivatization of the test sample with chiral reagents (Kanokmedhakul et al., 2006; Xu et al., 2020), were two main approaches to amplify their $\Delta\delta$ behavior and/or *J*-value differences among the various potential configurational isomers, for assigning their relative or absolute configurations.

Optimization of the NMR experiment, without chemical derivatization of the given compounds, is a direct, convenient, and reliable approach for discriminating the *threo* and *erythro* configurations of the acyclic vicinal diols in polyacetylenoids (Lee et al., 2022). The $^3J_{HH}$ values of these acyclic vicinal diol groups in DMSO d_6 were not so interpretable to distinguish the *threo* and *erythro* configurations, but they seem to follow an empirical rule in $CDCl_3$: a relatively larger value (more than 6.0 Hz) corresponds to a *threo* configuration, whereas a smaller value (< 5.0 Hz) corresponds to an *erythro* configuration. However, the poor solubility of polyacetylenoid glycosides in $CDCl_3$ limited the direct application of this rule. Furthermore, preparation of the aglycones by acid hydrolysis of the minor polyacetylenoids containing more than one sugar moiety was difficult due to structural instability. Higashibayashi and Kishi found that the $\Delta\delta$ ($\Delta\delta = \delta_{(R,R)} - \delta_{(S,S)}$) behaviors of acyclic secondary 1,2-diols in chiral bidentate NMR solvent [eg. (*R*,*R*)- and (*S*,*S*)-BMBA-*p*-Me] were significantly different, and accordingly developed a method to predict both the relative and absolute configurations of acyclic secondary 1,2-diols (Xu et al., 2017). And recently, Pei-Cheng Zhang's group found an excellent deuterated solvent, aceticacid d_4, enabling the collection of quality spectra that display a similar spectro-

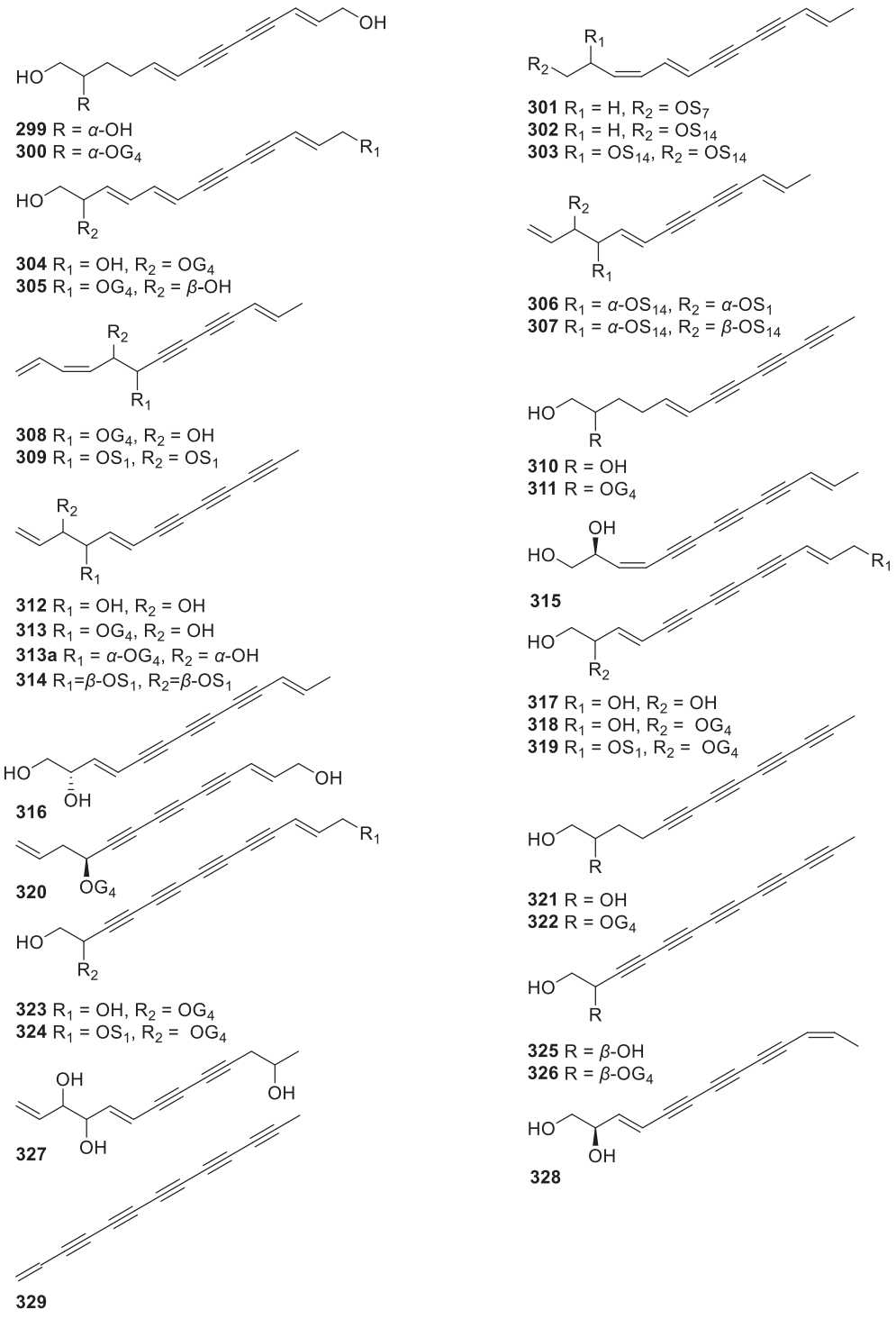

Fig. 6 Chemical structures of the linear C_{13}-polyacetylenoids.

scopic tendency as the nonpolar $CDCl_3$ solvent. Hence, the relative configurations of polyacetylenoid glycosides containing an acyclic vicinal diol group adjacent to an olefinic bond, an acetylenic bond, a thiophene ring, or a furan ring could be conveniently and reliably determined by ^{1}H NMR spectroscopy using aceticacid d_4/D_2O as the solvent. A relatively larger $^3J_{HH}$ value (7.0 Hz) was assigned to the *threo* configuration, whereas a smaller value (3.5 Hz) was assigned to the *erythro* configuration(Guo et al., 2017). what is more important, the proportions of aceticacid d_4 can be adjusted slightly based on the solubility of the samples to be tested.

Mosher's method provides another stereochemical solution but requires a certain amount of the tested compounds sufficient for hydrolysis and/or chemical derivatizations before further NMR analysis and/or ECD simulation and comparison. The common hydrolysis methods of polyacetylenoid glyco-

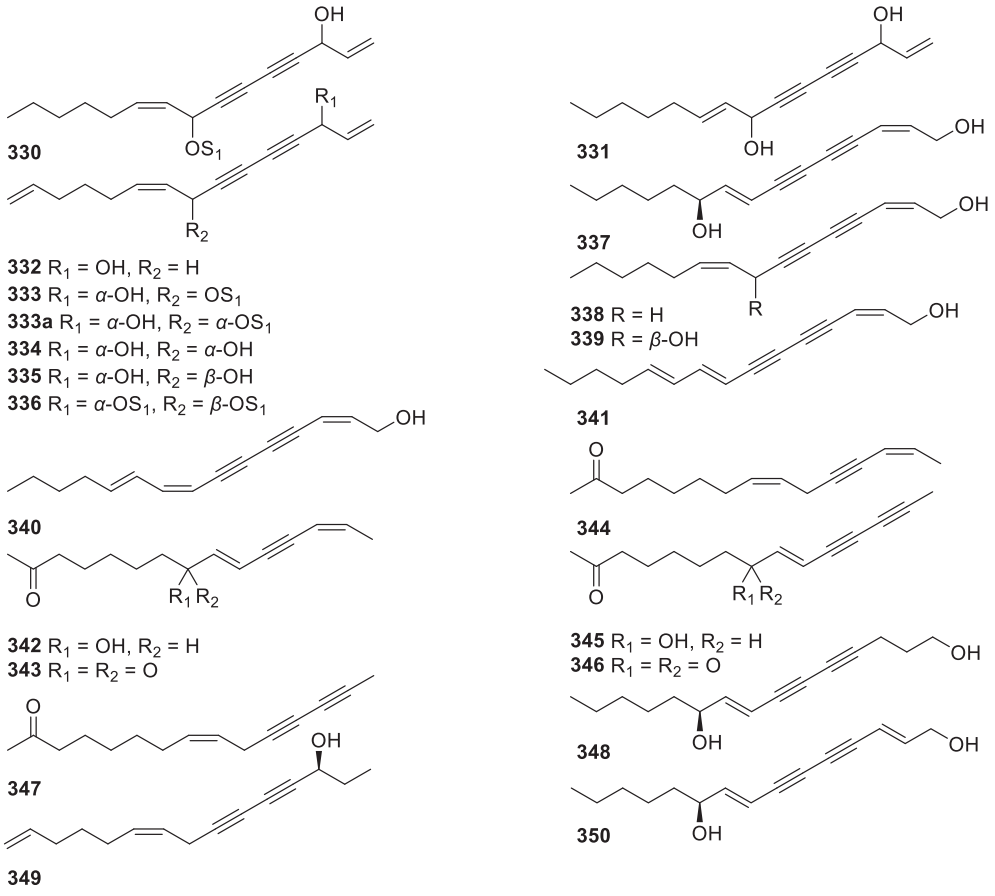

Fig. 7 Chemical structures of the linear C_{15}-polyacetylenoids.

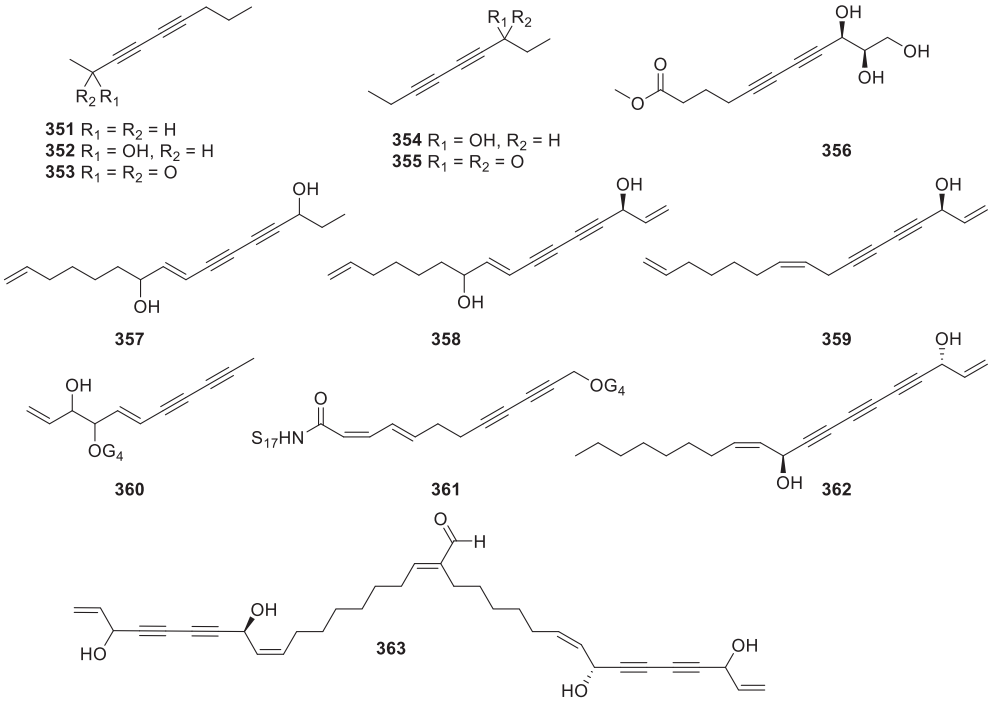

Fig. 8 Chemical structures of other linear polyacetylenoids.

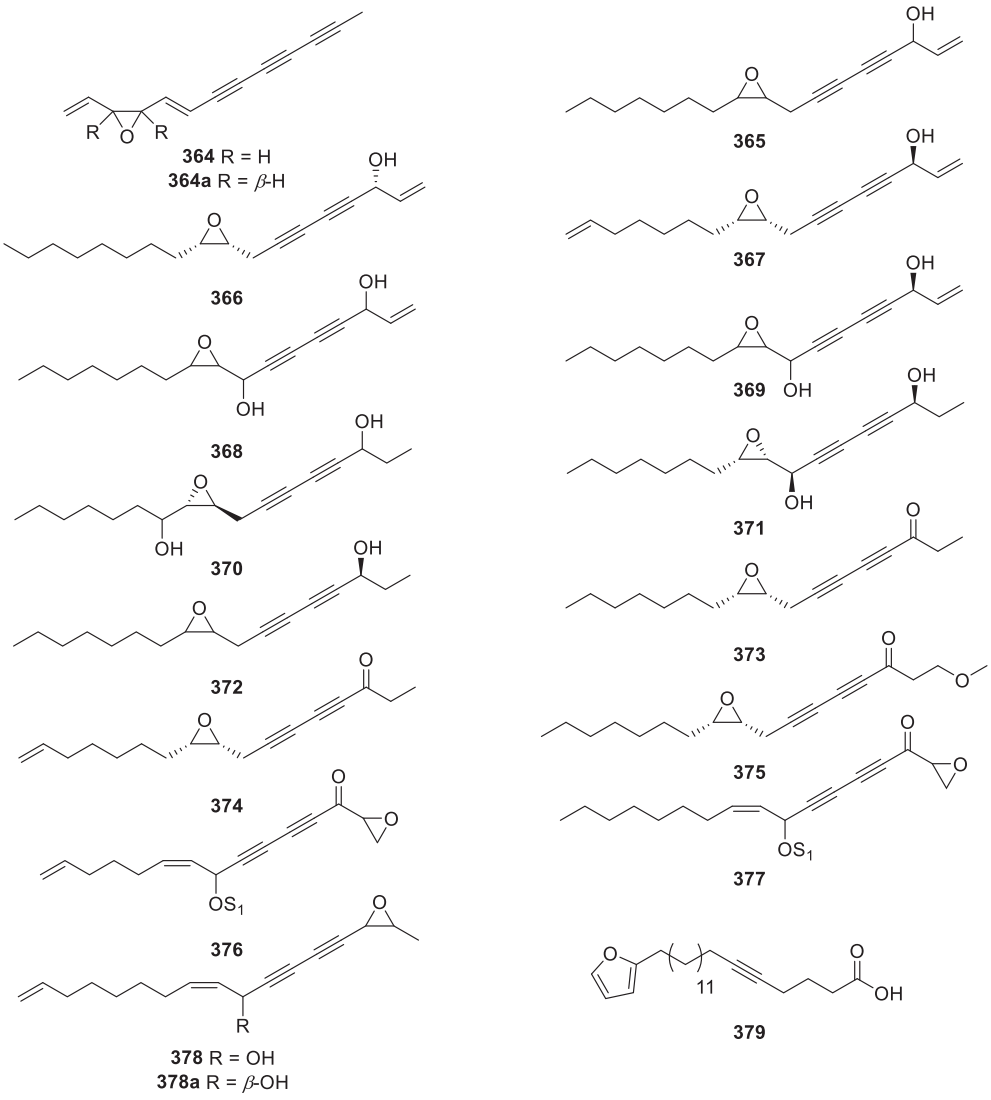

Fig. 9 Chemical structures of the monocyclic polyacetylenoids.

sides include: 1) Enzymatic hydrolysis, such as cellulase (Rücker et al., 1992), β-glucosidase (Wang et al., 2001), snailase (Jiang et al., 2015; Xu et al., 2017) and 2) Acid Hydrolysis, such as HCl/MeOH (Mei et al., 2008; Guo et al., 2017). And in the last two decades, the reagents dedicated to the chemical derivatization of saturated acyclic tertiary carbinols in the determination of relative and absolute stereochemistry of polyacetylenoids was mostly (*S*)-(+)- and (*R*)-(-)-α-methoxy-α-trifluoromethyl phenylacetyl chloride (MTPA) (Wang et al., 2001), occasionally (*S*)-(+)- and (*R*)-(-)-α-methoxyphenylacetic acid (MPA) (Jiang et al., 2015).

3. Botanic origins

As retrieved in the recent literature dating from 2000 to 2022, more than 485 polyacetylenoids, with a broad array of biological properties (Zhou et al., 2015), have been isolated from almost 110 species belonging to 11 families including Compositae, Apiaceae, Araliaceae, Campanulaceae, Annonaceae, Meliaceae, Simaroubaceae, Typhaceae, Olacaceae, Torricelliaceae and Cucurbitaceae, as summarized in Table 1. These 110 terrestrial species cover 45 Compositae species (251 polyacetylenoids), 34 Apiaceae species (113 polyacetylenoids), 13 Araliaceae species (67 polyacetylenoids), 8 Campanulaceae species (36 polyacetylenoids), 3 Annonaceae species (20 polyacetylenoids), 2 Meliaceae species (18 polyacetylenoids), and other 5 species belonging to the remaining 5 families (17 polyacetylenoids) (Fig. 12).

3.1. Compositae

Compositae is the largest source of polyacetylenoids that has ever been discovered so far. Since 2000, more than 250 polyacetylenoids have been isolated from Compositae species, among which, the top 6 polyacetylenoid-producing Compositae species ranked from most to least are *Atractylodes lancea*, *Carthamus tinctorius*, *Atractylodes macrocephala*, *Bidens pilosa*, *Desmanthodium guatemalense* and *Echinops ritro*. Most of them were C_{10}, C_{13}, and C_{14} polyacetylenoids. And, glycosylated polyacetylenoids account for nearly one-third of all

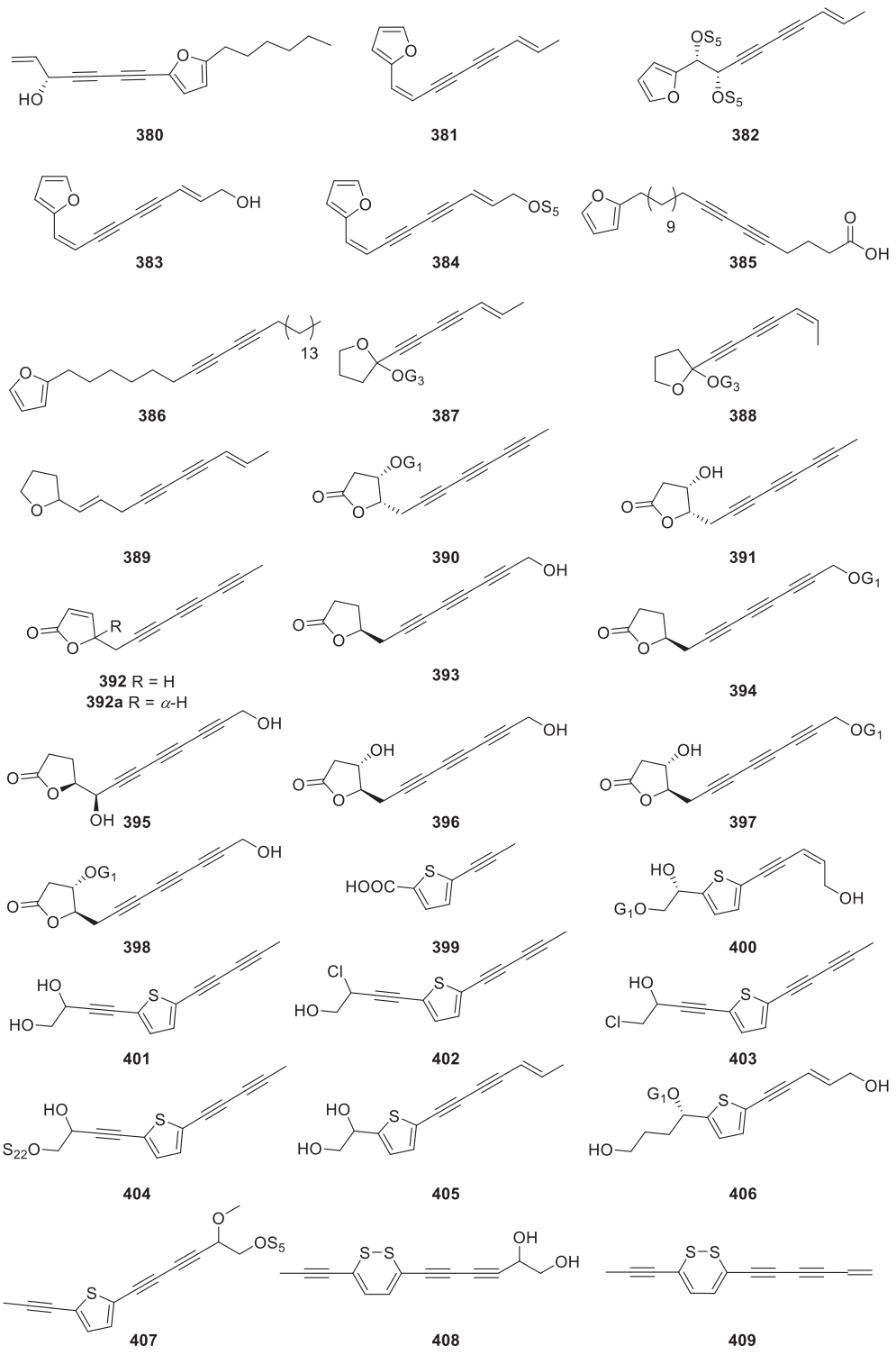

Fig. 9 (*continued*)

these isolated polyacetylenoids. As far as we know, most of the polyacetylenoids embedded with thiophene (thiofuran) ring(s) are originated from the plants in the Compositae family, in which C_{17} polyacetylenoids happen normally to be falcarinol-type.

3.2. Apiaceae

Some of the most bioactive (eg. antifungal, anti-inflammatory, anti-platelet-aggregatory, or antibacterial) polyacetylenoids have been found in plants of the Apiaceae family, including the well-known daily vegetables such as carrot, celery, and

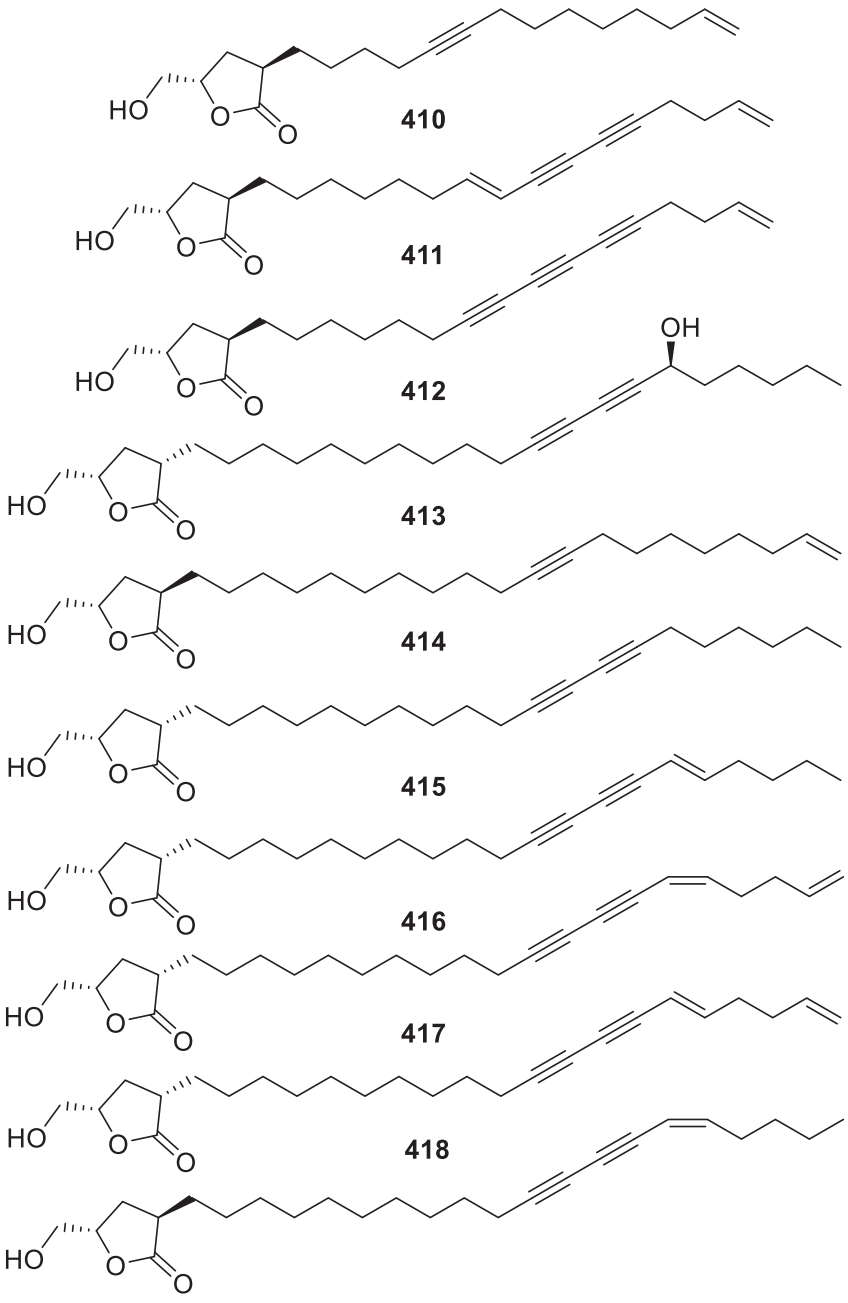

Fig. 9 (*continued*)

parsley (Christensen and Brandt 2006). As is reported, such genera as *Bupleurum* (*Bupleurum longiradiatum*), *Notopterygium* (eg. *Notopterygium incisum*), *Eryngium,* and *Pastinaca* in the Apiaceae family are rich in polyacetylenoid compounds, and falcarinol-type polyacetylenoids (C_{17}) represent the most widespread and representative polyacetylenoids in *Apiaceae* (Chen et al., 2015).

3.3. Araliaceae

In Araliaceae plants, *Ginseng* and *Oplopanax* genera are found to be rich in polyacetylenoids. Since last twenty years, 73 C_{17} and C_{18} predominating polyacetylenoids have been isolated from Araliaceae plants, and among them, falcarindiol, falcarinol and panaxydol occurred frequently with a wide range of biological activities, including anti-tumor (Sun et al., 2010), anti-pathogenic microbial (Yamazoe et al., 2007), and hair growth promoting effects (Suzuki et al., 2017).

3.4. Campanulaceae

From 2010 to 2022, phytochemistry studies on plants of the genera *Codonopsis* (eg. *Codonopsis pilosula*), *Lobelia* (eg. *Lobelia nummularia* Lam) and *Platycodon* (eg. *Platycodon grandiflorus*) led to the isolation of 38 polyacetylenoids, mainly C_{14} polyacetylenoids and most of which are glycosylated. Notably, lobetyol, lobetyolinin, lobetyolin occurring frequently in Campanulaceae plants, were found to possess beneficial anticancer properties (Bailly, 2020).

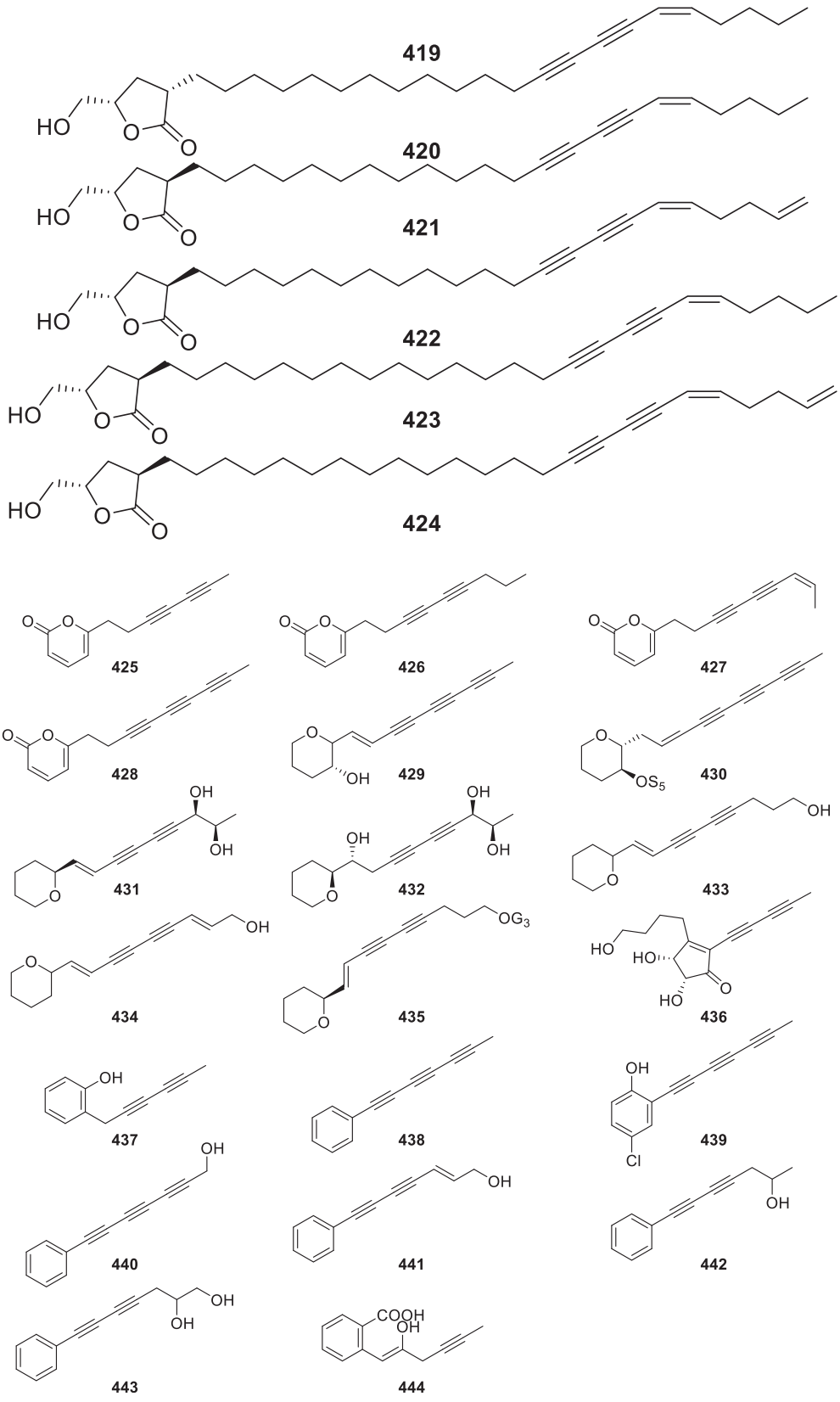

Fig. 9 (*continued*)

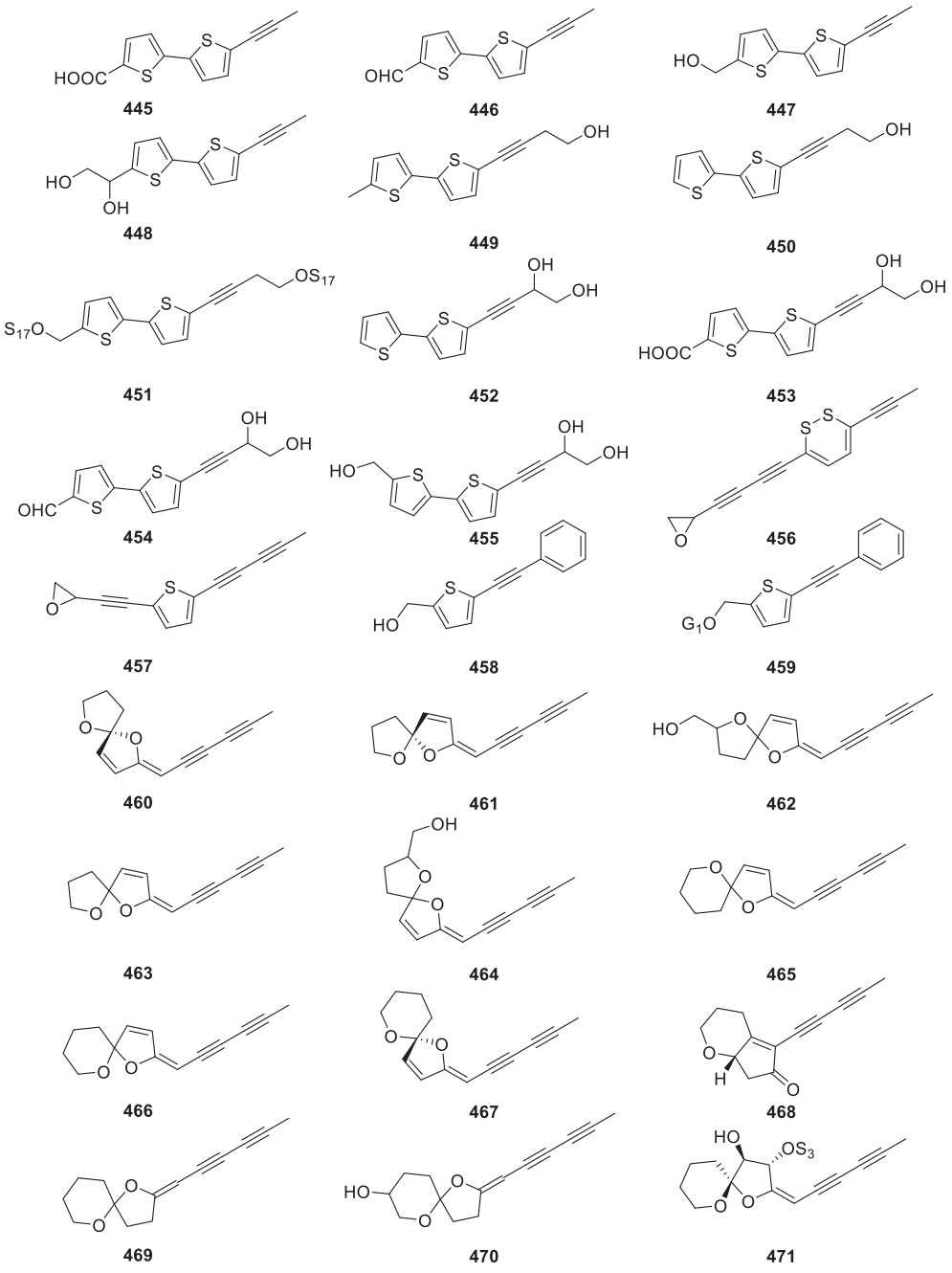

Fig. 10 Chemical structures of the bicyclic polyacetylenoids.

3.5. Species in other families

The *Mitrephora* and *Polyalthia* plants (Annonaceae family) contain mostly C_{18} polyacetylenoids in the form of polyacetylenoid ester or acid, following with C_{16}, C_{22}, and C_{24} polyacetylenoids. Few polyacetylenoids have been isolated from the plants of Meliaceae family, including *Toona ciliate* and *Swietenia mahagoni*, amongst which, *T. ciliate* mainly produces C_{17} and C_{18} polyacetylenoids while *S. mahagoni* affords mostly C_{14} and C_{17} polyacetylenoids, sharing similar skeletons as those from *T. ciliate*.

In addition to the above, some plants of other families, including Simaroubaceae, Olacaceae, Torricelliaceae and Cucurbitaceae, also occasionally biosynthesize polyacetylenoid metabolites during their growth cycle. Among them, the *Eurycoma longifolia* in family Simaroubaceae has been found to be able to produce the rare α-furanone-type monocyclic polyacetylenoids (Wang et al., 2017).

4. Analytical methods

So far, various separation-based and combined detection-based methods have been developed for qualitative and/or quantitative analyses of the polyacetylenoid compositions in terrestrial medicinal plants. Polyacetylenoids are usually extracted from fresh or dried plant material by an organic sol-

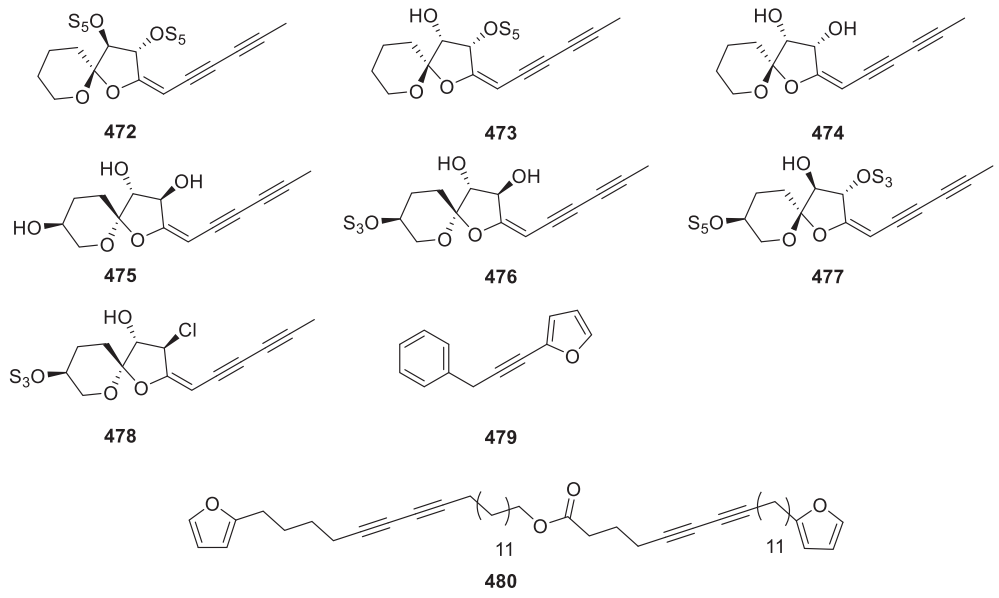

Fig. 10 (*continued*)

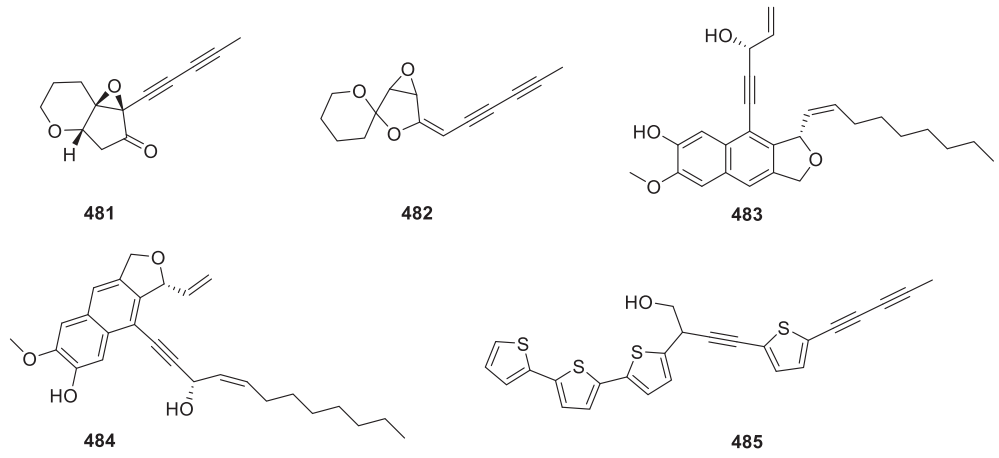

Fig. 11 Chemical structures of the other cyclic polyacetylenoids.

vent such as *n*-hexane (Pellati et al., 2012), ethyl acetate (Moricz et al., 2018), chloroform (Marčetić et al., 2014), ethanol (Silva et al., 2015), and methanol (He et al., 2014; Chen et al., 2018). Extraction methods for polyacetylenoid typically include reflux (Wang et al., 2017; Kim et al., 2018), sonication (He et al., 2014; Chen et al., 2018), supercritical fluid extraction (Tacchini et al., 2017), percolation (Silva et al., 2015), and hydrodistillation (Marcetic et al., 2013). Before analysis, polyacetylenoid samples are normally accumulated or prepared by repeated solvent extraction and/or thin-layer chromatography (TLC) on silica gel or by using a combination of silica gel CC and gel permeation CC on Sephadex LH-20 (Huang et al., 2011; Silva et al., 2015). Also, other special techniques such as centrifugal partition chromatography (CPC), counter-current chromatography (CCC) and elution-extrusion counter-current chromatography (EECCC), have been developed and adopted for the isolation of natural polyacetylenoids (Chen et al., 2018; Chen et al., 2021).

As summarized in Table 2, analysis of the main polyacetylenoid components is usually performed using thin-layer chromatography (TLC), high-performance thin-layer chromatography (HPTLC), high performance liquid chromatography (HPLC), ultra-high performance liquid chromatography (UHPLC), gas chromatography (GC), and effective detection of the marker components are always accomplished by using ultraviolet (UV), photo-diode array (PDA), diode array detector (DAD), mass spectrometry (MS), and flame ionization detector (FID) alone or in combinations. Generally, to obtain supplementary information, different types of detectors are often combined in one run, such as liquid chromatography-mass spectrometry (LC-MS) and the high-performance liquid chromatography-ultraviolet (HPLC-UV). Gas chromatography-mass spectrometry (GC–MS) is dedicated to the qualitative or semi-quantitative analysis of the polyacetylenoids in essential oils or nonpolar extracts of terrestrial medicinal plants (Liu et al., 2007).

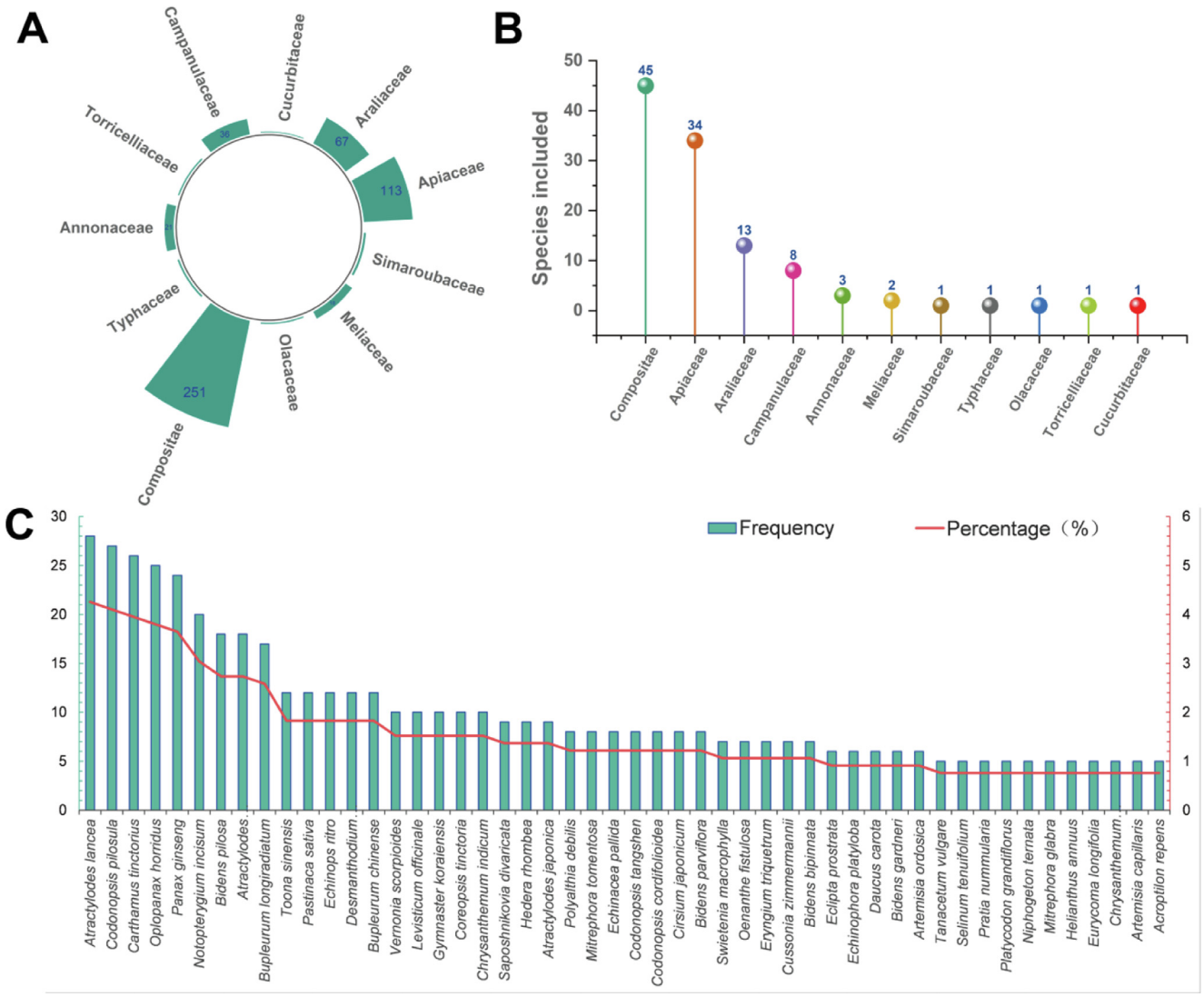

Fig. 12 Distribution of polyacetylenoids in different families of the terrestrial medicinal plants (A); The number of plant species in the major families containing polyacetylenoids (B); Frequency and the percentage of polyacetylenoids occurring in the main plant species (C).

4.1. Detection method

DAD and MS detectors are commonly used for qualitative and quantitative analysis of plant polyacetylenoids. The wavelength range for UV detection is 200–400 nm. Generally, the detection sensitivity above 230 nm is extremely low in the clue of the existence of few conjugated unsaturated bonds in their structures, and the excitation coefficients (ε) of these compounds (normally two triple bonds in conjugation) were commonly below 6000 at their characteristic UV-maxima. Instead, the UV sensitivity of the polyacetylenoids is improved approximately 10 times when detected at 205 nm and hence the detection of these compounds were commonly conducted at 205 nm (Christensen and Brandt 2006). However, additional co-eluting peaks may interfere with the analytes at 205 nm because no selective detection is possible in plants, such as carrot genotype (Pferschy-Wenzig et al., 2009). Therefore, more elaborate sample preparation is necessary. In general, two types of mass spectrometers are applied, quadrupole-time of flight (Q-TOF) and Q-Q-Q mass spectrometers, dedicated to qualitative and quantitative analysis of the polyacetylenoid constituents of plant origins, respectively. The most frequently used ion source is electrospray ionization (ESI).

4.2. TLC and HPTLC analyses

TLC and HPTLC are rapid separation and qualitative analytical techniques that can be used for routine chemical analysis and identification of the polyacetylenoid components in plants. For HPTLC and TLC analyses of polyacetylenoids, silica gel 60 F254 plates were often eluted with the following developing solvents: Petrol ether–ethyl acetate (3:1, *v*/*v*), hexane–ethyl acetate (1:1, *v*/*v*) (Prior et al., 2007), and *n*-hexane–isopropyl acetate (9:1, *v*/*v*) (Moricz et al., 2018). Normally, polyacetylenoids can be detected as dark black spots by spraying with vanillin (1% in MeOH) or sulfuric acid (5% in MeOH) before heating (Zidorn et al., 2005), or dark blue spots after spraying phosphomolybdic acid reagent and heating

Table 2 Determination methods for constituents of the polyacetylenoids.

Source	Method	Extract solvent	Column	Mobile phase	Detection condition	Plant part	Remark	Reference
D. carota	HPLC	EtOAc	Luna C18 column (100 mm × 4.6 mm, 5 μm)	H_2O (A) and MeCN (B)	205 nm	Roots	Fresh carrot juice: FaDOAc[a] 73 μg/L, FaOH[b] 233 μg/L	(Aguilo-Aguayo et al., 2014)
	HPLC-DAD	MeOH	Phenomenex Luna C18(2) column (100 mm × 3 mm, 3 μm)	MeCN (A) and H_2O (B) (70:30 *v*/*v*)	205 nm	Roots	/	(Kjellenberg et al., 2012)
	HPLC-DAD	EtOAc	Zorbax RX-C18 column (12.5 mm × 4.6 mm, 5 μm)	H_2O (A) and MeCN (B)	/	Roots	Carrot: FaOH[b] 85.13–244.85 μg/g DW[c]	(Hinds et al., 2017)
	HPLC-DAD-MS	MeOH	Phenomenex Aqua C18 column (250 mm × 21.2 mm, 5 μm)	H_2O (A) and MeCN (B)	205 nm	Roots	*A. sylvestris*: TP[f] 3.8 g/kg DW[c]; Celeriac: TP[f] < 0.1 g/kg DW[c]	(Kramer et al., 2011)
	HPLC-DAD	15% Aqueous EtOAc	Phenomenex Luna C18(2) column (150 mm × 4.6 mm, 3.0 μm)	H_2O (A) and MeCN (B)	205 nm	Roots	Peeled carrot: FaDOH[d] 6.4–30.4 mg/kg FW[e], FaDOAc[a] 10.2–21.6 mg/kg FW[e], FaOH[b] 35.2–67.0 mg/kg FW[e]	(Christensen and Kreutzmann 2007)
	HPLC-DAD and UPLC-TOFMS	EtOAc	Prodigy RP-C18 column (250 mm × 4.6 mm, 5 μm)	H_2O (A) and MeCN (B)	205 nm	Roots	Carrot: FaDOH[d] 222 μg/g DW[c], FaDOAc[a] 30 μg/g DW[c] and FaOH[b] 94 μg/g DW[c] in year 1, and 3–15% lower in year 2	(Soltoft et al., 2010)
	UPLC-PDA-MS	DCM + 0.1 % BHT	Waters Acquity UPLC® HSS SB-C18 column (2.1 mm × 100 mm, 1.8 μm)	H_2O + 5 mM NH_4OAc: MeOH:MeCN: EtOAc (A) (50:22.5:22.5:5) and MeCN: EtOAc (B) (50:50))	PDA: 190–800 nm; *m*/*z* 100–1400	/	Whole raw small carrots: FaOH[b] 18 mg/kg FW[e], FaDOH[d] 35 mg/kg FW[e]; Peeled blanched round carrots: FaOH[b] 2.9 mg/kg FW[e], FaDOH[d] 13 mg/kg FW[e]	(Bijttebier et al., 2014)
B. pilosa	HPLC	*n*-Hexane	Aglient ZORBAX SB-C18 column (150 mm × 4.6 mm, 5 μm)	H_2O (A) and MeCN (B)	254 nm	Whole grass	/	(Chen et al., 2021)
	HPLC	70% aqueous EtOH	Phenomenex Luna C18 column (250 mm × 4.6 mm, 5 μm)	H_2O (A) and MeCN (B)	245 nm	Leaves	/	(Chen et al., 2020)
	HPLC-DAD-MS	EtOAc	Phenomenex Luna C18 (5 μm)	H_2O (A) and MeCN (B) both containing 0.05% trifluoroacetic acid	240 nm	Flowers	TP[f] 15.9–76.9 mg/g in methanolic extract, 25.8–100.9 mg/g in ethyl acetate fractionate	(Lee et al., 2013)
B. pilosa L. var. radiata (BPR), *B. pilosa* L. var. pilosa (BPP), *and* *B. pilosa* L. var. minor (BPM)	HPLC	MeOH	Phenomenex Luna C18(2) column (150 mm × 2.0 mm, 3 μm)	H_2O (A) and MeCN (B) both containing 0.05% trifluoroacetic acid	240 nm	Leaves	2-*β*-D-glucopyranosyloxy-1-hydroxy-5(*E*)-tridecene-7,9,11-triyne, cytopiloyne, 3-*β*-D-glucopyranosyloxy-1-hydroxy-6(*E*)-tetradecene-8,10,12-triyne 0.61 ± 0.02%,	(Chien et al., 2009)

Table 2 (*continued*)

Source	Method	Extract solvent	Column	Mobile phase	Detection condition	Plant part	Remark	Reference
							0.44 ± 0.02%, and 0.32 ± 0.01% in BPR, 0.17 ± 0.01%, 0.19 ± 0.01%, and 0.27 ± 0.01% in BPP and 0.16 ± 0.02%, 0.15 ± 0.02%, and 0.27 ± 0.01% in BPM, respectively	
	GC-EI-MS	Supercritical CO_2	RTX-5 MS capillary column (30 m × 0.25 mm, 0.25 μm)	He	/	Whole plants	/	(Chien et al., 2009)
P. ginseng	HPLC-DAD-MS	MeOH	Prevail C18 rocket column (33 mm × 7 mm, 3.0 μm)	H_2O (A) and MeCN (B)	203 nm	Leaves, roots	Polyacetylenoids 1.93–2.72 mg/g	(Qian et al., 2009)
	UPLC-PDA	15% aqueous EtOH	Acquity UPLC BEH-C18 column (50 mm × 2.1 mm, 1.7 μm)	MeCN (16%) in H_2O	265 nm	Roots	Panaxfuraynes A and B < 3 and 2 ng/g, respectively	(Lee et al., 2010)
	GC–MS	70% aqueous MeOH	DB-5 column (5% phenyl-methylpolysiloxane, 30 m × 0.25 mm, 0.25 μm)	He	/	Roots	/	(Park et al., 2013)
	GC–MS	Hexane	OV-1 capiliary column (30 m × 0.25 mm, 0.25 mm)	He	*m*/*z* 40–500	Roots	Nona-3,5-diyne 85.6%, nona-3,5-diyn-2-one 3.0%, nona-4,6-diyn-3-one 2.5%, nona-3,5-diyn-2-ol 2.2%, and nona-4,6-diyn-3-ol 3.1% in the total volatiles	(Herrmann et al., 2013)
E. pallida	HPLC	*n*-Hexane	Chromolith performance RP-18e column (100 mm × 4.6 mm)	H_2O (A) and MeCN (B)	210 nm	Roots	8-Hydroxy-tetradec-(9*E*)-ene-11,13-diyn-2-one, 8-Hydroxy-pentadec-(9*E*)-ene-11,13-diyn-2-one, 8-Hydroxy-pentadeca-(9*E*,13*Z*)-dien-11-yn-2-one, Pentadec-(9*E*)-ene-11,13-diyne-2,8-dione, Pentadeca-(9*E*,13*Z*)-dien-11-yne-2,8-dione, Tetradec-(8*Z*)-ene-11,13-diyn-2-one, Pentadec-(8*Z*)-ene-11,13-diyn-2-one, Pentadeca-(8*Z*,13*Z*)-dien-11-yn-2-one 0.09–1.13 mg/g	(Pellati et al., 2007)
	HPLC-DAD-(ESI)MS	MeOH with 0.1% HCOOH	Ascentis C18 column (250 mm × 4.6 mm, 5 μm)	H_2O (A) and MeCN (B) both containing 0.1% formic acid	DAD:190–450 nm	Roots	TP[f] 5.46 ± 0.23 mg/g	(Pellati et al., 2012)
	HPLC-UV/DAD and ESI-	*n*-Hexane	Ascentis Express C18 column	H_2O (A) and MeCN (B)	DAD:190–500 nm,	Roots	/	(Tacchini et al., 2017)

(*continued on next page*)

Table 2 (*continued*)

Source	Method	Extract solvent	Column	Mobile phase	Detection condition	Plant part	Remark	Reference
	MS		(150 mm × 3.0 mm, 2.7 μm)		210 nm; *m*/*z* 100–1700			
A. annua	HPLC-DAD	MeOH	Hypersil ODS2 RP-18 column (250 mm × 4.6 mm, 5.0 μm)	H_2O (A) and MeCN (B)	190–400 nm	Hairy roots	/	(Zhai and Zhong 2010)
	LC-DAD/APCI-MS	*n*-Hexane	Eclipse C18 (150 mm × 4.6 mm, 5 μm)	0.05% TFA in H_2O (A) and MeCN (B)	DAD: 200–600 nm, 220, 254, 280, 354 nm	Aerial parts	/	(Ivarsen et al., 2014)
B. longiradiatum	HPLC-DAD-MS	CH_2Cl_2	TSKgel ODS-100 V C18 column (150 mm × 4.6 mm, 3 μm)	H_2O (A) and MeCN (B)	DAD: 190–400 nm, 254 nm	Whole plants	Bupleurotoxin 2.25–0.18 mg/g, acetylbupleurotoxin 3.91–0.02 mg/g, and bupleurynol 1.00–0.03 mg/g	(Huang et al., 2011)
	LC-Q-TOF-MS	Serum metabolites	Eclipse plus C18 column (100 mm × 3.6 mm, 1.8 μm)	MeCN (A) and 0.1% formic acid H_2O (B)	*m*/*z* 80–1000	Roots	/	(Zhang et al., 2014)
C. Radix	HPLC-UV	MeOH	YMC-Pack ODS-A column (20 mm × 250 mm, S-5 μm, 12 nm)	MeCN (A) and 0.1% phosphoric acid H_2O (B)	215 nm	Roots	/	(He et al., 2014)
	UHPLC-Q-TOF-MS and UHPLC-MS/MS	Plasma and tissue	Acquity UPLC HSS T3 column (100 mm × 2.1 mm, 1.8 μm)	H_2O (A) and MeCN (B) both containing 0.1% formic acid	*m*/*z* 100–1200	Roots	/	(Xie et al., 2023)
P. quinquefolium	HPLC	100% Aqueous MeOH – 80% aqueous MeOH	Purospher STAR RP-18 column (250 mm × 4 mm, 5 μm)	H_2O (A) and MeCN (B)	203 nm	Roots	TP[f] 2560 mg/kg FW[e] in root hairs, 910 mg/kg FW[e] in lateral roots and 570 mg/kg FW[e] in main roots	(Christensen et al., 2006)
	GC–MS	Hexane	DM-1 capiliary column (methyl siloxane, 30 mm × 0.25 mm, 0.25 mm)	He	*m*/*z* 159	Roots	Type I: FaOH[b] 156.07 mg/kg, Panaxydol 556.74 mg/kg Type Ⅱ: FaOH[b] 372.10 mg/kg, Panaxydol 503.41 mg/kg	(Wang et al., 2010)
T. vulgare	HPTLC-UV/Vis/FLD-EDA-HRMS	EtOAc	/	MeCN (A) and H_2O both containing 0.1% formic acid	254, 366 nm	Roots	/	(Moricz et al., 2018)
A. podagraria	HPLC	MeOH	Nucleosil-3C-18 column (100 mm × 4.6 mm)	MeCN (A) and H_2O (B) both containing 0.1% formic acid	/	Roots, leaves, stems, flowers	FaOH[b] 88 mg/g in flowers	(Prior et al., 2007)
A. maritima	HPLC	$CHCl_3$	Inertsil ODS-column (250 mm × 4.6 mm, 3.5 μm)	H_2O:MeOH (20:80)	480 nm	Roots	Pentayeneene 3.3%, thiarubrine A 2.6%, thiarubrine A epoxide 1.0%, and thiarubrine A diol	(AbouZid et al., 2007)

Table 2 (*continued*)

Source	Method	Extract solvent	Column	Mobile phase	Detection condition	Plant part	Remark	Reference
C. asiatica	HPLC	90% Aqueous MeOH	Symmetry 300™ C18 (150 mm × 3.9 mm, 5 μm)	H_2O (A) and MeCN (B)	/	Leaves	0.2%	(Randriamampionona et al., 2007)
L. inflata	HPLC	HCl: MeOH (1:1, *v*/*v*)	Hypersil MOS column (250 mm × 4 mm)	H_2O (A) and MeCN (B).	270 nm	Hairy roots	Lobetyolin 3.6% and lobetyolinin 0.8–1.6%	(Bálványos et al., 2004)
P. pseudo-ginseng subsp. *pseudo-ginseng*	HPLC	EtOAc	YMC-Pack A-612 (NH_2) (150 mm × 6 mm)	MeOH:H_2O (80:20)	202 nm	Roots, rhizomes	FaOH[b] 0.028%	(Tanaka et al., 2000)
Panax species (*white ginseng*; *red ginseng*; *P. Japonicus*; *P. Noteginseng*)	HPLC	MeOH	LiChrosorb RP-18 (250 mm × 4.6 mm)	H_2O (A) and MeCN / MeOH (B)	254 nm	Roots	TP[f] content of *white ginseng* 0.020–0.073%, *red ginseng* 0.019–0.055%, *P. quinquefolium* 0.067–0.080%, *P. japonicus* 0.004–0.006%, and *P. noteginseng* 0.045–0.056%	(Washida and Kitanaka 2003)
D. carota; *P. satica*	HPLC-UV	MeCN	Luna C18 column (4.6 mm, 5 μm)	H_2O (A) and MeCN (B)	205 nm	Roots	Carrots: FaDOH[d] 158.3 mg/kg, FaDOAc[a] 55.5 mg/kg, FaOH[c] 277.5 mg/kg; Parsnips: FaDOH[d] 252.1 mg/kg, FaOH[b] 330.7 mg/kg in parsnips	(Koidis et al., 2012)
C. taxa; *C. pilosula*; *C. pilosula* var. modesta and *C. tangshen*	HPLC-DAD	MeOH	YMC-Pack Pro-C18 column (250 mm × 4.6 mm, 5 μm)	MeCN (A) and 0.1 % (*v*/*v*) phosphoric acid H_2O (B)	215 nm	Roots	*C. pilosula:* lobetyolin 0.034–0.720 mg/g; *C. pilosula* var. modesta: lobetyolin 0.008–1.302 mg/g	(He et al., 2014)
A. graveolens	HPLC-DAD	CH_2Cl_2	Zorbax Rx-C18 (150 mm × 4.6 mm, 3.5 μm)	H_2O (A) and MeCN (B)	205 nm	Roots	/	(Zidorn et al., 2005)
P. sativa	HPLC/LC-Q-TOF-MS	MeCN	Phenomenex Luna C18 columns (100 mm × 4.6 mm, 5 μm; 100 mm × 2 mm, 2.5 μm)	H_2O (A) and MeCN (B)	205 nm; *m*/*z* 100–1000	Roots	/	(Rawson et al., 2010)
A. macrocephala or *A. japonica*	HPLC/ESI-MS	MeOH	INNO C18 column (250 mm × 4.6 mm, 5 μm)	MeCN (A) and H_2O (B) both containing 0.1% formic acid	254 nm	Roots	/	(Kim et al., 2018)
Radix Bupleuri	UHPLC-DAD/ESI-MS	Serum samples	Acquity BEH C18 column (50 mm × 2.1 mm, 1.7 μm)	0.1% formic acid H_2O (A) and MeCN (B)	ESI probe in both positive and negative ion modes	Roots	/	(Gao et al., 2020)
A. membranaceus and *C. pilosula*	UPLC-Q-TOF-MS	H_2O	Acquity BEH C18 (100 mm × 2.1 mm, 1.7 μm)	H_2O (A) and MeCN (B) both containing 0.1% (*v*/*v*) formic acid	*m*/*z* 100–1700 in negative mode and 50–1600 in positive	Roots	/	(Chau et al., 2016)

(*continued on next page*)

Table 2 (*continued*)

Source	Method	Extract solvent	Column	Mobile phase	Detection condition	Plant part	Remark	Reference
					mode			
O. horridus	UPLC/Q-TOF-MS	Human fecal specimens	Waters Acquity UPLC HSS C8 column (100 mm × 2.1 mm, 1.7 μm)	0.1% formic acid H_2O (A) and MeCN (B)	Dual electrospray ionization (ESI) source	Root bark	/	(Wang et al., 2020)
C. pilosula	UPLC-MS/MS	Rat plasma	ZORBAX Extend-C18 column (100 mm × 2.1 mm, 1.8 μm)	MeCN (A) and H_2O (B) both containing 0.1% formic acid	278 nm	Roots	/	(Dong et al., 2021)
M. chamomilla	UHPLC-PDA-Q-TOF-MS	MeOH	Acquity UPLCTM BEH Shield RP18 column (100 mm × 2.1 mm, 1.7 μm)	H_2O (A) and MeCN (B) both containing 0.05% formic acid	*m*/*z* 50–1500; 190–600 nm	Whole plant	/	(Avula et al., 2014)
B. gardneri	LC-ESI-MS	CH_2Cl_2 and EtOAc	Onyx C18 (15 mm × 4.6 mm)	H_2O (A) and MeCN (B) both added 1% (*v*/*v*) acetic acid	/	Leaves, stems	/	(Silva et al., 2015)
P. grandiflorum	HR-TOF-MS	MeOH	Agilent ZORBAX® SB-C18 column (150 mm × 4.6 mm, 5 μm)	H_2O (A) and MeCN (B)	DAD:210 nm	Roots	/	(Chen et al., 2018)
T. procumbens	GC-FID	Hexane	HP-5 capiliary columns (5% phenylmethylsiloxane, 30 m × 0.320 mm, 0.25 μm)	N_2	/	Roots, stems, leaves, flowers, fruits	/	(Larque-Garcia et al., 2020)
C. acaulis	GC-FID	EtOH	HP-5 capillary column (30 m × 0.32 mm, 0.25 μm)	He	/	Plant material	/	(Strzemski et al., 2019)
E. bannaticus and *E. sphaerocephalus*	GC–MS	Et_2O	DB-5MS capiliary columns (5% phenylmethylsiloxane, 30 m × 0.25 mm, 0.25 mm)	He	RI: C_7–C_{40} alkanes	Roots	/	(Radulovic and Denic 2013)
E. yuccifolium	GC–MS	Essential oil	Chrompack CPSil 5 CB capillary column (polydimethylsiloxane, 25 m)	He	/	Whole plants	Leaves oil: FaOH[b] 9.6%; stalk oil: FaOH[b] 3.2%	(Ayoub et al., 2006)
S. africana	GC–MS	Essential oil	BP-1 capillary column (polydimethylsiloxane, 50 m × 0.22 mm, 0.25 μm); BP-20 capillary column (polyethylene glycol, 50 m × 0.22 mm, 0.25 μm)	GC: H_2; MS: He	/	Aerial parts	(*E*)-2-(2′,4′-Hexadiynylidene)-1,6-dioxaspiro [4.4]-nona-3,7-diene (7.3%) (*E*)-tonghaosu 3.8%	(Malti et al., 2019)

Table 2 (*continued*)

Source	Method	Extract solvent	Column	Mobile phase	Detection condition	Plant part	Remark	Reference
P. ginseng, *ginseng*, *notoginseng*, *American ginseng*	GC-EI-MS	*n*-Hexane	DM-1 MS column (30 mm × 0.25 mm, 0.25 μm)	He	SIM *m/z*: 159, 121	Roots	FaOH[b] 84.2–261.8 μg/g and panaxydol 102.7–247.4 μg/g	(Liu et al., 2007)
E. palmatum	GC-FID and GC–MS	CH_2Cl_2	HP-5 MS column (30 m × 0.25 mm, 0.25 μm)	He	*m/z* 35–550, RI: *n*-alkanes (C_8–C_{20} and C_{21}–C_{40})	Aerial parts, roots	/	(Marčetić et al., 2014)
S. tenuifolium	GC-FID and GC–MS	Essential oil	Elite-5 MS capillary column (30 m × 0.32 mm, 0.32 mm)	He	RI: *n*-alkane series (C_6–C_{32})	Underground parts	/	(Chauhan et al., 2012)

[a] FaDOAc, Falcarindiol-3-acetate; [b] FaOH, Falcarinol; [c] DW, dry weight; [d] FaDOH, Falcarindiol; [e] FW, fresh weight; [f] TP, Total polyacetylenoids.

(Larque-Garcia et al., 2020). Recently, a situ effect-directed analysis by integrating HPTLC, chemical derivatization, and high-resolution mass spectrometry (HRMS) detection (HPTLC-UV/Vis/FLD-EDA-HRMS) was developed to profile and identify the antibacterial polyacetylenoids in root extracts of tansy (Moricz et al., 2018).

4.3. HPLC and UHPLC analyses

4.3.1. In vitro analysis

Till now, HPLC and UHPLC have been two of the most common techniques for quality assessment of the plant-originated polyacetylenoids, due to their availability, ease of operation, high sensitivity and reproducibility, good resolution and linearity, and the ability to analyze multiple components in a single run. For HPLC and UHPLC analyses of these polyacetylenoids, the most frequently equipped column for the separation is the RP-C_{18} columns, including Onyx C18 (Silva et al., 2015), Acquity BEH C18 (Chau et al., 2016), Ascentis Express C18 (Tacchini et al., 2017), Zorbax RX-C18 (Hinds et al., 2017), INNO C18 (Kim et al., 2018), Phenomenex Luna C18 (Chen et al., 2020), and Agilent ZORBAX SB-C18 (Chen et al., 2021), with methanol–water or acetonitrile–water containing 0.1–0.3% formic acid, acetic acid or phosphoric acid as the mobile phases. Notably, the use of acetic acid or phosphoric acid in the mobile phase not only afforded a satisfactory baseline that led to MS spectra of higher quality, but also produced many clusters, which were used for internal calibration to allow the molecular formulae of polyacetylenoids to be easily found (Silva et al., 2015). PDA and/or MS were used as the common detectors, and ESI and atmospheric pressure chemical ionization (APCI) was commonly used as the ion sources for MS detection. However, UV detection seems more suitable than ESI-MS for polyacetylenoids, because of the lack of low ionization by ESI, which requires high concentrations of the target compound in the samples to produce satisfactory results.

In order to improve the ionization for ESI detection of polyacetylenoids, a post-column sodiation is often used to show a good MS spectrum. Since ion suppression can happen in the ESI source, the added sodium must be low and carefully controlled. Polyacetylenoids present the electron pairs (non-bounded) of oxygen in their chemical structures that can interact with metals hence they show preferentially sodiated ions. The coordination reactions of polyacetylenoids with sodium can take place by oxygen of sugar, or even the oxygen from the polyacetylenic aglycone (Silva et al., 2015). Actually, polyacetylenoids are non-detectable among the deprotonated molecular ions $[M - H]^-$, thus, the electrospray ionization in positive ion mode (ESI^+) seems a good choice for the detection of the polyacetylenoids (Soltoft et al., 2010; Wen-Chin et al., 2013), which showed $[M + H]^+$ and $[M + Na]^+$ ions, as well as some other fragment ions, such as $[M - H_2O + H]^+$ and $[M + H - CH_3COOH]^+$ (Huang et al., 2011). Amongst them, the $[M + H]^+$ ions showed lower abundance than the $[M - H_2O + H]^+$ ions due to the easy dehydration of the protonated molecular ion for those hydroxylated polyacetylenoids, such as falcarinol (FaOH), falcarindiol (FaDOH) and falcarindiol-3-acetate (FaDOAc). For example, the relative abundances of the $[FaDOH + H]^+$ ion and the $[FaDOAc + H]^+$ ion were only 2 and 9%, respectively, while

the $[FaOH + H]^+$ ion couldn't be observed in the (+)-ESI mode. Instead, $[M - H_2O + H]^+$ ions of FaDOH and FaDOAc showed abundances of 75–100% and a more modest 21% for that of FaOH (Soltoft et al., 2010). Interestingly, dimeric ion species were predominant in the ESI spectrum of falcarinol, recorded with the mobile phase containing MeOH. From the foregoing, a positive ESI detection with a mobile phase of MeCN-H_2O-0.1% HCOOH was found to be most appropriate for the determination of FaOH, with the ion adduct at *m/z* 268 $[FaOH + H - H_2O + MeCN]^+$ in 100% relevant abundance, together with those at *m/z* 309 $[FaOH + H - H_2O + 2MeCN]^+$, 182 $[FaOH + H - H_2O - C_6H_{14} + MeCN]^+$, and etc. in lower relevant abundances (Pferschy-Wenzig et al., 2009).

Nevertheless, the MS spectrometric behaviour of FaOH, FaDOH and FaDOAc was comprehensively studied by ionization using an APCI interface in the positive ionization mode, with methanol–water as the mobile phase. For FaOH, no ionization at all was observed in APCI detection with MeCN-containing mobile phases, while a MeOH eluted APCI detection yielded rather complex MS spectra, with *m/z* 259 $[FaOH + H - H_2O + MeOH]^+$ and 227 $[FaOH + H - H_2O]^+$ as the most abundant ion adducts, accompanied with a considerable degree of the usually concentration-dependent dimeric ion species. Therefore, a linear calibration curve over a wide concentration range is quite difficult to obtain (Pferschy-Wenzig et al., 2009). Incredibly, FaOH generated an ion at *m/z* 243 $[M - 1]^+$, suggesting either a hydride subtraction $[M - H]^+$ or a dehydrogenation of the protonated molecule ion $[(M + H) - H_2]^+$ (Kramer et al., 2011).

4.3.2. Pharmacokinetics analysis

For those active polyacetylenoids, finding out their half-life, bioavailability, toxicity, and other pharmacokinetic (PK) properties would help us understand how the body may respond to the intake of the polyacetylenoids. Recently, UPLC-PDA, UHPLC-Q Extractive Orbitrap MS/MS, or UPLC/Q-TOF-MS method has been successfully applied to study the pharmacokinetic and biotransformation properties of plant polyacetylenoids (Lee et al., 2010; Avula et al., 2014; Dong et al., 2021; Xie et al., 2023). Four polyacetylenoids, including compounds **341** [(2*Z*,8*E*,10*E*)-pentadecatriene-4,6-diyn-1-ol], **107** (bupleurynol), **340** [(2*Z*,8*Z*,10*E*)-pentadecatriene-4,6-diyne-1-ol], and **104** [(2*Z*,8*Z*,10*E*)-heptadecatriene-4,6-diyne-1-ol], could be detected in rat serum after a single intragastric (i.g.) administration of the petroleum ether extract (22.5, 45.0, 90.0 g/kg) of *Radix Bupleuri* to rats. Among them, **341** and **107** showed a fast distribution phase followed by a relatively slow elimination phase ($t_{1/2z}$, 4–7 h), however, **340** and **104** could not be detected in rat serum. The reason for this may be either the existence of the less stable *Z*-configuration of C8/C9 in their structures, which may undergo a *trans*-isomerism *in vivo*, or the limitation of their original contents in *Radix Bupleuri* (Liu et al., 2015). The major biotransformation routes of **341** and **107** involved oxidation and glucuronidation as indicated by the combined analytical results of UHPLC-Q Extractive Orbitrap MS/MS and Compound Discoverer 2.0, which can facilitate us the understanding of an individual's response and accomplishing the drug–drug interaction prediction for us (Gao et al., 2020).

Furthermore, by applying UPLC/Q-TOF-MS analysis, 37 metabolites could be identified from the biotransformed *Oplopanax horridus* extract (OHE) with the enteric microbiome of healthy human subjects. Among the seven polyacetylenoids originally identified in OHE, only oplopantriol A (**206a**) was detected to be extensively biotransformed (94.7%), and demethylation and dehydroxylation may be the two major metabolic pathways. All these microbial metabolites are more hydrophobic than the parent oplopantriol A, and are expected to show more potent anticancer activity than their parent compound (Wang et al., 2020). Another, Xie *et al*. established a rapid, sensitive, and selective UPLC-MS/MS method for the simultaneous quantitative and semi-quantitative determination of the rat metabolites of lobetyol (**148**). As a result, a total of 47, 30 and 34 metabolites of lobetyol, lobetyolin (**149**) and lobetyolinin (**151**), respectively, were found in all the rat liver microsomes (RLMs), human liver microsomes (HLMs), and rat plasma, bile, feces, and urine samples, concerning mainly the metabolic pathways of oxidation, glucuronidation and glutathione conjugation (Xie et al., 2023).

UPLC–MS/MS Method has also been developed to evaluate the pharmacokinetic properties of polyacetylenoid monomers *in vivo*. In rat plasma, after administration of lobetyolin and *Codonopsis pilosula* extract (CPE), the elimination half-times ($t_{1/2}$) and the areas under the concentration–time curve were statistically different between the two treatments, but there was no significant difference between them in the time to reach the maximum plasma concentration (T_{max}) and the maximum concentration (C_{max}). Notably, the bioavailability of lobetyolin (3.90%) was lower than CPE's (6.97%), indicating that this compound may either be absorbed poorly or metabolized extensively in rats. Therefore, the methods to enhance its oral absorption should be further studied (Dong et al., 2021). Using the similar method, the pharmacokinetics of falcarinol (**19**) was elucidated *in vivo*. Falcarinol had a half-life of 1.5 hr. after an intravenous injection (5 mg/kg), while 5.9 hr. after an oral administration (20 mg/kg) with a moderate bioavailability of 50.4%. Falcarinol also shows a low metabolism and slow absorption in the clue of its highly lipid-soluble property (Tashkandi et al., 2020).

4.4. GC analysis

Gas chromatography (GC), coupled with a FID and/or a EI-MS detection, has been most frequently adopted to detect the polyacetylenic components in volatile (essential) oils or nonpolar extracts of the terrestrial medicinal plants. Separation of the polyacetylenoids can be achieved on various types of fused silica gel capillary GC columns including DB-5MS (Park et al., 2013; Radulovic and Denic 2013; Wnorowski et al., 2020), DM-1 (Liu et al., 2007; Wang et al., 2010), RTX-5 (Chien et al., 2009), Elite-5 (Chauhan et al., 2012), SPB-1 (de Carvalho Augusto et al., 2020) and HP-5 (Benelli et al., 2020; Larque-Garcia et al., 2020), coated with 5% phenylmethylsiloxane (Benelli et al., 2020) or cross-linked methylsiloxane (Wang et al., 2010). Compared with HPLC/UHPLC-UV method, GC–MS has much lower LOD and

LOQ, assuring its suitability for the analysis of such polyacetylenoids with extremely low abundance in plants as exemplified by ginseng (Liu et al., 2007). Quantitative analysis of them was carried out in selected ion monitoring (SIM) mode, in whose chromatograms seldom interference was found near the peaks of compounds, allowing accurate determination. Then, ions at m/z 159 and m/z 121 were selected for scanning with the aim of the detection of falcarinol and panaxydol, respectively (Liu et al., 2007; Wang et al., 2010).

In addition to the above, Strzemski *et al*. established a fast and low-cost voltammetric methodology for determination of carlina oxide (**479**), one major volatile constituent of *Carlina* plants. The results were quite similar to those obtained using HPLC and GC methods, with the differences in mean contents < 8.51%, and the values of relative standard deviation obtained for all analyzed samples were 1.5–3.1% (< 5%), revealing excellent repeatability of the method (Strzemski et al., 2019).

5. Pharmacology

Falcarinol-type polyacetylenoids are widely present in vegetables including carrots and parsley, and some food-medicine herbs as exemplified by *P. ginseng* and *C. pilosula*. They exert diverse pharmacological actions and hold potential as health-promoting and therapeutic agents (P Christensen 2011). For example, falcarinol and falcarindiol, both exhibit anti-inflammatory, anti-tumor, hepatoprotective and some other interesting bioactivities. Besides, other types of polyacetylenoids including lobetylolin, lobetyol and panaxytriol were frequently reported to possess beneficial pharmacological activities against cancer (colorectal cancer, lung cancer, gastric cancer, etc.) (Bailly, 2020; Kobaek-Larsen et al., 2017; Liu et al., 2022). Herein, we try to draw a brief outline of the latest pharmacological achievements on the fore-mentioned falcarinol- and lobetyol-types of polyacetylenoids.

5.1. Falcarinol and falcarindiol

Falcarinol could upregulate intestinal heme oxygenase-1 and modify plasma cytokine IL-4, IL-13, IL-9 and IL-10 profile in late-phase lipopolysaccharide (LPS)-induced acute inflammation in C57BL/6 mice. Hence, a diet rich in falcarinol is anti-inflammatory, immunomodulatory and can have beneficial effects on inflammatory gastrointestinal as well as other inflammatory disorders (Stefanson and Bakovic 2020).

Notably, dietary supplements with falcarinol and falcarindiol reduced the number of neoplastic lesions as well as the growth rate of the polyps, suggesting a preventive effect of falcarinol and falcarindiol on the development of colorectal cancer (Kobaek-Larsen et al., 2017). And, falcarinol and falcarindiol isolated from *Daucus carota* could prevent the formation of colon tumor induced by azomethane in rats (Kobaek-Larsen et al., 2017). Furthermore, orally administered falcarinol significantly reduced lung tumorigenesis in KrasG12D/ñ transgenic mice and mice carrying NSCLC xenografts without detectable toxicity, as a novel natural Hsp90 inhibitor that effectively eliminates both non-CSC (cancer stem-like cells) and CSC populations of NSCLC (Non-small cell lung cancer) by blocking *N*- and *C*-terminal ATP pockets without inducing Hsp70 expression (Le et al., 2018).

5.2. Lobetylolin, lobetyol and panaxytriol

Lobetyolin (LBT) suppressed lung cancer in a mouse model by inhibiting epithelial-mesenchymal transition (Liu et al., 2022). Xanthine oxidase (XO) catalyzes the formation of uric acid from xanthine, concerning a critical metabolic pathway related to hyperuricemia and gout. Oral administration of LBT at 50 mg/kg significantly reduced the activity of hepatic XO *in vivo* (Yoon and Cho 2021).

A recent study has revealed a key aspect of the mode of action of LBT, with the discovery of the capacity of the compound to inhibit glutamine metabolism and specifically, to down-regulate the amino acid transporter ASCT2, in a p53-dependent manner. Human ASCT2 is a trimeric protein (also known as SLC1A5) acting as a sodium-dependent neutral amino acid antiporter. Its transport activity can be modulated by lipophilic molecules, like the antagonist V-9302 which is a potent anticancer agent, sulfonamide/sulfonic acid esters linked to a hydrophobic group, and cholesterol. Given the diverse functional roles of hASCT2, the blockade of this transporter can have multiple implications in human diseases, not only in cancer. Interestingly, LBT-containing extracts and TCM prescriptions (eg. Weikang Keli), lobetyol, and other polyacetylenoids structurally close to lobetyol, such as 4,6,12-tetradecatriene-8,10-diyne-1,3,14-triol and panaxytriol, were demonstrated to show significant inhibitory activities against gastric cancer lines. Nowadays, efficient treatments are lacking for advanced gastric cancer. Thus, it would be worth a lot to investigate the further therapeutic potential of such polyacetylenoid glycosides in this indication (Bailly, 2020; He et al., 2020).

6. Conclusion and discussion

6.1. Conclusion

This review covers the research updates on the polyacetylenic phytochemicals and their distribution, botanic origins, NMR characteristics and analytical methods, as well as a brief bioactivity sketch of some representative polyacetylenoids in terrestrial medicinal plants by excavating various literature dating from 2000 to 2023. Herein, 363 linear polyacetylenoids and 122 cyclic ones with chain lengths of $C_{8–19}$, C_{21}, $C_{23–25}$, C_{27}, C_{29}, and C_{33}, have been collated from the terrestrial medicinal plants, belonging mostly to the families of Compositae, Apiaceae, Araliaceae, Campanulaceae, Annonaceae, and Meliaceae. Their molecular scaffolds occurred mainly to be the polyacetylenoids with carbon lengths of C_{17}, C_{14}, C_{18}, C_{10}, C_{13}, C_{15}, with 14 main types of polyacetylenic terminals. And their representative NMR characteristics and the determination methods of the related configurations have also been included. Further, the analytical methods of polyacetylenoid compounds and/or extracts are summarized. HPLC, UHPLC and GC analysis, as well as the co-location technology, have been widely used for *in vitro* or *in vivo* determination and quantification of the polyacetylenoids. And finally, the plant origins and a brief outline of the bioactivities of several representative polyacetylenoids were also referred to in this Review.

6.2. Discussion

6.2.1. Polyacetylenic phytochemicals and their distribution

In the last two decades, more than 485 polyacetylenoids have been isolated from almost 110 kinds of terrestrial herbs. Linear polyacetylenoids dominate about 85% of all the 485 polyacetylenoids, with C_{17}-polyacetylenoids ranked in the top 1. The moiety of hepta-4,6-diyne is normally embedded in their polyacetylenic terminals. As is known, plant polyacetylenoids are widely distributed in plants of families Compositae and Apiaceae. Not very early, due to the low contents in their botanical origins, they come to people's attention on account of their intrinsic special triple-bond functionalities and fatty acid-like carbon chains. In view of biosynthesis pathways, most of them are falciferol-derived, showing anticancer and other diverse pharmacological activities. It is worth noting that polyacetylenoid glycosides hold important potential as one of the anti-tumor active ingredients for future anti-tumor compounds and traditional Chinese medicine preparations.

6.2.2. Analytical methods and quality control

As shown in Table 2, common analytical methods of plant polyacetylenoids were summarized and HPLC-MS, UHPLC-MS and GC–MS represented the main methods ever reported. Several well-known active polyacetylenoids including falcarinol, falcarindiol, falcarindiol-3-acetate, lobetyol, lobetyolin, and lobetyolinin, have been frequently selected out as the maker components for both qualitative determination and quantitative analysis of those specific herbs, considering their valuable bioactivities *in vitro* and/or *in vivo*. Several studies had revealed that the ratio of polyacetylenoids such as panaxydol/falcarinol can be proposed as an important marker for differentiating *Asian ginseng, Notoginseng, and* cultivated *American ginseng*, indicating that analysis of the ratios of the major polyacetylenoid constituents, to some extent, may supply a guideline for distinguishing certified herbs from their counterfeit species (Wang et al., 2010).

Unfortunately, they are unstable and highly lipophilic, their low metabolism and slow absorption *in vivo* as exemplified by falcarinol and lobetyolin are key problems to be overcome for future in-depth exploitation (Tashkandi et al., 2020; Dong et al., 2021). Hence, there is still an urgent need for highly rapid, convenient, and cost-effective methods, artificial synthesis, biosynthesis, and phytochemical separation for high production of active and structurally stable polyacetylenoids to light their pharmacological effects. Moreover, their plasma concentrations for exerting biological functions *in vivo* are still unclear.

6.2.3. Pharmacology of polyacetylenoids

As reviewed by Negri, Xie and Wang (Negri 2015; Xie and Wang 2022), at the current stage, *in-vivo* preclinical studies are still needed as they play essential and vital roles in the assessment and supervision of the clinical functions of those polyacetylenoids. Up-to-date laboratory researches, especially *in vitro* evaluations at the cellular level, on the pharmacological properties of polyacetylenoids are extensive. However, there are few *in-vivo* scale pharmacological and pharmacokinetic studies on the active plant polyacetylenoids, as bioavailability and metabolism of the polyacetylenoids are critically important for future research and development of such drugs.

Studies have shown that a generous intake of fruits and vegetables can promote people's health. And aliphatic C_{17} polyacetylenoids, represented by the common falcarinol-type polyacetylenoids abundant in foods, fruits and vegetables of the family Apiaceae, may act as the potential functional molecules promoting the consumer's health. As far as we know, there are still numerous falcarinol-type polyacetylenoids that have not been fully studied due to their unavailable production in larger amounts, although some of them have been tested out to show favorable anticancer or anti-tumor activities. Therefore, in addition to conducting more and more *in-vivo* preclinical studies and even trials in the clinic to achieve the ideal intake dosage for health-promoting effects, there is also a necessary to improve their bioavailability by structural modification or synthesize methods, as well as their yield in plants (foods, fruits, or vegetables) by developing new genotypes and/or processing techniques (*eg*. large-scale extraction and isolation) (Christensen 2011).

Currently, polyacetylenoids in red ginseng extract composed of panaxynol and panaxydol has furtherly been found to possess beauty-related bioactivities such as skin care and hair generation, by alleviating even eliminating the symptoms of acne (Hou et al., 2019). And, hydroxylated polyacetylenoids isolated from *P. ginseng* may provide therapeutic benefits for hair growth disorders (*eg*. alopecia) by inhibiting neurotrophins from binding to the receptors (Suzuki et al., 2017). Therefore, in addition to the abovementioned health-promoting, skin care, and hair generation potentials, it is speculated that polyacetylenoids will possess good research prospect and important value in applications as perfume, appetite enhancer and natural preservative (Xie and Wang 2022). And, polyacetylenoids from terrestrial medicinal plants show great future potentials to be developed into health care products and new drugs in treatment of a wide array of pathologies.

Author contributions

The idea of putting forward innovative ideas and summarizing the whole review were done by Hong-Hua Wu. Jia-Xin Lai and Su-Fang Dai collated documents and summarize objective laws cooperatively. Jia-Xin Lai was responsible for drafting the manuscript with critical suggestions from Hong-Hua Wu. Li-Hua Zhang, Yan-Xu. Chang and Wen-Zhi. Yang assisted with the revision of the manuscript.

Declaration of Competing Interest

The authors declare that they have no known competing financial interests or personal relationships that could have appeared to influence the work reported in this paper.

Acknowledgments

This work was financially supported by grants (No. 21ZYJDJC00080 and 22ZYJDSS00040) from the Tianjin Committee of Science and Technology of China and a grant (No. 62231025) from the Major Program of National Natural Science Foundation of China.

Appendix A. Supplementary material

Supplementary data to this article can be found online at https://doi.org/10.1016/j.arabjc.2023.105137.

References

AbouZid, S., Orihara, Y., Kawanaka, M., 2007. Molluscicidal activity of polyacetylenes from *Ambrosia maritima* hairy roots. Nat. Prod. Commun. 2, 177–180. https://doi.org/10.1177/1934578X0700200214.

Aguilo-Aguayo, I., Brunton, N., Rai, D.K., et al, 2014. Polyacetylene levels in carrot juice, effect of pH and thermal processing. Food Chem. 152, 370–377. https://doi.org/10.1016/j.foodchem.2013.11.146.

Ahmed, A.A., Bishr, M.M., El-Shanawany, M.A., et al, 2005. Rare trisubstituted sesquiterpenes daucanes from the wild *Daucus carota*. Phytochemistry 66, 1680–1684. https://doi.org/10.1016/j.phytochem.2005.05.010.

Appendino, G., Pollastro, F., Verotta, L., et al, 2009. Polyacetylenes from sardinian *Oenanthe fistulosa*: a molecular clue to risus sardonicus. J. Nat. Prod. 72, 962–965. https://doi.org/10.1021/np8007717.

Avonto, C., Rua, D., Lasonkar, P.B., et al, 2017. Identification of a compound isolated from German chamomile (*Matricaria chamomilla*) with dermal sensitization potential. Toxicol. Appl. Pharmacol. 318, 16–22. https://doi.org/10.1016/j.taap.2017.01.009.

Avula, B., Wang, Y.H., Wang, M., et al, 2014. Quantitative determination of phenolic compounds by UHPLC-UV-MS and use of partial least-square discriminant analysis to differentiate chemo-types of Chamomile/Chrysanthemum flower heads. J. Pharm. Biomed. Anal. 88, 278–288. https://doi.org/10.1016/j.jpba.2013.08.037.

Ayoub, N., Al-Azizi, M., König, W., et al, 2006. Essential oils and a novel polyacetylene from *Eryngium yuccifolium* Michaux. (Apiaceae). Flavour Fragrance J. 21, 864–868. https://doi.org/10.1002/ffj.1631.

Baek, S.C., Yi, S.A., Lee, B.S., et al, 2021. Anti-adipogenic polyacetylene glycosides from the florets of Safflower (*Carthamus tinctorius*). Biomedicines 9. https://doi.org/10.3390/biomedicines9010091.

Bailly, C., 2020. Anticancer properties of lobetyolin, an essential component of radix *Codonopsis* (Dangshen). Nat. Prod. Bioprospect. 11, 143–153. https://doi.org/10.1007/s13659-020-00283-9.

Bálványos, I., Kursinszki, L., Bányai, P., et al, 2004. Analysis of polyacetylenes by HPLC in hairy root cultures of *Lobelia inflata* cultivated in bioreactor. Chromatographia 60, S235–S238. https://doi.org/10.1365/s10337-004-0188-x.

Baranska, M., Schulz, H., Christensen, L.P., 2006. Structural changes of polyacetylenes in American ginseng root can be observed in situ by using Raman spectroscopy. J. Agric. Food Chem. 54, 3629–3635. https://doi.org/10.1021/jf060422d.

Baur, R., Simmen, U., Senn, M., et al, 2005. Novel plant substances acting as beta subunit isoform-selective positive allosteric modulators of GABAA receptors. Mol. Pharmacol. 68, 787–792. https://doi.org/10.1124/mol.105.011882.

Benelli, G., Pavoni, L., Zeni, V., et al, 2020. Developing a highly stable carlina acaulis essential oil nanoemulsion for managing *Lobesia botrana*. Nanomater. (Basel) 10. https://doi.org/10.3390/nano10091867.

Bijttebier, S., D'Hondt, E., Noten, B., et al, 2014. Automated analytical standard production with supercritical fluid chromatography for the quantification of bioactive C17-polyacetylenes: A case study on food processing waste. Food Chem. 165, 371–378. https://doi.org/10.1016/j.foodchem.2014.05.093.

Blunder, M., Liu, X., Kunert, O., et al, 2014. Polyacetylenes from radix et rhizoma *Notopterygii incisi* with an inhibitory effect on nitric oxide production *in vitro*. Planta Med. 80, 415–418. https://doi.org/10.1055/s-0034-1368196.

Bouzergoune, F., Ciavatta, M.L., Bitam, F., et al, 2016. Phytochemical study of *Eryngium triquetrum*: isolation of polyacetylenes and lignans. Planta Med. 82, 1438–1445. https://doi.org/10.1055/s-0042-110316.

Buskuhl, H., Freitas, R.A., Monache, F.D., et al, 2009. A new polyacetylene from *Vernonia scorpioides* (Lam.) Pers. (Asteraceae) and its *in vitro* antitumoral activity. J. Braz. Chem. Soc. 20, 1327–1333. https://doi.org/10.1016/j.cbi.2017.11.003.

Butler, S.M., Wallig, M.A., Nho, C.W., et al, 2013. A polyacetylene-rich extract from *Gymnaster koraiensis* strongly inhibits colitis-associated colon cancer in mice. Food Chem. Toxicol. 53, 235–239. https://doi.org/10.1016/j.fct.2012.11.049.

Cao, T.Q., Vu, N.K., Woo, M.H., et al, 2020. New polyacetylene and other compounds from *Bupleurum chinense* and their chemotaxonomic significance. Biochem. Syst. Ecol. 92. https://doi.org/10.1016/j.bse.2020.104090.

Cavin, A., Potterat, O., Wolfender, J.L., et al, 1998. Use of on-flow LC/1H NMR for the study of an antioxidant fraction from *Orophea enneandra* and isolation of a polyacetylene, lignans, and a tocopherol derivative. J. Nat. Prod. 61 (12), 1497–1501. https://doi.org/10.1021/np980203p.

Chang, B.Y., Lee, S.K., Kim, D.E., et al, 2020. Effect of echinalkamide identified from *Echinacea purpurea* (L.) Moench on the inhibition of osteoclastogenesis and bone resorption. Sci. Rep. 10, 10914. https://doi.org/10.1038/s41598-020-67890-x.

Chauhan, R.S., Nautiyal, M.C., Tava, A., et al, 2012. Chemical composition of the volatile oil from the roots of *Selinum tenuifolium* Wall. Helvetica Chim. Acta 95, 780–787. https://doi.org/10.1002/hlca.201100480.

Chen, P.Y., Hsieh, M.J., Tsai, Y.T., et al, 2020. Transformation and characterization of delta12-fatty acid acetylenase and delta12-oleate desaturase potentially involved in the polyacetylene biosynthetic pathway from *Bidens pilosa*. Plants (Basel) 9. https://doi.org/10.3390/plants9111483.

Chen, B., Liu, Z., Zhang, Y., et al, 2018. Application of high-speed counter-current chromatography and HPLC to separate and purify of three polyacetylenes from *Platycodon grandiflorum*. J. Sep. Sci. 41, 789–796. https://doi.org/10.1002/jssc.201700767.

Chen, W.-H., Ma, X.-M., Wu, Q.-X., et al, 2008. Chemical-constituent diversity of *Tridax procumbens*. Can. J. Biochem. 86, 892–898. https://doi.org/10.1139/v08-097.

Chen, Y., Peng, S., Luo, Q., et al, 2015. Chemical and pharmacological progress on polyacetylenes isolated from the family apiaceae. Chem. Biodivers. 12, 474–502. https://doi.org/10.1002/cbdv.201300396.

Chen, Z., Tian, Z., Zhang, Y., et al, 2021. Separation of chemical constituents in *Bidens pilosa* Linn. var. radiata Sch. Bip. by elution-extrusion counter-current chromatography using two new three-phase solvent systems. J. Sep. Sci. 44, 3540–3550. https://doi.org/10.1002/jssc.202100330.

Cheung, S.S.C., Hasman, D., Khelifi, D., et al, 2019. Devil's club falcarinol-type polyacetylenes inhibit pancreatic cancer cell proliferation. Nutr. Cancer 71, 301–311. https://doi.org/10.1080/01635581.2018.1559931.

Chianese, G., Sirignano, C., Shokoohinia, Y., et al, 2018. TRPA1 modulating C(14) polyacetylenes from the iranian endemic plant *Echinophora platyloba*. Molecules 23. https://doi.org/10.3390/molecules23071750.

Chien, S.C., Young, P.H., Hsu, Y.J., et al, 2009. Anti-diabetic properties of three common *Bidens pilosa* variants in Taiwan. Phytochemistry 70, 1246–1254. https://doi.org/10.1016/j.phytochem.2009.07.011.

Chobot, V., Vytlačilová, J., Kubicová, L., et al, 2006. Phototoxic activity of a thiophene polyacetylene from *Leuzea carthamoides*. Fitoterapia 77, 194–198. https://doi.org/10.1016/j.fitote.2006.01.001.

Choi, Y.E., Ahn, H., Ryu, J.H., 2000. Polyacetylenes from *angelica gigas* and their inhibitory activity on nitric oxide synthesis in activated macrophages. Biol. Pharm. Bull. 23, 884–886. https://doi.org/10.1248/bpb.23.884.

Choi, H.G., Choi, H., Lee, J.-H., et al, 2016. Anti-inflammatory activity of a novel acetylene isolated from the roots of *Angelica tenuissima* Nakai. Helvetica Chim. Acta 99, 447–451. https://doi.org/10.1002/hlca.201500507.

Christensen, L.P., 2011. Aliphatic C(17)-polyacetylenes of the falcarinol type as potential health promoting compounds in food plants of the Apiaceae family. Recent Pat. Food Nutr. Agric. 3, 64–77. https://doi.org/10.2174/2212798411103010064.

Christensen, L.P., 2020. Bioactive C17 and C18 acetylenic oxylipins from terrestrial plants as potential lead compounds for anticancer drug development. Molecules 25, 2568. https://doi.org/10.3390/molecules25112568.

Christensen, L.P., Brandt, K., 2006. Bioactive polyacetylenes in food plants of the Apiaceae family: occurrence, bioactivity and analysis. J. Pharm. Biomed. Anal. 41, 683–693. https://doi.org/10.1016/j.jpba.2006.01.057.

Christensen, L.P., Kreutzmann, S., 2007. Determination of polyacetylenes in carrot roots (*Daucus carota* L.) by high-performance liquid chromatography coupled with diode array detection. J. Sep. Sci. 30, 483–490. https://doi.org/10.1002/jssc.200600325.

Christensen, L.P., Jensen, M., Kidmose, U., 2006. Simultaneous determination of ginsenosides and polyacetylenes in American ginseng root (*Panax quinquefolium* L.) by high-performance liquid chromatography. J. Agric. Food Chem. 54, 8995–9003. https://doi.org/10.1021/jf062068p.

P Christensen, L., 2011. Aliphatic C17-polyacetylenes of the falcarinol type as potential health promoting compounds in food plants of the Apiaceae family. Recent Pat. Food, Nutr. Agric. 3, 64-77. https://doi.org/10.2174/2212798411103010064

Chau, S. L., Huang, Z. B., Song, Y. G., et al., 2016. Comprehensive quantitative analysis of SQ injection using multiple chromatographic technologies. molecules. 21, https://doi.org/10.3390/molecules21081092.

Chung, I.M., Song, H.K., Kim, S.J., et al, 2011. Anticomplement activity of polyacetylenes from leaves of *Dendropanax morbifera* Leveille. Phytother. Res. 25, 784–786. https://doi.org/10.1002/ptr.3336.

Chung, H.H., Ting, H.M., Wang, W.H., et al, 2021. Elucidation of enzymes involved in the biosynthetic pathway of bioactive polyacetylenes in *Bidens pilosa* using integrated omics approaches. J. Exp. Bot. 72, 525–541. https://doi.org/10.1093/jxb/eraa457.

Corell, M., Sheehy, E., Evans, P., et al, 2013. Absolute configuration of falcarinol (9*Z*-heptadeca-1,9-diene-4,6-diyn-3-ol) from *Pastinaca Sativa*. Nat. Prod. Commun. 8. https://doi.org/10.1177/1934578x1300800824.

Dall'Acqua, S., Maggi, F., Minesso, P., et al, 2010. Identification of non-alkaloid acetylcholinesterase inhibitors from *Ferulago campestris* (Besser) Grecescu (Apiaceae). Fitoterapia 81, 1208–1212. https://doi.org/10.1016/j.fitote.2010.08.003.

Dang, N.H., Zhang, X., Zheng, M., et al, 2005. Inhibitory constituents against cyclooxygenases from *Aralia cordata* Thunb. Arch. Pharm. Res. 28, 28–33. https://doi.org/10.1007/BF02975131.

Dat, N.T., Cai, X.F., Shen, Q., et al, 2005. Gymnasterkoreayne G, a new inhibitory polyacetylene against NFAT transcription factor from *Gymnaster koraiensis*. Chem. Pharm. Bull. (Tokyo) 53, 1194–1196. https://doi.org/10.1248/cpb.53.1194.

Dawid, C., Dunemann, F., Schwab, W., et al, 2015. Bioactive C17-polyacetylenes in carrots (*Daucus carota* L.): current knowledge and future perspectives. J. Agric. Food Chem. 63, 9211–9222. https://doi.org/10.1021/acs.jafc.5b04357.

De Carvalho Augusto, R., Merad, N., Rognon, A., et al, 2020. Molluscicidal and parasiticidal activities of *Eryngium triquetrum* essential oil on Schistosoma mansoni and its intermediate snail host Biomphalaria glabrata, a double impact. Parasit. Vectors 13, 486. https://doi.org/10.1186/s13071-020-04367-w.

Dembitsky, V.M., 2006. Anticancer activity of natural and synthetic acetylenic lipids. Lipids 41, 883–924. https://doi.org/10.1007/s11745-006-5044-3.

Djebara, A., Ciavatta, M.L., Mathieu, V., et al, 2019. Oxygenated C (17) polyacetylene metabolites from Algerian *Eryngium tricuspidatum* L. roots: structure and biological activity. Fitoterapia 138,. https://doi.org/10.1016/j.fitote.2019.104355 104355.

Dong, J., Cheng, M., Xue, R., et al, 2021. Comparative pharmacokinetic and bioavailability study of lobetyolin in rats after administration of lobetyolin and *Codonopsis pilosula* extract by ultra-performance LC-tandem mass spectrometry. Biomed. Chromatogr. 35, e5125. https://doi.org/10.1002/bmc.5125.

Emad, F., Khalafalah, A.K., El Sayed, M.A., et al, 2020. Three new polyacetylene glycosides (PAGs) from the aerial part of *Launaea capitata* (Asteraceae) with anti-biofilm activity against Staphylococcus aureus. Fitoterapia 143,. https://doi.org/10.1016/j.fitote.2020.104548 104548.

Feng, Z.M., Xu, K., Wang, W., et al, 2018. Two new thiophene polyacetylene glycosides from *Atractylodes lancea*. J. Asian Nat. Prod. Res. 20, 531–537. https://doi.org/10.1080/10286020.2018.1458841.

Feng, X., Zhong, G., Dengba, D., et al, 2017. Two new polyhydroxyl polyacetylenes from fruits of *Herpetospermum caudigerum*. J. Nat. Med. 71, 574–577. https://doi.org/10.1007/s11418-017-1079-4.

Fois, B., Bianco, G., Sonar, V.P., et al, 2017. Phenylpropenoids from *Bupleurum fruticosum* as anti-human rhinovirus species a selective capsid binders. J. Nat. Prod. 80, 2799–2806. https://doi.org/10.1021/acs.jnatprod.7b00648.

Fukuyama, N., Shibuya, M., Orihara, Y., 2012. Antimicrobial polyacetylenes from *Panax ginseng* hairy root culture. Chem. Pharm. Bull. (Tokyo) 60, 377–380. https://doi.org/10.1248/cpb.60.377.

Gafner, F., Epstein, W., Reynolds, G., et al, 1988. Human maximization test of falcarinol, the principal contact allergen of English ivy and Algerian ivy (Hedera helix, *H. canariensis*). Contact Dermatitis 19, 125–128. https://doi.org/10.1111/j.1600-0536.1988.tb05509.x.

Gao, Y., Mi, J., Zhang, C.L., et al, 2019. Three new polyacetylene glycosides from the roots of *Heracleum dissectum* and their triglyceride accumulating activities in 3T3-L1 cells. Chem. Biodivers. 16, e1800424.

Gao, X.X., Zhang, F., Xing, J., et al, 2020. Metabolic profiling of RB-2 and RB-4, two analogs of polyacetylene from *Bupleurum*. J. Asian Nat. Prod. Res. 22, 1045–1064. https://doi.org/10.1080/10286020.2019.1681409.

Geng, C.A., Huang, X.Y., Chen, X.L., et al, 2015. Three new anti-HBV active constituents from the traditional Chinese herb of Yin-Chen (*Artemisia scoparia*). J. Ethnopharmacol. 176, 109–117. https://doi.org/10.1016/j.jep.2015.10.032.

Govindan, G., Sambandan, T.G., Govindan, M., et al, 2007. A bioactive polyacetylene compound isolated from *Centella asiatica*. Planta Med. 73, 597–599. https://doi.org/10.1055/s-2007-981521.

Grant, C.V., Cai, S., Risinger, A.L., et al, 2020. CRISPR-Cas9 genome-wide knockout screen identifies mechanism of selective activity of dehydrofalcarinol in mesenchymal stem-like triple-negative breast cancer cells. J. Nat. Prod. 83, 3080–3092. https://doi.org/10.1021/acs.jnatprod.0c00642.

Gung, B.W., 2009. Total synthesis of polyyne natural products. Comptes Rendus Chim. 12, 489–505. https://doi.org/10.1016/j.crci.2008.08.014.

Guo, J., Wang, A., Yang, K., et al, 2017. Isolation, characterization and antimicrobial activities of polyacetylene glycosides from *Coreopsis tinctoria* Nutt. Phytochemistry 136, 65–69. https://doi.org/10.1016/j.phytochem.2016.12.023.

Hansen, L., Boll, P.M., 1986. Polyacetylenes in Araliaceae: their chemistry, biosynthesis and biological significance. Phytochemistry 25, 285–293. https://doi.org/10.1016/S0031-9422(00)85468-0.

Hansen, L., Hammershøy, O., Boll, P.M., 1986. Allergic contact dermatitis from falcarinol isolated from *Schefflera arboricola*. Contact Dermatitis 14, 91–93. https://doi.org/10.1111/j.1600-0536.1986.tb01167.x.

Hao, W., Xing-Jun, W., Yong-Yao, C., et al, 2005. Up-regulation of M1 muscarinic receptors expressed in CHOm1 cells by panaxynol via cAMP pathway. Neurosci. Lett. 383, 121–126. https://doi.org/10.1016/j.neulet.2005.03.062.

He, J., Shen, Y., Jiang, J.S., et al, 2011. New polyacetylene glucosides from the florets of *Carthamus tinctorius* and their weak anti-inflammatory activities. Carbohydr Res. 346, 1903–1908. https://doi.org/10.1016/j.carres.2011.06.015.

He, W., Tao, W., Zhang, F., et al, 2020. Lobetyolin induces apoptosis of colon cancer cells by inhibiting glutamine metabolism. J. Cell Mol. Med. 24, 3359–3369. https://doi.org/10.1111/jcmm.15009.

He, J.Y., Zhu, S., Goda, Y., et al, 2014. Quality evaluation of medicinally-used *Codonopsis* species and Codonopsis Radix based on the contents of pyrrolidine alkaloids, phenylpropanoid and polyacetylenes. J. Nat. Med. 68, 326–339. https://doi.org/10.1007/s11418-013-0801-0.

He, J.Y., Zhu, S., Komatsu, K., 2014. HPLC/UV analysis of polyacetylenes, phenylpropanoid and pyrrolidine alkaloids in medicinally used *Codonopsis* species. Phytochem. Anal. 25, 213–219. https://doi.org/10.1002/pca.2494a.

Herrmann, F., Hamoud, R., Sporer, F., et al, 2011. Carlina oxide–a natural polyacetylene from *Carlina acaulis* (Asteraceae) with potent antitrypanosomal and antimicrobial properties. Planta Med. 77, 1905–1911. https://doi.org/10.1055/s-0031-1279984.

Herrmann, F., Sporer, F., Tahrani, A., et al, 2013. Antitrypanosomal properties of *Panax ginseng* C. A. Meyer: new possibilities for a remarkable traditional drug. Phytother. Res. 27, 86–98. https://doi.org/10.1002/ptr.4692.

Hinds, L., Kenny, O., Hossain, M.B., et al, 2017. Evaluating the antibacterial properties of polyacetylene and glucosinolate compounds with further identification of their presence within various carrot (*Daucus carota*) and broccoli (*Brassica oleracea*) cultivars using high-performance liquid chromatography with a diode array detector and ultra performance liquid chromatography-tandem mass spectrometry analyses. J. Agric. Food Chem. 65, 7186–7191. https://doi.org/10.1021/acs.jafc.7b02029.

Hou, J.H., Shin, H., Jang, K.H., et al, 2019. Anti-acne properties of hydrophobic fraction of red ginseng (*Panax ginseng* CA Meyer) and its active components. Phytother. Res. 33, 584–590. https://doi.org/10.1002/ptr.6243.

Hu, H.-M., Bai, S.-M., Chen, L.-J., et al, 2018. Chemical constituents from *Bidens bipinnata* Linn. Biochem. Syst. Ecol. 79, 44–49. https://doi.org/10.1016/j.bse.2018.05.005.

Huang, H.Q., Su, J., Zhang, X., et al, 2011. Qualitative and quantitative determination of polyacetylenes in different *Bupleurum* species by high performance liquid chromatography with diode array detector and mass spectrometry. J. Chromatogr. A 1218, 1131–1138. https://doi.org/10.1016/j.chroma.2010.12.007.

Huang, H.-Q., Zhang, X., Shen, Y.-H., et al, 2009. Polyacetylenes from *Bupleurum longiradiatum*. J. Nat. Prod. 72, 2153–2157. https://doi.org/10.1021/np900534v.

Ishimaru, K., Osabe, M., Yan, L., et al, 2003. Polyacetylene glycosides from Pratia nummularia cultures. Phytochemistry 62, 643–646. https://doi.org/10.1016/S0031-9422(02)00669-6.

Ito, A., Cui, B., Chavez, D., et al, 2001. Cytotoxic polyacetylenes from the twigs of *Ochanostachys amentacea*. J. Nat. Prod. 64, 246–248. https://doi.org/10.1021/np000484c.

Ivarsen, E., Fretté, X.C., Christensen, K.B., et al, 2014. Bioassay-guided chromatographic isolation and identification of antibacterial compounds from *Artemisia annua* L. that inhibit Clostridium perfringens growth. J. AOAC Int. 97, 1282–1290. https://doi.org/10.5740/jaoacint.sgeivarsen.

Jelodarian, Z., Shokoohinia, Y., Rashidi, M., et al, 2017. New polyacetylenes from *Echinophora cinerea* (Boiss.) Hedge et Lamond. Nat. Prod. Res. 31, 2256–2263. https://doi.org/10.1080/14786419.2017.1300797.

Jeong, D., Dong, G.Z., Lee, H.J., et al, 2019. Anti-inflammatory compounds from *Atractylodes macrocephala*. Molecules 24. https://doi.org/10.3390/molecules24101859.

Jeong, G.S., Kwon, O.K., Park, B.Y., et al, 2007. Lignans and coumarins from the roots of *Anthriscus sylvestris* and their increase of caspase-3 activity in HL-60 cells. Biol. Pharm. Bull. 30, 1340–1343. https://doi.org/10.1248/bpb.30.1340.

Ji, Y., Feng, X., Xiao, C.C., et al, 2010. A new polyacetylene glycoside from the rhizomes of *Atractylodes lancea*. Chin. Chem. Lett. 21, 850–852. https://doi.org/10.1016/j.cclet.2010.03.026.

Jiang, Y.P., Liu, Y.F., Guo, Q.L., et al, 2015. C14-Polyacetylene glucosides from *Codonopsis pilosula*. J. Asian Nat. Prod. Res. 17, 601–614. https://doi.org/10.1080/10286020.2015.1041932.

Jiao, P., Tseng-Crank, J., Corneliusen, B., et al, 2014. Lipase inhibition and antiobesity effect of *Atractylodes lancea*. Planta Med. 80, 577–582. https://doi.org/10.1055/s-0034-1368354.

Jin, L., Zhou, W., Li, R., et al, 2021. A new polyacetylene and other constituents with anti-inflammatory activity from *Artemisia halodendron*. Nat. Prod. Res. 35, 1010–1013. https://doi.org/10.1080/14786419.2019.1610962.

Johnson, J.A., Webster, D., Gray, C.A., 2013. The Canadian medicinal plant *Heracleum maximum* contains antimycobacterial diynes and furanocoumarins. J. Ethnopharmacol. 147, 232–237. https://doi.org/10.1016/j.jep.2013.03.009.

Jung, H.J., Min, B.S., Park, J.Y., et al, 2002. Gymnasterkoreaynes A-F, cytotoxic polyacetylenes from *Gymnaster koraiensis*. J. Nat. Prod. 65, 897–901. https://doi.org/10.1021/np0104018.

Kang, M.J., Kwon, E.B., Ryu, H.W., et al, 2018. Polyacetylene from *Dendropanax morbifera* alleviates diet-induced obesity and hepatic steatosis by activating AMPK signaling pathway. Front. Pharmacol. 9, 537. https://doi.org/10.3389/fphar.2018.00537.

Kanokmedhakul, S., Kanokmedhakul, K., Kantikeaw, I., et al, 2006. 2-substituted furans from the roots of *Polyalthia evecta*. J. Nat. Prod. 69, 68–72. https://doi.org/10.1021/np0503202.

Killeen, D.P., Sansom, C.E., Lill, R.E., et al, 2013. Quantitative Raman spectroscopy for the analysis of carrot bioactives. J. Agric. Food Chem. 61, 2701–2708. https://doi.org/10.1021/jf3053669.

Kim, M.I., Kim, J.H., Syed, A.S., et al, 2018. Application of ccentrifugal partition chromatography for bioactivity-guided purification of antioxidant-response-element-inducing constituents from *Atractylodis Rhizoma* Alba. Molecules 23. https://doi.org/10.3390/molecules23092274.

Kim, B.R., Paudel, S.B., Nam, J.W., et al, 2020. Constituents of *Coreopsis lanceolata* flower and their dipeptidyl peptidase IV inhibitory effects. Molecules 25. https://doi.org/10.3390/molecules25194370.

Kjellenberg, L., Johansson, E., Gustavsson, K.E., et al, 2012. Polyacetylenes in fresh and stored carrots (*Daucus carota*): relations to root morphology and sugar content. J. Sci. Food Agric. 92, 1748–1754. https://doi.org/10.1002/jsfa.5541.

Klein, J.B., Nowill, A.E., Franchi Jr, G.C., et al, 2013. Cytotoxic, antitumour and antimetastatic activity of two new polyacetylenes isolated from *Vernonia scorpioides* (Lam.) Pers. Basic Clin. Pharmacol. Toxicol. 113, 307–315. https://doi.org/10.1111/bcpt.12098.

Kobaek-Larsen, M., El-Houri, R.B., Christensen, L.P., et al, 2017. Dietary polyacetylenes, falcarinol and falcarindiol, isolated from carrots prevents the formation of neoplastic lesions in the colon of azoxymethane-induced rats. Food Funct. 8, 964–974. https://doi.org/10.1039/c7fo00110j.

Koidis, A., Rawson, A., Tuohy, M., et al, 2012. Influence of unit operations on the levels of polyacetylenes in minimally processed carrots and parsnips: An industrial trial. Food Chem. 132, 1406–1412. https://doi.org/10.1016/j.foodchem.2011.11.128.

Konovalov, D., 2014. Polyacetylene compounds of plants of the Asteraceae family. Pharm. Chem. J. 48, 613–631. https://doi.org/10.1007/s11094-014-1159-7.

Kramer, M., Muhleis, A., Conrad, J., et al, 2011. Quantification of polyacetylenes in apiaceous plants by high-performance liquid chromatography coupled with diode array detection. Z. Naturforsch. C. J. Biosci. 66, 319–327. https://doi.org/10.1515/znc-2011-7-801.

Kraus, W., 2003. Investigation of biologically active natural products using online LC-bioassay, LC-NMR, and LC-MS techniques. J. Toxicol. Toxin Rev. 22, 495–508. https://doi.org/10.1081/txr-120026909.

Kuklev, D.V., Dembitsky, V.M., 2014. Epoxy acetylenic lipids: their analogues and derivatives. Prog. Lipid Res. 56, 67–91. https://doi.org/10.1016/j.plipres.2014.08.001.

Kuo, Y.H., Lo, J.M., Chan, Y.F., 2002. Cytotoxic components from the leaves of *Schefflerataiwaniana*. J. Chin. Chem. Soc. 49, 427–431. https://doi.org/10.1002/jccs.200200067.

Kurimoto, S.I., Fujita, H., Kawaguchi, S., et al, 2021. Kamiohnoyneosides A and B, two new polyacetylene glycosides from flowers of edible Chrysanthemum "Kamiohno". J. Nat. Med. 75, 167–172. https://doi.org/10.1007/s11418-020-01443-4.

Larque-Garcia, H., Torres-Tapia, L.W., Vera-Ku, M., et al, 2020. Quantitative seasonal variation of the falcarinol-type polyacetylene (3*S*)-16,17-didehydrofalcarinol and its spatial tissue distribution in Tridax procumbens. Phytochem. Anal. 31, 183–190. https://doi.org/10.1002/pca.2878.

Le, J., Lu, W., Xiong, X., et al, 2015. Anti-inflammatory constituents from *Bidens frondosa*. Molecules 20, 18496–18510. https://doi.org/10.3390/molecules201018496.

Le, H.T., Nguyen, H.T., Min, H.Y., et al, 2018. Panaxynol, a natural Hsp90 inhibitor, effectively targets both lung cancer stem and non-stem cells. Cancer Lett. 412, 297–307. https://doi.org/10.1016/j.canlet.2017.10.013.

Lee, S.M., Bae, K.H., Sohn, H.J., 2009. Panaxfuraynes A and B, two new tetrahydrofuranic polyacetylene glycosides from *Panax ginseng* C. A. Meyer. Tetrahedron Lett. 50, 416–418. https://doi.org/10.1016/j.tetlet.2008.11.020.

Lee, S.W., Kim, K., Rho, M.C., et al, 2004. New Polyacetylenes, DGAT inhibitors from the roots of *Panax ginseng*. Planta Med. 70, 197–200. https://doi.org/10.1055/s-2004-815534.

Lee, S.H., Kim, J.G., Le, T.P.L., et al, 2022. Polyacetylenes from the roots of *Cirsium japonicum* var. ussuriense. Phytochemistry 202,. https://doi.org/10.1016/j.phytochem.2022.113319 113319.

Lee, S.M., Lee, H.B., Lee, C.G., 2010. A convenience UPLC/PDA method for the quantitative analysis of panaxfuraynes A and B from *Panax ginseng*. Food Chem. 123, 955–958. https://doi.org/10.1016/j.foodchem.2010.05.002.

Lee, J., Lee, Y.J., Kim, J., et al, 2015. Pyranocoumarins from root extracts of *Peucedanum praeruptorum* dunn with multidrug resistance reversal and anti-inflammatory activities. Molecules 20, 20967–20978. https://doi.org/10.3390/molecules201219738.

Lee, W.C., Peng, C.C., Chang, C.H., et al, 2013. Extraction of antioxidant components from *Bidens pilosa* flowers and their uptake by human intestinal Caco-2 cells. Molecules 18, 1582–1601. https://doi.org/10.3390/molecules18021582.

Li, W., 2022. Isolobetyol, a new polyacetylene derivative from *Platycodon grandiflorum* root. Nat. Prod. Res. 36, 466–469. https://doi.org/10.1080/14786419.2020.1779269.

Li, C., Lee, D., Graf, T.N., et al, 2009. Bioactive constituents of the stem bark of *Mitrephora glabra*. J. Nat. Prod. 72, 1949–1953. https://doi.org/10.1021/np900572g.

Li, Y.L., Li, J., Wang, N.L., et al, 2008. Flavonoids and a new polyacetylene from *Bidens parviflora* Willd. Molecules 13, 1931–1941. https://doi.org/10.3390/molecules13081931.

Li, X.R., Liu, J., Peng, C., et al, 2021. Polyacetylene glucosides from the florets of *Carthamus tinctorius* and their anti-inflammatory activity. Phytochemistry 187,. https://doi.org/10.1016/j.phytochem.2021.112770 112770.

Li, L.-B., Xiao, G.-D., Xiang, W., et al, 2019. Novel substituted thiophenes and sulf-polyacetylene ester from *Echinops ritro* L. Molecules 24, 805. https://doi.org/10.3390/molecules24040805.

Li, M., Zeng, M., Zhang, J., et al, 2021. Anti-inflammatory dendranacetylene A, a new polyacetylene glucoside from the flower of *Chrysanthemum morifolium* Ramat. Nat. Prod. Res. 35, 5692–5698. https://doi.org/10.1080/14786419.2020.1825425.

Lin, M., Zhang, W., Su, J., 2016. Toxic polyacetylenes in the genus *Bupleurum* (Apiaceae)–distribution, toxicity, molecular mechanism and analysis. J. Ethnopharmacol. 193, 566–573. https://doi.org/10.1016/j.jep.2016.12.043.

Liu, Y., Du, D., Liang, Y., et al, 2015. Novel polyacetylenes from *Coreopsis tinctoria* Nutt. J. Asian Nat. Prod. Res. 17, 744–749. https://doi.org/10.1080/10286020.2014.996138.

Liu, J., Fang, Y., Yang, L., et al, 2015. A qualitative, and quantitative determination and pharmacokinetic study of four polyacetylenes from Radix *Bupleuri* by UPLC-PDA-MS. J. Pharm. Biomed. Anal. 111, 257–265. https://doi.org/10.1016/j.jpba.2015.04.002.

Liu, X., Kunert, O., Blunder, M., et al, 2014. Polyyne hybrid compounds from *Notopterygium incisum* with peroxisome proliferator-activated receptor gamma agonistic effects. J. Nat. Prod. 77, 2513–2521. https://doi.org/10.1021/np500605v.

Liu, X., Latkolik, S., Atanasov, A.G., et al, 2017. *Bupleurum chinense* roots: a bioactivity-guided approach toward saponin-type NF-kappaB inhibitors. Planta Med. 83, 1242–1250. https://doi.org/10.1055/s-0043-118226.

Liu, J.-H., Lee, C.-S., Leung, K.-M., et al, 2007. Quantification of two polyacetylenes in radix *ginseng* and roots of related *Panax* species using a gas chromatography–mass spectrometric method. J. Agric. Food Chem. 55, 8830–8835. https://doi.org/10.1021/jf070735o.

Liu, L., Liu, Z., Yang, L., et al, 2022. Lobetyolin suppressed lung cancer in a mouse model by inhibiting epithelial-mesenchymal transition. Eur. J. Histochem. 66 (3), 3423. https://doi.org/10.4081/ejh.2022.3423.

Liu, L.-L., Wang, R., Shi, Y.-P., 2011. Chrysindins A-D, Polyacetylenes from the flowers of *Chrysanthemum indicum*. Planta Med. 77, 1806–1810. https://doi.org/10.1055/s-0030-1271138.

Liu, Y., Zhao, J., Chen, Y., et al, 2016. Polyacetylenic oleanane-type triterpene saponins from the roots of *Panax japonicus*. J. Nat. Prod. 79, 3079–3085. https://doi.org/10.1021/acs.jnatprod.6b00748.

Lu, Q.-X., Xiong, H., Du, Y., et al, 2020. Polyacetylenes and flavonoids from the stems and leaves of *Pyrethrum tatsienense*. Phytochem. Lett. 40, 130–134. https://doi.org/10.1016/j.phytol.2020.10.009.

Malti, C.E.W., Baccati, C., Mariani, M., et al, 2019. Biological activities and chemical composition of *Santolina Africana* Jord. et Fourr. aerial part essential oil from Algeria: occurrence of polyacetylene derivatives. Molecules 24. https://doi.org/10.3390/molecules24010204.

Marcetic, M.D., Lakusic, B.S., Lakusic, D.V., et al, 2013. Variability of the root essential oils of *Seseli rigidum* Waldst. & Kit. (Apiaceae) from different populations in Serbia. Chem. Biodivers. 10, 1653–1666. https://doi.org/10.1002/cbdv.201200439.

Marčetić, M., Petrović, S., Milenković, M., et al, 2014. Composition, antimicrobial and antioxidant activity of the extracts of *Eryngium palmatum* Pančić and Vis. (Apiaceae). Open Life Sci. 9, 149–155. https://doi.org/10.2478/s11535-013-0247-0.

Matsunaga, H., Katano, M., Yamamoto, H., et al, 1990. Cytotoxic activity of polyacetylene compounds in *Panax ginseng* CA Meyer. Chem. Pharm. Bull. 38, 3480–3482. https://doi.org/10.1248/cpb.38.3480.

Mei, R.Q., Lu, Q., Hu, Y.F., et al, 2008. Three new polyyne (= polyacetylene) glucosides from the edible roots of *Codonopsis cordifolioidea*. Helvetica Chim. Acta 91, 90–96. https://doi.org/10.1002/hlca.200890018.

Meng, X., Li, B.B., Lin, X., et al, 2019. New polyacetylenes glycoside from *Eclipta prostrate* with DGAT inhibitory activity. J. Asian Nat. Prod. Res. 21, 501–506. https://doi.org/10.1080/10286020.2018.1452914.

Meot-Duros, L., Cerantola, S., Talarmin, H., et al, 2010. New antibacterial and cytotoxic activities of falcarindiol isolated in *Crithmum maritimum* L. leaf extract. Food Chem. Toxicol. 48, 553–557. https://doi.org/10.1016/j.fct.2009.11.031.

Mi, C.N., Wang, H., Chen, H.Q., et al, 2019. Polyacetylenes from the roots of *Swietenia macrophylla* King. Molecules 24. https://doi.org/10.3390/molecules24071291.

Minto, R.E., Blacklock, B.J., 2008. Biosynthesis and function of polyacetylenes and allied natural products. Prog. Lipid Res. 47, 233–306. https://doi.org/10.1016/j.plipres.2008.02.002.

Moricz, A.M., Ott, P.G., Morlock, G.E., 2018. Discovered acetylcholinesterase inhibition and antibacterial activity of polyacetylenes in tansy root extract via effect-directed chromatographic

fingerprints. J. Chromatogr. A 1543, 73–80. https://doi.org/10.1016/j.chroma.2018.02.038.
Murata, K., Iida, D., Ueno, Y., et al, 2017. Novel polyacetylene derivatives and their inhibitory activities on acetylcholinesterase obtained from *Panax ginseng* roots. J. Nat. Med. 71, 114–122. https://doi.org/10.1007/s11418-016-1036-7.
Nakagawa, H., Takaishi, Y., Fujimoto, Y., et al, 2004. Chemical constituents from the Colombian medicinal plant Maytenus laevis. J. Nat. Prod. 67, 1919–1924. https://doi.org/10.1021/np040006s.
Nakano, H., Cantrell, C.L., Mamonov, L.K., et al, 2011. Echinopsacetylenes A and B, new thiophenes from *Echinops transiliensis*. Org. Lett. 13, 6228–6231. https://doi.org/10.1021/ol202680a.
Negri, R., 2015. Polyacetylenes from terrestrial plants and fungi: recent phytochemical and biological advances. Fitoterapia 106, 92–109. https://doi.org/10.1016/j.fitote.2015.08.011.
Ngo, T.M., Vu, T.O., Cao, T.Q., et al, 2021. Polyacetylenes and flavonoids isolated from flowers of *Carthamus tinctorius*. Chem. Nat. Compd. 57, 635–640. https://doi.org/10.1007/s10600-021-03439-2.
Ntumba, J.K., Tshiongo, C.M., Mifundu, M.N., et al, 2018. Effective antimalarial activities of alpha-hydroxy diynes isolated from *Ongokea gore*. Planta Med. 84, 806–812. https://doi.org/10.1055/s-0043-124974.
Nur, E.A.A., Ohshiro, T., Kobayashi, K., et al, 2020. Inhibition of cholesteryl ester synthesis by polyacetylenes from *Atractylodes* rhizome. Bioorg. Med. Chem. Lett. 30,. https://doi.org/10.1016/j.bmcl.2020.126997 126997.
Pan, Y., Lowary, T.L., Tykwinski, R.R., 2009. Naturally occurring and synthetic polyyne glycosides. Can. J. Chem. 87, 1565–1582. https://doi.org/10.1139/v09-117.
Pan, W., Zhang, Y., Xu, B., et al, 2006. Two new naturally occurring optical polyacetylene compounds from *Torricellia angulata* var intermedia and the determination of their absolute configurations. Nat. Prod. Res. 20, 1098–1104. https://doi.org/10.1080/14786410600743951.
Panter, K.E., Gardner, D.R., Stegelmeier, B.L., et al, 2011. Water hemlock poisoning in cattle: Ingestion of immature *Cicuta maculata* seed as the probable cause. Toxicon 57, 157–161. https://doi.org/10.1016/j.toxicon.2010.11.009.
Panthama, N., Kanokmedhakul, S., Kanokmedhakul, K., 2010. Polyacetylenes from the roots of *Polyalthia debilis*. J. Nat. Prod. 73, 1366–1369. https://doi.org/10.1021/np1001913.
Park, H.E., Lee, S.Y., Hyun, S.H., et al, 2013. Gas chromatography/mass spectrometry-based metabolic profiling and differentiation of ginseng roots according to cultivation age using variable selection. J. AOAC Int. 96, 1266–1272. https://doi.org/10.5740/jaoacint.12-195.
Park, J., Min, B., Jung, H., et al, 2002. Polyacetylene glycosides from *Gymnaster koraiensis*. Chem. Pharm. Bull. (Tokyo) 50, 685–687. https://doi.org/10.1248/cpb.50.685.
Park, B.Y., Min, B.S., Oh, S.R., et al, 2004. Isolation and anticomplement activity of compounds from *Dendropanax morbifera*. J. Ethnopharmacol. 90, 403–408. https://doi.org/10.1016/j.jep.2003.11.002.
Patil, B.S., Jayaprakasha, G.K., Murthy, K.N.C., et al, 2012. Emerging trends in dietary components for preventing and combating disease. ACS Publications. https://doi.org/10.1021/bk-2012-1093.fw001.
Pellati, F., Calo, S., Benvenuti, S., et al, 2006. Isolation and structure elucidation of cytotoxic polyacetylenes and polyenes from *Echinacea pallida*. Phytochemistry 67, 1359–1364. https://doi.org/10.1016/j.phytochem.2006.05.006.
Pellati, F., Calo, S., Benvenuti, S., 2007. High-performance liquid chromatography analysis of polyacetylenes and polyenes in *Echinacea pallida* by using a monolithic reversed-phase silica column. J. Chromatogr. A 1149, 56–65. https://doi.org/10.1016/j.chroma.2006.11.038.
Pellati, F., Orlandini, G., Benvenuti, S., 2012. Simultaneous metabolite fingerprinting of hydrophilic and lipophilic compounds in *Echinacea pallida* by high-performance liquid chromatography with diode array and electrospray ionization-mass spectrometry detection. J. Chromatogr. A 1242, 43–58. https://doi.org/10.1016/j.chroma.2012.04.025.
Perry, N.B., Span, E.M., Zidorn, C., 2001. Aciphyllal—a C34-polyacetylene from *Aciphylla scott-thomsonii* (Apiaceae). Tetrahedron Lett. 42, 4325–4328. https://doi.org/10.1016/s0040-4039(01)00720-1.
Pferschy-Wenzig, E.M., Getzinger, V., Kunert, O., et al, 2009. Determination of falcarinol in carrot (*Daucus carota* L.) genotypes using liquid chromatography/mass spectrometry. Food Chem. 114, 1083–1090. https://doi.org/10.1016/j.foodchem.2008.10.042.
Phan, N.H.T., Thuan, N.T.D., Hien, N.T.T., et al, 2022. Polyacetylene and phenolic constituents from the roots of *Codonopsis javanica*. Nat. Prod. Res. 36, 2314–2320. https://doi.org/10.1080/14786419.2020.1833200.
Pollo, L.A.E., Bosi, C.F., Leite, A.S., et al, 2013. Polyacetylenes from the leaves of *Vernonia scorpioides* (Asteraceae) and their antiproliferative and antiherpetic activities. Phytochemistry 95, 375–383. https://doi.org/10.1016/j.phytochem.2013.07.011.
Pollo, L.A.E., Frederico, M.J., Bortoluzzi, A.J., et al, 2018. A new polyacetylene glucoside from *Vernonia scorpioides* and its potential antihyperglycemic effect. Chem. Biol Interact. 279, 95–101. https://doi.org/10.1016/j.cbi.2017.11.003.
Prior, R.M., Lundgaard, N.H., Light, M.E., et al, 2007. The polyacetylene falcarindiol with COX-1 activity isolated from *Aegopodium podagraria* L. J. Ethnopharmacol. 113, 176–178. https://doi.org/10.1016/j.jep.2007.05.005.
Purup, S., Larsen, E., Christensen, L.P., 2009. Differential effects of falcarinol and related aliphatic C(17)-polyacetylenes on intestinal cell proliferation. J. Agric. Food Chem. 57, 8290–8296. https://doi.org/10.1021/jf901503a.
Qian, Z.M., Lu, J., Gao, Q.P., et al, 2009. Rapid method for simultaneous determination of flavonoid, saponins and polyacetylenes in folium ginseng and radix *ginseng* by pressurized liquid extraction and high-performance liquid chromatography coupled with diode array detection and mass spectrometry. J. Chromatogr. A 1216, 3825–3830. https://doi.org/10.1016/j.chroma.2009.02.065.
Quintana, N., Weir, T.L., Du, J., et al, 2008. Phytotoxic polyacetylenes from roots of Russian knapweed *(Acroptilon repens* (L.) DC.). Phytochemistry 69, 2572–2578. https://doi.org/10.1016/j.phytochem.2008.07.015.
Radulovic, N.S., Denic, M.S., 2013. Essential oils from the roots of *Echinops bannaticus* Rochel ex Schrad. and *Echinops sphaerocephalus* L. (Asteraceae): chemotaxonomic and biosynthetic aspects. Chem. Biodivers. 10, 658–676. https://doi.org/10.1002/cbdv.201200330.
Rahman, M.A., Cho, S.C., Song, J., et al, 2007. Dendrazawaynes A and B, antifungal polyacetylenes from *Dendranthema zawadskii* (Asteraceae). Planta Med. 73, 1089–1094. https://doi.org/10.1055/s-2007-981576.
Randriamampionona, D., Diallo, B., Rakotoniriana, F., et al, 2007. Comparative analysis of active constituents in *Centella asiatica* samples from Madagascar: Application for ex situ conservation and clonal propagation. Fitoterapia 78, 482–489. https://doi.org/10.1016/j.fitote.2007.03.016.
Rashid, M.A., Gustafson, K.R., Cardellina 2nd, J.H., et al, 2001. Absolute stereochemistry and anti-HIV activity of minquartynoic acid, a polyacetylene from *Ochanostachys amentacea*. Nat. Prod. Lett. 15, 21–26. https://doi.org/10.1080/10575630108041253.
Rawson, A., Koidis, A., Rai, D.K., et al, 2010. Influence of Sous Vide and water immersion processing on polyacetylene content and instrumental color of parsnip (*Pastinaca sativa*) disks. J. Agric. Food Chem. 58, 7740–7747. https://doi.org/10.1021/jf100517p.

Redl, K., Breu, W., Davis, B., et al, 1994. Anti-inflammatory active polyacetylenes from *Bidens campylotheca*. Planta Med. 60, 58–62. https://doi.org/10.1055/s-2006-959409.

Renate, S., Ernst-Peter, E.-M., Christian, Z., et al, 2002. Phenylpropanoids and polyacetylenes from *Ligusticum mutellina* (Apiaceae) of tyrolean origin. Sci. Pharm. 70, 101–109. https://doi.org/10.3797/scipharm.aut-02-12.

Resch, M., Heilmann, J., Steigel, A., et al, 2001. Further phenols and polyacetylenes from the rhizomes of *Atractylodes lancea* and their anti-inflammatory activity. Planta Med. 67, 437–442. https://doi.org/10.1055/s-2001-15817.

Resetar, M., Liu, X., Herdlinger, S., et al, 2020. Polyacetylenes from *Oplopanax horridus* and *Panax ginseng*: Relationship between structure and PPARγ activation. J. Nat. Prod. 83, 918–926. https://doi.org/10.1021/acs.jnatprod.9b00691.

Rollinger, J.M., Zidorn, C., Dobner, M.J., et al, 2003. Lignans, phenylpropanoids and polyacetylenes from *Chaerophyllum aureum* L. (Apiaceae). Z. Naturforsch. C. J. Biosci. 58, 553–557. https://doi.org/10.1515/znc-2003-7-818.

Roman, M., Baranski, R., Baranska, M., 2011. Nondestructive Raman analysis of polyacetylenes in Apiaceae vegetables. J. Agric. Food Chem. 59, 7647–7653. https://doi.org/10.1021/jf202366w.

Rücker, G., Kehrbaum, S., Sakulas, H., et al, 1992. Acetylenic glucosides from *Microglossa pyrifolia*. Planta Med. 58, 266–269. https://doi.org/10.1055/s-2006-961450.

Rui, M., Chou, G., 2022. Three new polyacetylenes from *Atractylodes japonica* Koidz.ez Kitam. Nat. Prod. Res. 36, 2063–2070. https://doi.org/10.1080/14786419.2020.1845673.

Sanchez-Ramos, M., Marquina-Bahena, S., Alvarez, L., et al, 2021. Phytochemical, pharmacological, and biotechnological study of *Ageratina pichinchensis*: A native species of Mexico. Plants (Basel) 10. https://doi.org/10.3390/plants10102225.

Santos, P., Busta, L., Yim, W.C., et al, 2022. Structural diversity, biosynthesis, and function of plant falcarin-type polyacetylenic lipids. J. Exp. Bot. 73, 2889–2904. https://doi.org/10.1093/jxb/erac006.

Schinkovitz, A., Stavri, M., Gibbons, S., et al, 2008. Antimycobacterial polyacetylenes from *Levisticum officinale*. Phytother. Res. 22, 681–684. https://doi.org/10.1002/ptr.2408.

Schwaiger, S., Adams, M., Seger, C., et al, 2004. New constituents of *Leontopodium alpinum* and their in *vitro* leukotriene biosynthesis inhibitory activity. Planta Med. 70, 978–985. https://doi.org/10.1055/s-2004-832625.

Senn, M., Gunzenhauser, S., Brun, R., et al, 2007. Antiprotozoal polyacetylenes from the Tanzanian medicinal plant *Cussonia zimmermannii*. J. Nat. Prod. 70, 1565–1569. https://doi.org/10.1021/np0702133.

Shigemori, H., Seshimoto, F., Won Hong, S., et al, 2011. New antibacterial polyacetylenes from sunflower (*Helianthus annuus* L.) seedlings. Heterocycles 83. https://doi.org/10.3987/com-11-12161.

Silva, D.B., Rodrigues, E.D., da Silva, G.V., et al, 2015. Post-column sodiation to enhance the detection of polyacetylene glycosides in LC-DAD-MS analyses: an example from *Bidens gardneri* (Asteraceae). Talanta 135, 87–93. https://doi.org/10.1016/j.talanta.2014.12.024.

Soltoft, M., Eriksen, M.R., Trager, A.W., et al, 2010. Comparison of polyacetylene content in organically and conventionally grown carrots using a fast ultrasonic liquid extraction method. J. Agric. Food Chem. 58, 7673–7679. https://doi.org/10.1021/jf101921v.

Song, J.H., Kwak, S., Kim, H., et al, 2019. *Dendropanax morbifera* branch water extract increases the immunostimulatory activity of RAW264.7 macrophages and primary mouse splenocytes. J. Med. Food 22, 1136–1145. https://doi.org/10.1089/jmf.2019.4424.

Stavri, M., Ford, C.H., Bucar, F., et al, 2005. Bioactive constituents of *Artemisia monosperma*. Phytochemistry 66, 233–239. https://doi.org/10.1016/j.phytochem.2004.11.010.

Stefanson, A., Bakovic, M., 2020. Dietary polyacetylene falcarinol upregulated intestinal heme oxygenase-1 and modified plasma cytokine profile in late phase lipopolysaccharide-induced acute inflammation in CB57BL/6 mice. Nutr. Res. 80, 89–105. https://doi.org/10.1016/j.nutres.2020.06.014.

Strzemski, M., Wojciak-Kosior, M., Sowa, I., et al, 2019. Methodological approach to determine carlina oxide - a main volatile constituent of *Carlina acaulis* L. essential oil. Talanta 191, 504–508. https://doi.org/10.1016/j.talanta.2018.09.005.

Sun, S., Du, G.J., Qi, L.W., et al, 2010. Hydrophobic constituents and their potential anticancer activities from Devil's Club (*Oplopanax horridus* Miq.). J. Ethnopharmacol. 132, 280–285. https://doi.org/10.1016/j.jep.2010.08.026.

Sun, Y., Sun, Y.P., Liu, Y., et al, 2022. Four new polyacetylenes from the roots of *Saposhnikovia divaricata*. Nat. Prod. Res. 36, 3579–3586. https://doi.org/10.1080/14786419.2020.1869973.

Sun, J., Wang, L., Wang, M., et al, 2016. Two new polyacetylene glycosides from the roots of *Codonopsis tangshen* Oliv. Nat. Prod. Res. 30, 2338–2343. https://doi.org/10.1080/14786419.2016.1174230.

Suzuki, A., Matsuura, D., Kanatani, H., et al, 2017. Inhibitory effects of polyacetylene compounds from *Panax ginseng* on Neurotrophin. Biol. Pharm. Bull. 40, 1784–1788. https://doi.org/10.1248/bpb.b17-00205.

Suzuki, A., Matsuura, D., Kanatani, H., et al, 2017. Inhibitory effects of polyacetylene compounds from *Panax ginseng* on neurotrophin receptor-mediated hair growth. Biol. Pharm. Bull. 40, 1784–1788. https://doi.org/10.1248/bpb.b17-00205.

Tacchini, M., Spagnoletti, A., Brighenti, V., et al, 2017. A new method based on supercritical fluid extraction for polyacetylenes and polyenes from *Echinacea pallida* (Nutt.) Nutt. roots. J. Pharm. Biomed. Anal. 146, 1–6. https://doi.org/10.1016/j.jpba.2017.07.053.

Tai, J., Cheung, S.S.C., Ou, D., et al, 2014. Antiproliferation activity of Devil's club (*Oplopanax horridus*) and anticancer agents on human pancreatic cancer multicellular spheroids. Phytomedicine 21, 506–514. https://doi.org/10.1016/j.phymed.2013.10.003.

Tanaka, O., Han, E.-C., Yamaguchi, H., et al, 2000. Saponins of plants of *Panax* species collected in central Nepal, and their chemotaxonomical significance. III. Chem. Pharm. Bull. 48, 889–892. https://doi.org/10.1248/cpb.48.889.

Tashkandi, H., Chaparala, A., Peng, S., et al, 2020. Pharmacokinetics of panaxynol in mice. J. Cancer Sci. Clin. Ther. 4, 133–143. https://doi.org/10.26502/jcsct.5079059.

Thorson, J.S., Sievers, E.L., Ahlert, J., et al, 2000. Understanding and exploiting nature's chemical arsenal: the past, present and future of calicheamicin research. Curr. Pharm. Des. 6, 1841–1879. https://doi.org/10.2174/1381612003398564.

Tobinaga, S., Sharma, M.K., Aalbersberg, W.G., et al, 2009. Isolation and identification of a potent antimalarial and antibacterial polyacetylene from *Bidens pilosa*. Planta Med. 75, 624–628. https://doi.org/10.1055/s-0029-1185377.

Towers, G., 1986. Significance of phototoxic phytochemicals in insect herbivory. J. Chem. Ecol. 12, 813–821. https://doi.org/10.1007/bf01020253.

Towers, G., Arnason, T., Wat, C.K., et al, 1979. Phototoxic polyacetylenes and their thiophene derivatives [effects on human skin]. Contact Dermatitis 5, 140–144. https://doi.org/10.1111/j.1600-0536.1979.tb04825.x.

Tuyen, N.Q., Hoa, L.T.P., Huong, L.T.D., et al, 2018. Heptadeca-8-en-4,6-diyne-3,10-diol – A new cytotoxic polyacetylene from Vietnamese *Panax stipuleanatus*. Chem. Nat. Compd. 54, 156–157. https://doi.org/10.1007/s10600-018-2280-8.

Um, Y.R., Kong, C.-S., Lee, J.I., et al, 2010. Evaluation of chemical constituents from *Glehnia littoralis* for antiproliferative activity against HT-29 human colon cancer cells. Process Biochem. 45, 114–119. https://doi.org/10.1016/j.procbio.2009.08.016.

Utrilla, M., Navarro, M., Jimenez, J., et al, 1995. Santolindiacetylene, a polyacetylene derivative isolated from the essential oil of *Santolina canescens*. J. Nat. Prod. 58, 1749–1752. https://doi.org/10.1021/np50125a018.

Venkatesan, T., Choi, Y.W., Lee, J., et al, 2018. Falcarindiol inhibits LPS-induced inflammation via attenuating MAPK and JAK-STAT signaling pathways in murine macrophage RAW 264.7 cells. Mol. Cell Biochem. 445, 169–178. https://doi.org/10.1007/s11010-017-3262-z.

Wang, Q., Hao, J., Gong, J., et al, 2020. Isolation and structure elucidation of two new compounds from *artemisia Ordosica* Krasch. Nat. Prod. Res. 34, 1862–1867. https://doi.org/10.1080/14786419.2018.1564298.

Wang, J.R., Leung, C.Y., Ho, H.M., et al, 2010. Quantitative comparison of ginsenosides and polyacetylenes in wild and cultivated American ginseng. Chem. Biodiversity 7, 975–983. https://doi.org/10.1002/cbdv.200900264.

Wang, N.H., Taniguchi, M., Tsuji, D., et al, 2003. Four guaianolides from *Sinodielsia yunnanensis*. Chem. Pharm. Bull. (Tokyo) 51, 68–70. https://doi.org/10.1248/cpb.51.68.

Wang, C.Z., Wan, J.Y., Wan, J., et al, 2020. Human intestinal microbiota derived metabolism signature from a North American native botanical *Oplopanax horridus* with UPLC/Q-TOF-MS analysis. Biomed. Chromatogr. 34, e4911.

Wang, K.D.G., Wang, J., Xie, S.-S., et al, 2016. New naturally occurring diacetylenic spiroacetal enol ethers from *Artemisia selengensis*. Tetrahedron Lett. 57, 32–34. https://doi.org/10.1016/j.tetlet.2015.11.049.

Wang, R., Wu, Q.X., Shi, Y.P., 2010. Polyacetylenes and flavonoids from the aerial parts of *Bidens pilosa*. Planta Med. 76, 893–896. https://doi.org/10.1055/s-0029-1240814.

Wang, S., Xu, Y., Jiang, W., et al, 2013. Isolation and identification of constituents with activity of inhibiting nitric oxide production in RAW 264.7 macrophages from *Gentiana triflora*. Planta Med. 79, 680–686. https://doi.org/10.1055/s-0032-1328460.

Wang, N., Yao, X., Ishii, R., et al, 2001. Antiallergic agents from natural sources. 3. structures and inhibitory effects on nitric oxide production and histamine release of five novel polyacetylene glucosides from *Bidens parviflora* WILLD. Chem. Pharm. Bull. (Tokyo) 49, 938–942. https://doi.org/10.1248/cpb.49.938.

Wang, M., Zou, H., Chen, Q., et al, 2017. Isolation of new polyacetylenes from the roots of *Eurycoma longifolia* via high-speed counter-current chromatography. J. Chromatogr. B Analyt. Technol. Biomed. Life Sci. 1055–1056, 39–44. https://doi.org/10.1016/j.jchromb.2017.03.038.

Washida, D., Kitanaka, S., 2003. Determination of polyacetylenes and ginsenosides in *Panax* species using high performance liquid chromatography. Chem. Pharm. Bull. 51, 1314–1317. https://doi.org/10.1248/cpb.51.1314.

Wat, C.-K., Biswas, R., Graham, E., et al, 1979. Ultraviolet-mediated cytotoxic activity of phenylheptatriyne from *Bidens pilosa* L. J. Nat. Prod. 42, 103–111. https://doi.org/10.1021/np50001a005.

Wei, W.C., Lin, S.Y., Lan, C.W., et al, 2016. Inhibiting MDSC differentiation from bone marrow with phytochemical polyacetylenes drastically impairs tumor metastasis. Sci. Rep. 6, 36663. https://doi.org/10.1038/srep36663.

Wen-Chin, L., Chiung-Chi, P., Chi-Huang, C., et al, 2013. Extraction of antioxidant components from *Bidens pilosa* flowers and their uptake by human intestinal Caco-2 cells. Molecules 18, 1582–1601. https://doi.org/10.3390/molecules18021582.

Wnorowski, A., Wnorowska, S., Wojas-Krawczyk, K., et al, 2020. Toxicity of carlina oxide-a natural polyacetylene from the *Carlina acaulis* roots-*in vitro* and *in vivo* study. Toxins (Basel) 12. https://doi.org/10.3390/toxins12040239.

Wongsomboon, P., Rattanajak, R., Kamchonwongpaisan, S., et al, 2021. Unique polyacetylenic ester-neolignan derivatives from *Mitrephora tomentosa* and their antimalarial activities. Phytochemistry 183,. https://doi.org/10.1016/j.phytochem.2020.112615 112615.

Wu, L.-W., Chiang, Y.-M., Chuang, H.-C., et al, 2004. Polyacetylenes function as anti-angiogenic agents. Pharm. Res. 21, 2112–2119. https://doi.org/10.1023/b:pham.0000048204.08865.41.

Xi, F.M., Li, C.T., Han, J., et al, 2014. Thiophenes, polyacetylenes and terpenes from the aerial parts of *Eclipata prostrate*. Bioorg. Med. Chem. 22, 6515–6522. https://doi.org/10.1016/j.bmc.2014.06.051.

Xiao, M.-T., Luo, D.-W., Ke, Z., et al, 2014. A novel polyacetylene from the aerial parts of *Artemisia lactiflora*. Phytochem. Lett. 8, 52–54. https://doi.org/10.1016/j.phytol.2014.01.008.

Xie, Q., Wang, C., 2022. Polyacetylenes in herbal medicine: A comprehensive review of its occurrence, pharmacology, toxicology, and pharmacokinetics (2014–2021). Phytochemistry, 113288. https://doi.org/10.1016/j.phytochem.2022.113288.

Xie, Q., Wang, H., Guan, H., et al, 2023. The *in vitro*/*in vivo* metabolic pathways analysis of lobetyol, lobetyolin, and lobetyolinin, three polyacetylenes from Codonopsis Radix, by UHPLC-Q/TOF-MS and UHPLC-MS/MS. J. Pharm. Biomed. Anal. 223,. https://doi.org/10.1016/j.jpba.2022.115140 115140.

Xu, K., Jiang, J.S., Feng, Z.M., et al, 2016. Bioactive sesquiterpenoid and polyacetylene glycosides from *Atractylodes lancea*. J. Nat. Prod. 79, 1567–1575. https://doi.org/10.1021/acs.jnatprod.6b00066.

Xu, K., Feng, Z.-M., Jiang, J.-S., et al, 2017. Sesquiterpenoid and C 14 -polyacetylene glycosides from the rhizomes of *Atractylodes lancea*. Chin. Chem. Lett. 28, 597–601. https://doi.org/10.1016/j.cclet.2016.10.036.

Xu, K., Feng, Z.M., Yang, Y.N., et al, 2017. Four new C(10)-polyacetylene glycosides from the rhizomes of *Atractylodes lancea*. J. Asian Nat. Prod. Res. 19, 121–127. https://doi.org/10.1080/10286020.2016.1247811.

Xu, W.J., Li, J.H., Zhou, M.M., et al, 2020. Toonasindiynes A-F, new polyacetylenes from *Toona sinensis* with cytotoxic and anti-inflammatory activities. Fitoterapia 146,. https://doi.org/10.1016/j.fitote.2020.104667 104667.

Xu, K., Yang, P.F., Yang, Y.N., et al, 2017. Direct assignment of the threo and erythro configurations in polyacetylene glycosides by ^{1}H NMR spectroscopy. Org. Lett. 19, 686–689. https://doi.org/10.1021/acs.orglett.6b03855.

Yamazoe, S., Hasegawa, K., Suenaga, K., et al, 2006. Growth inhibitory polyacetylenes from galls of *Hedera rhombea* bean. Nat. Prod. Commun. 1, 87–94. https://doi.org/10.1177/1934578X0600100202.

Yamazoe, S., Hasegawa, K., Ito, J., et al, 2007. Hederyne A, a new antimicrobial polyacetylene from galls of *Hedera rhombea* Bean. J. Asian Nat. Prod. Res. 9, 537–540. https://doi.org/10.1080/10286020600882379.

Yamazoe, S., Hasegawa, K., Shigemori, H., 2007. Growth inhibitory indole acetic acid polyacetylenic ester from Japanese ivy (*Hedera rhombea* Bean). Phytochemistry 68, 1706–1711. https://doi.org/10.1016/j.phytochem.2007.03.036.

Yang, M.C., Seo, D.S., Choi, S.U., et al, 2008. Polyacetylenes from the roots of cultivated-wild ginseng and their cytotoxicity *in vitro*. Arch. Pharm. Res. 31, 154–159. https://doi.org/10.1007/s12272-001-1134-1.

Yang, M.C., Kwon, H.C., Kim, Y.J., et al, 2010. Oploxynes A and B, polyacetylenes from the stems of *Oplopanax elatus*. J. Nat. Prod. 73, 801–805. https://doi.org/10.1021/np900628j.

Yang, S., Shen, T., Zhao, L., et al, 2014. Chemical constituents of *Lobelia chinensis*. Fitoterapia 93, 168–174. https://doi.org/10.1016/j.fitote.2014.01.007.

Yao, C.M., Yang, X.W., 2014. Bioactivity-guided isolation of polyacetylenes with inhibitory activity against NO production in LPS-activated RAW264.7 macrophages from the rhizomes of *Atractylodes macrocephala*. J. Ethnopharmacol. 151, 791–799. https://doi.org/10.1016/j.jep.2013.10.005.

Yeboah, G.N., Owusu, F.W.A., Archer, M.A., et al, 2022. Bridelia ferruginea Benth.; An ethnomedicinal, phytochemical, pharmacological and toxicological review. Heliyon 8, e10366. https://doi.org/10.1016/j.heliyon.2022.e10366.

Yim, S.H., Kim, H.J., Lee, I.S., 2003. A polyacetylene and flavonoids from *Cirsium rhinoceros*. Arch. Pharm. Res. 26, 128–131. https://doi.org/10.1007/BF02976657.

Yokosuka, A., Tatsuno, S., Komine, T., et al, 2017. Chemical constituents of the roots and rhizomes of *Saposhnikovia divaricata* and their cytotoxic activity. Nat. Prod. Commun. 12, 255–258. https://doi.org/10.1177/1934578X1701200229.

Yoon, I.S., Cho, S.S., 2021. Effects of lobetyolin on xanthine oxidase activity in *vitro* and in *vivo*: weak and mixed inhibition. Nat. Prod. Res. 35, 1667–1670. https://doi.org/10.1080/14786419.2019.1622108.

Yoshikawa, M., Nishida, N., Ninomiya, K., et al, 2006. Inhibitory effects of coumarin and acetylene constituents from the roots of *Angelica furcijuga* on D-galactosamine/lipopolysaccharide-induced liver injury in mice and on nitric oxide production in lipopolysaccharide-activated mouse peritoneal macrophages. Bioorg. Med. Chem. 14, 456–463. https://doi.org/10.1016/j.bmc.2005.08.038.

Zhai, D.D., Zhong, J.J., 2010. Simultaneous analysis of three bioactive compounds in *Artemisia annua* hairy root cultures by reversed-phase high-performance liquid chromatography-diode array detector. Phytochem. Anal. 21, 524–530. https://doi.org/10.1002/pca.1226.

Zhang, S., Cheng, F., Yang, L., et al, 2020. Chemical constituents from *Glehnia littoralis* and their chemotaxonomic significance. Nat. Prod. Res. 34, 2822–2827. https://doi.org/10.1080/14786419.2019.1586697.

Zhang, Z., Lu, C., Liu, X., et al, 2014. Global and targeted metabolomics reveal that Bupleurotoxin, a toxic type of polyacetylene, induces cerebral lesion by inhibiting GABA receptor in mice. J. Proteome Res. 13, 925–933. https://doi.org/10.1021/pr400968c.

Zhang, Y., Shi, S., Zhao, M., et al, 2013. Coreosides A-D, C14-polyacetylene glycosides from the capitula of *Coreopsis tinctoria* and its anti-inflammatory activity against COX-2. Fitoterapia 87, 93–97. https://doi.org/10.1016/j.fitote.2013.03.024.

Zhao, Y., Geng, C.A., Sun, C.L., et al, 2014. Polyacetylenes and anti-hepatitis B virus active constituents from *Artemisia capillaris*. Fitoterapia 95, 187–193. https://doi.org/10.1016/j.fitote.2014.03.017.

Zheng, X., Zheng, X., Zhang, C., et al, 2019. Cytotoxic polyacetylenes isolated from the roots and rhizomes of *Notopterygium incisum*. Chin. Chem. Lett. 30, 428–430. https://doi.org/10.1016/j.cclet.2018.09.011.

Zhou, Z.F., Menna, M., Cai, Y.S., et al, 2015. Polyacetylenes of marine origin: chemistry and bioactivity. Chem. Rev. 115, 1543–1596. https://doi.org/10.1021/cr4006507.

Zhu, Y.J., Li, C.H., Yu, S.H., et al, 2021. Two new polyacetylene glucosides and a new caffeoyl derivative with angiogenic activity from *Bidens parviflora* Willd. Phytochem. Lett. 42, 82–86. https://doi.org/10.1016/j.phytol.2021.01.005.

Ziaratnia, S.M., Ohyama, K., Hussein, A.-A.-F., et al, 2009. Isolation and identification of a novel chlorophenol from a cell suspension culture of *Helichrysum aureonitens*. Chem. Pharm. Bull. 57, 1282–1283. https://doi.org/10.1248/cpb.57.1282.

Zidorn, C., Johrer, K., Ganzera, M., et al, 2005. Polyacetylenes from the Apiaceae vegetables carrot, celery, fennel, parsley, and parsnip and their cytotoxic activities. J. Agric. Food Chem. 53, 2518–2523. https://doi.org/10.1021/jf048041s.

Zloh, M., Bucar, F., Gibbons, S., 2007. Quantum chemical studies on structure activity relationship of natural product polyacetylenes. Theor. Chem. Acc. 117, 247–252. https://doi.org/10.1007/s00214-006-0148-7.

Bernart., M. W., J. H. Cardellina., M. S. Balaschak., et al., 1996. Cytotoxic falcarinol oxylipins from *Dendropanax arboreus*. J. Nat. Prod. 59, 748-753. https://doi.org/10.1021/np960224o